

HOMOEOLGOUS RECOMBINATION-BASED CHROMOSOME ENGINEERING FOR
PHYSICAL MAPPING AND INTROGRESSION IN WHEAT AND ITS RELATIVES

AEGILOPS SPELTOIDES AND *THINOPYRUM ELONGATUM*

A Dissertation
Submitted to the Graduate Faculty
of the
North Dakota State University
of Agriculture and Applied Science

By

Mingyi Zhang

In Partial Fulfillment of the Requirements
for the Degree of
DOCTOR OF PHILOSOPHY

Major Program:
Genomics and Bioinformatics

January 2020

Fargo, North Dakota

North Dakota State University
Graduate School

Title
HOMOELOGOUS RECOMBINATION-BASED CHROMOSOME
ENGINEERING FOR PHYSICAL MAPPING AND INTROGRESSION
IN WHEAT AND ITS RELATIVES *AEGILOPS SPELTOIDES* AND
THINOPYRUM ELONGATUM

By

Mingyi Zhang

The Supervisory Committee certifies that this *disquisition* complies with North Dakota
State University's regulations and meets the accepted standards for the degree of

DOCTOR OF PHILOSOPHY

SUPERVISORY COMMITTEE:

Xiwen Cai

Chair

Phillip McClean

Steven S. Xu

Justin D. Faris

Zhaohui Liu

Approved:

January 22, 2020

Date

Phillip McClean

Department Chair

ABSTRACT

Wheat (genome AABBDD) is one of the essential crops, offering approximate 20% of human calorie consumption worldwide. Allopolyploidization of three diploid ancestors led to hexaploid wheat with narrowed genetic variation. Chromosome engineering is an applicable approach to restore the evolutionarily-omitted genetic diversity by homoeologous chromosomes recombination between wheat and its relatives. Two diploid relatives of wheat, *Thinopyrum elongatum* (genome EE) and *Aegilops speltoides* (genome SS), containing favorable genes, are used as gene resources for alien introgression and genome diversification in wheat. An advanced and effective experiment procedure was developed and applied for the production, recovery, detection, and characterization of homoeologous recombinants. Meanwhile, a novel recombinant chromosome recovery strategy was exploited with improved efficiency and accuracy.

In this study, recombinants of wheat chromosomes 3B and 7B with their homoeologous chromosomes in *Th. elongatum* and *Ae. speltoides* (i.e. 3B-3E, 7B-7E, and 7B-7S) were produced and detected. Totally, 81 3B-3E recombinants and four aberrations involving in distinct chromosomal regions were developed in three recombination cycles by fluorescent genomic *in situ* hybridization (FGISH). The secondary and tertiary recombination breakpoints occurred toward the proximal regions comparing to the primary recombination under this advanced recombination procedure. A novel recovery strategy was used to recover 7B-7E and 7B-7S homoeologous recombinants by chromosome-specific markers and FGISH verification. Marker-based pre-screening and subsequent FGISH verification identified 29 7B-7E and 61 7B-7S recombinants, seven 7B-7E and four 7B-7S Robertsonian translocations, one 7E and five 7S telocentric chromosomes, and three 7S deletions. All the recombinants and aberrations were genotyped by high-throughput wheat 90K single nucleotide polymorphism (SNP) assay and the

recombination breakpoints were physically mapped to wheat chromosome 3B or 7B according to their FGISH patterns, SNP results, and wheat reference genome sequence. Chromosome 3B was physically partitioned into 38 bins with 429 SNPs. Meanwhile, 44 distinct bins were resolved for chromosome 7B with 523 SNPs. A composite bin map was constructed for chromosomes 3B and 7B, respectively, with a comprehensive analysis of FGISH and SNPs results. In summary, this project provides a unique physical framework for further wheat genome studies and diversifies the wheat genome for germplasm development in wheat breeding.

ACKNOWLEDGEMENTS

I would thank everyone who has supported and assisted me during my whole doctoral study. First and foremost, I would like to express my deepest gratitude to my supervisor, Dr. Xiwen Cai, whose wealth of knowledge, research attitude, and his encouragement and patience make a great impact on my life and guide me through my doctoral program.

I would sincerely appreciate my graduate committee members, Drs. Phillip McClean, Steven S. Xu, Justin D. Faris, and Zhaohui Liu, who have supported my research goals and improved my professional studies.

I would like to thank Dr. Shiaoman Chao, who has helped me on wheat 90K SNP genotyping and GenomeStudio operating. I also express my sincere thanks to our lab technician, Wei Zhang, who helped me on the course's study and experiment execution. I extend my grateful thanks for my previous and current lab members, Rachel McArthur, Xianwen Zhu, Shaungfeng Ren, Tatiana Danilova, Yadav Gyawali, and Somo Ibrahim for their friendship and collaboration.

I would also express my gratitude to the Program of Genomics and Bioinformatics, the Department of Plant Sciences, North Dakota State University (NDSU) for providing me this opportunity to pursue my Ph.D.

Nobody has been more important than my family members during my Ph.D. studies. I would thank my parents and brother for their support and inspiration. I wish to thank my husband, Qing Sun, and my daughter, Chloe Sun, to provide endless love and happiness for me.

TABLE OF CONTENTS

ABSTRACT.....	iii
ACKNOWLEDGEMENTS.....	v
LIST OF TABLES.....	ix
LIST OF FIGURES.....	x
CHAPTER 1. GENERAL INTRODUCTION.....	1
References.....	3
CHAPTER 2. LITERATURE REVIEW.....	7
Wheat origin, evolution, and domestication.....	7
Taxonomy of wheat.....	7
Origin and evolutionary of polyploid wheat.....	9
Domestication of wheat.....	10
Wheat genome and chromosomes.....	11
Wheat genome.....	11
Wheat chromosomes.....	13
Chromosome engineering-based gene introgression in wheat.....	14
Wheat gene pools.....	14
Chromosome engineering in wheat.....	15
Gene introgression in wheat and its relatives.....	16
Meiotic homoeologous recombination-based alien introgression.....	17
References.....	19
CHAPTER 3. PARTITIONING AND PHYSICAL MAPPING OF WHEAT CHROMOSOME 3B AND ITS HOMOEOLOGUE 3E IN <i>THINOPYRUM</i> <i>ELONGATUM</i> BY INDUCING HOMOEOLOGOUS RECOMBINATION.....	30
Abstract.....	30
Introduction.....	31

Material and methods	34
Plant materials	34
Homoeologous recombination population development.....	34
Molecular cytogenetic analysis	34
Molecular marker analyses.....	36
Results	36
Induction and recovery of 3B-3E recombinants and aberrations	36
Detection and delineation of 3B-3E recombinants and aberrations by FGISH.....	38
FGISH-based physical analysis of 3B-3E recombination breakpoints	43
Homoeologous recombination-based physical mapping of wheat chromosome 3B.....	44
Development of chromosome 3E-specific STARP markers and construction of a comparative physical map for chromosomes 3E, 3B, 3A, and 3D.....	47
Discussion	50
References	54
CHAPTER 4. DISSECTION AND PHYSICAL MAPPING OF WHEAT CHROMOSOME 7B BY INDUCING MEIOTIC RECOMBINATION WITH ITS HOMOEOLOGUES IN <i>AEGILOPS SPELTOIDES</i> AND <i>THINOPYRUM ELONGATUM</i>	60
Abstract	60
Introduction	61
Materials and methods	64
Plant materials	64
Construction of the <i>ph1b</i> -induced homoeologous recombination populations.....	64
Molecular markers analysis.....	64
Cytogenetic analysis.....	65
Microscopy	66
Results	67

Development and validation of chromosome-specific STARP markers for the detection of 7B-7E and 7B-7S recombinants	67
Pre-screening and verification of 7B-7E and 7B-7S recombinants and aberrations by STARP markers and FGISH	70
Homoeologous recombination-based delineation and dissection of wheat chromosome 7B.....	73
Construction of the composite bin map for wheat chromosome 7B	77
Discussion	78
References	82
APPENDIX A. THE 3B-3E RECOMBINANTS/ABERRATIONS AND THEIR CHROMOSOME CONSTITUTIONS	88
APPENDIX B. MEASUREMENT AND SIZE CALCULATION OF THE 3B-3E RECOMBINANT CHROMOSOMES	92
APPENDIX C. THE GENETIC AND PHYSICAL POSITION OF SNPS ASSIGNED TO THE COMPOSITE BIN MAP	105
APPENDIX D. PHYSICAL POSITION OF THE RECOMBINATION BREAKPOINTS IN THE CRITICAL 3B-3E RECOMBINANTS USED FOR THE CONSTRUCTION OF THE COMPOSITE BIN MAP.....	116
APPENDIX E. PRIMER SEQUENCES AND PHYSICAL LOCATIONS OF THE CHROMOSOME-SPECIFIC STARP MARKERS.....	118
APPENDIX F. THE 7B-7E AND 7B-7S RECOMBINANTS/ABERRATIONS AND THEIR COMPOSITIONS AND PEDIGREE	121
APPENDIX G. POLYMORPHIC SNPS ASSIGNED TO THE CHROMOSOME 7B	126
APPENDIX H. PHYSICAL POSITIONS OF THE RECOMBINATION BREAKPOINTS OF THE REPRESENTATIVE 7B-7E AND 7B-7S RECOMBINANTS.....	139
APPENDIX I. THE COMPOSITE BIN MAP OF CHROMOSOME 7B AND PARTITIONED CHROMOSOME BASED ON 7B-7E RECOMBINANTS AND 7B-7S RECOMBINANTS	141
APPENDIX J. SNP-BASED PHYSICAL MAPPING OF THE 7B-7E AND 7B-7S RECOMBINATION-RESOLVED BINS FOR CHROMOSOME 7B	142

LIST OF TABLES

<u>Table</u>	<u>Page</u>
2.1. The classification of Triticum genus.....	8
3.1. 3B-3E homoeologous recombinants detected in the primary, secondary, and tertiary recombination populations.....	40
3.2. Chromosome 3E-specific STARP markers spanning distinct regions along the entire chromosome.....	48
4.1. SNP-derived STARP markers specific for the 7B-7E and 7B-7S homoeologous pairs.....	68
4.2. Six categories of 7B-7E and 7B-7S recombinants and aberrations	72

LIST OF FIGURES

<u>Figure</u>	<u>Page</u>
3.1. Induction, recovery, detection, and characterization of 3B-3E homoeologous recombinants.....	35
3.2. FGISH patterns of <i>ph1b</i> mutant-induced 3B-3E homoeologous pairing as a rod bivalent (a) and a ring bivalent (b) in the special genotype that was double monosomic for 3B and 3E, and homozygous for <i>ph1b</i>	38
3.3. FGISH-painted 3B-3E recombinant chromosomes and aberrations in the seven categories.....	40
3.4. Distribution of primary, secondary, and tertiary 3B-3E recombinants and aberrations in the following seven categories: <i>I</i> -Terminal recombinants with a large 3E segment; <i>II</i> -Terminal recombinants with a large 3B segment; <i>III</i> -Interstitial recombinants with a large 3E pericentromeric region flanked by 3B terminal segments; <i>IV</i> -Interstitial recombinants with a small 3E segment within one or both arms; <i>V</i> -Double recombinant [V1 (3ES·3EL-3BL) + V2 (3DS·3DL(?)·3EL)]; <i>VI</i> -Robertsonian translocations (3ES·3BL and 3BS·3EL); <i>VII</i> -Telocentric chromosomes of 3E; <i>VIII</i> -Telocentric chromosomes of 3E.....	41
3.5. FGISH images illustrating three cycles (primary, secondary, and tertiary) of <i>ph1b</i> -induced 3B-3E homoeologous recombination and resultant recombinants.....	42
3.6. Distribution of the three rounds (primary, secondary, and tertiary) of 3B-3E recombination breakpoints on the centromere-telomere axis.....	44
3.7. The genetic and physical positions of 3B-3E polymorphic SNPs on chromosome 3B.....	45
3.8. Integrative SNP genotyping and FGISH analysis of 3B-3E recombinants.....	46
3.9. Comparative physical map of <i>Th. elongatum</i> chromosome 3E and wheat chromosomes 3A, 3B, and 3D at 22 chromosome 3E-specific STARP (i.e. SNP) marker loci.....	49
4.1. Diagram showing induction, recovery, detection, and characterization of 7B-7E and 7B-7S homoeologous recombinants.....	65
4.2. Ideogram of wheat chromosome 7B (red), <i>Th. elongatum</i> chromosome 7E (green), and <i>Ae. speltoides</i> chromosome 7S (green) illustrating chromosome-specific molecular markers for the detection of meiotic homoeologous recombinants and chromosome aberrations.....	66
4.3. Detection of 7B-7E and 7B-7S recombinants by chromosome-specific STARP markers (a) and verification of the recombinants by FGISH (b).....	69

4.4. FGISH-painted 7B-7E and 7B-7S recombinant chromosomes and aberrations in six categories, including Category 1 (I & II) - terminal recombinants with a small 7B segment, Category 2 (III & IV) - terminal recombinants with a small 7E or 7S segment, Category 3 (V) -interstitial recombinants, Category 4 (VI) - Robertsonian translocation, Category 5 (VII) -telocentric 7E or 7S chromosomes, and Category 6 (VIII) - chromosome 7E or 7S deletions..	71
4.5. Polymorphic SNPs of the homoeologous pair 7B-7E and 7B-7S (<i>a</i>) and their genetic and physical positions on chromosome 7B (<i>b</i>).....	74
4.6. Graphical representation of the 26 7B-7E recombinants (<i>top</i>) and 38 7B-7S recombinants (<i>bottom</i>), showing their SNP genotypes and FGISH patterns.	76
4.7. Composite bin map of wheat chromosome 7B and corresponding partitioned chromosome 7B.	78

CHAPTER 1. GENERAL INTRODUCTION

Common wheat (*Triticum aestivum* L., $2n = 6x = 42$, AABBDD) is an allohexaploid with three subgenomes. It originated from two distinct spontaneous hybridizations involving three diploid ancestors (McFadden and Sears, 1946; Riley et al., 1958a; Dvorak et al., 1993; Huang et al., 2002; Jauhar, 2007; Feldman and Levy, 2012; Pont et al., 2019). The first hybridization occurred between *Triticum urartu* ($2n = 2x = 14$, AA) and *Aegilops speltoides*-related lineage ($2n = 2x = 14$, BB) and the second one occurred between *T. turgidum* ($2n = 4x = 28$, AABB) and *Ae. tauschii* ($2n = 2x = 14$, DD) (Kihara, 1944; McFadden and Sears, 1946; Dvorak et al., 1993; Blake et al., 1999; Petersen et al., 2006; Feldman and Levy, 2012; Zhang et al., 2018a; Pont et al., 2019). The ancestor of the wheat B subgenome remains obscure. A recent study reported that the wheat B genome was evolved from multiple ancestors, and *Ae. speltoides* is one of them (Zhang et al., 2018a). Hexaploid wheat has a narrowed genetic variation due to the allopolyploid origin of its genome. This has made wheat vulnerable to many biotic and abiotic threats (Brown et al., 2009; Peng et al., 2011; Faris, 2014; Marcussen et al., 2014; Zhang et al., 2019).

Wheat chromosome engineering is the technology to modify chromosome number, ploidy, or structure for wheat genetic improvement. It has been used to incorporate favorable genes from wheat relatives into the wheat genome for germplasm and variety development (Zhang et al., 2019). Construction of wheat-alien addition, substitution, or translocation lines can incorporate alien genes into the wheat genome. Alien chromosomes may contain favorable as well as deleterious genes. Thus, the addition and substitution lines are generally not utilized directly in wheat breeding for variety development. Instead, they are used as bridge materials for alien introgression in pre-breeding. Wheat-alien translocations involving distinct alien

chromosome segments can reduce the linkage drag and minimize the chance of incorporating undesirable genes into the wheat genome.

Wheat-alien translocations can be induced by irradiation, gametocidal chromosome or meiotic homoeologous recombination. Irradiation and gametocidal genes (*Gc*) induce chromosome breakage and fusion randomly. Meiotic homoeologous recombination produces reciprocal translocations, which are genetically more stable than irradiation- or *Gc* gene- induced translocations. Homoeologous recombination-based chromosome engineering is an effective approach for alien gene introgression and wheat genome studies. Wheat relatives containing favorable genes are used as donors for gene introgression and wheat genome diversification. The wild relatives of wheat *Aegilops speltoides* and *Thinopyrum elongatum* contain various beneficial genes, including those for resistance to stem rust, stripe rust, SNB, or tan spot. They were used in this study for wheat chromosome dissection and introgression. However, the meiotic homoeologous recombination frequency is low because of the existence of *Ph* (pairing homoeologous) genes in wheat, which ensure homologous pairing and prevent homoeologous pairing. The absence of *Ph* gene, such as nullisomy for *Ph1* and *ph1b* mutant, induces homoeologous pairing and recombination (Riley and Chapman, 1958b; Riley et al., 1959; Sears, 1977; Qi et al., 2007). The *ph1b*-induced homoeologous recombination produces compensating translocations useful for wheat germplasm and variety development in wheat breeding.

Alien chromosomes or segments can be differentiated from wheat chromosomes by fluorescent genomic *in situ* hybridization (FGISH) as well as molecular markers (Schwarzacher et al., 1992; Cai et al., 1998; Zhang et al. 2018b). FGISH allows for a direct visualization of wheat and alien chromosomes and their recombination, but it is a time-consuming process. The SNP-derived PCR markers, including semi-thermal asymmetric reverse PCR (STARP) and

kompetitive allele specific PCR (KASP), have been developed and applied to recover homoeologous recombinants (Neelam et al. 2013; Long et al., 2017; Zhang et al., 2017, 2018b). The molecular marker-mediated recombinant detection can be verified by FGISH. The integrative molecular marker and FGISH analysis offers an effective approach for wheat-alien recombinant detection in an improved throughput (Zhang et al., 2018b; Zhang et al. 2020).

There were three aims involved in this study. The first aim was to develop an advanced and efficient procedure to induce, recover, detect, and characterize meiotic homoeologous recombination. The second aim was to manipulate wheat chromosomes 3B and 7B through meiotic recombination with its homoeologous counterparts in *Ae. speltooides* and *Th. elongatum*, respectively, for the development of homoeologous recombinants. The third aim was to dissect and physical map wheat chromosome 3B and 7B using the high-throughput genotyping platform for the construction of a composite bin map for chromosome 3B and 7B, respectively.

References

- Avni R, Nave M, Barad O, Baruch K, Twardziok SO, Gundlach H, Hale L, Mascher M, Spannagl M, Wiebe K, Jordan KW, Golan G, Deek J, Ben-Zvi G, Himmelbach A, MacLachlan RP, Sharpe AG, Fritz A, Ben-David R, Budak H, Fahima T, Korol A, Faris JD, Hernandez A, Mikel MA, Levy AA, Steffenson B, Maccaferri M, Tuberosa R, Cattivelli L, Faccioli P, Ceriotti A, Kashkush K, Pourkheirandish M, Komatsuda T, Eilam T, Sela H, Sharon A, Ohad N, Chamovitz DA, Mayer KFX, Stein N, Ronon G, Peleg Z, Pozniak CJ, Akhunov ED, Distelfeld A (2017) Wild emmer genome architecture and diversity elucidate wheat evolution and domestication. *Science* 357:93–97
- Blake NK, Leffert BR, Lavin M, Talbert LE (1999) Phylogenetic reconstruction based on low copy DNA sequence data in an allopolyploid: The B genome of wheat. *Genome* 42:351–360
- Brown TA, Jones MK, Powell W, Allaby RG (2009) The complex origins of domesticated crops in the Fertile Crescent. *Trends Ecol Evol* 24:103–109
- Cai X, Jones S, Murray T (1998) Molecular cytogenetic characterization of Thinopyrum and wheat–Thinopyrum translocated chromosomes in a wheat Thinopyrum amphiploid. *Chromosome Res* 6:185–189
- Dvorak J, Terlizzi P, Zhang HB, Resta P (1993) The evolution of polyploidy wheats: Identification of the A genome donor species. *Genome* 36:21–31

- Faris JD (2014) Wheat domestication: key to agricultural revolutions past and future. In: Tuberosa R, Graner A, Frison E (eds) Genomics of plant genetic resources. vol 1. Managing, sequencing and mining genetic resources, Springer, Netherlands, pp 439–464
- Feldman M, Levy AA (2012) Genome evolution due to allopolyploidization in wheat. *Genetics* 192:763–774
- Huang S, Sirikhachornkit A, Su X, Faris J, Gill B, Haselkorn R, Gornicki P (2002) Genes encoding plastid acetyl–CoA carboxylase and 3–phosphoglycerate kinase of the *Triticum/Aegilops* complex and the evolutionary history of polyploid wheat. *Proc Natl Acad Sci USA* 99:8133–8138
- Jauhar PP (2007) Meiotic restitution in wheat polyhaploids (amphihaploids), a potent evolutionary force. *J Hered* 98:188–193
- Kihara H (1944) Discovery of the DD–analyser, one of the ancestors of vulgare wheat. *Agric Hortic* 19:889–890
- Ling HQ, Ma B, Shi XL, Liu H, Dong LL, Sun H, Cao YH, Gao Q, Zheng SS, Li Y, Yu Y, Du HL, Qi M, Li Y, Lu HW, Yu H, Cui Y, Wang N, Chen CL, Wu HL, Zhao Y, Zhang JC, Li YW, Zhou WJ, Zhang BR, Hu WJ, Eijk MJT, Tang JF, Witsenboer HMA, Zhao SC, Li ZS, Zhang AM, Wang DW, Liang CZ (2018) Genome sequence of the progenitor of wheat A subgenome *Triticum urartu*. *Nature* 557:424–428
- Long Y, Chao WS, Ma G, Xu SS, Qi L (2017) An innovative SNP genotyping method adapting to multiple platforms and throughputs. *Theor Appl Genet* 130:597–607
- Luo MC, Gu YQ, Puiu D, Wang H, Twardziok SO, Deal KR, Huo N, Zhu T, Wang L, Wang Y, McGuire PE, Liu S, Long H, Ramasamy RK, Rodriguez JC, Van SL, Yuan L, Wang Z, Xia Z, Xiao L, Anderson OD, Ouyang S, Liang Y, Zimin AV, Perrea G, Qi P, Bennetzen JL, Dai X, Dawson MW, Müller H, Kugler K, Rivarola-Duarte L, Spannagl M, Mayer KFX, Lu FH, Becan MW, Lerou P, Li P, You FM, Sun Q, Liu Z, Lyons E, Wicher T, Zalzberg SL, Devos KM, Dvořák J (2017) Genome sequence of the progenitor of the wheat D genome *Aegilops tauschii*. *Nature* 551:498–502
- Marcussen T, Sandve SR, Heier L, Spannagl M, Pfeifer M, IWGSC, Jakobsen KS, Wulff BBH, Steuernagel B, Mayer KFX, Olsen OA (2014) Ancient hybridizations among the ancestral genomes of bread wheat. *Science* 345:1250092–1–4
- McFadden ES, Sears ER (1946) The origin of *Triticum speltoides* and its free–threshing hexaploid relatives. *J Hered* 37:107–116
- Oerke EC (2006) Crop losses to pests. *J Agric Sci* 144:31–43
- Peng JH, Sun D, Nevo E (2011) Domestication evolution, genetics and genomics in wheat. *Mol Breeding* 28:281–301

- Petersen G, Seberg O, Yde M, Berthelsen K (2006) Phylogenetic relationships of *Triticum* and *Aegilops* and evidence for the origin of the A, B, and D genomes of common wheat (*Triticum aestivum*). *Mol Phylogenet Evol* 39:70–82
- Pont C, Leroy T, Seidel M, Tondelli A, Duchemin W, Armisen D, Lang D, Bustos-Korts D, Goué N, Balfourier F, Molnar-Lang M, Lage J, Kilian B, Ozkan H, Waite D, Dyer S, Alaux M, Letellier T, Russell J, Keller B, Eeuwijk F, Spannagl M, Mayer K, Waugh R, Stein N, Cattivelli L, Haberer G, Charmet G, Salse J (2019) Tracing the Ancestry of Modern Bread Wheats. *Nature Genetics* accepted. *Nature Genetics* 51:905–911
- Qi LL, Friebe B, Zhang P, Gill BS (2007) Homoeologous recombination, chromosome engineering and crop improvement. *Chromosome Res* 15:3–19
- Riley R, Unrau J, Chapman V (1958a) Evidence on the origin of the B genome of wheat. *J Hered* 49:90–98
- Riley R, Chapman V (1958b) Genetic control of the cytologically diploid behaviour of hexaploid wheat. *Nature* 182:713–715
- Riley R, Chapman V, Kimber G (1959) Genetic control of chromosome pairing in intergeneric hybrids with wheat. *Nature* 185:1244–1246
- Schwarzacher T, Anamthawat-Jónsson K, Harrison GE, Islam AKMR, Jia JZ, King IP, Leitch AR, Miller TE, Reader SM, Rogers WJ, Shi M, Heslop-Harrison JS (1992) Genomic *in situ* hybridization to identify alien chromosomes and chromosome segments in wheat. *Theor Appl Genet* 84:365–375
- Sears ER (1977) An induced mutant with homoeologous pairing in common wheat. *Can J Genet Cytol* 19:585–593
- International Wheat Genome Sequencing Consortium (IWGSC) (2018) Shifting the limits in wheat research and breeding using a fully annotated reference genome. *Science* 361:6403
- Zhang M, Zhang W, Zhu X, Sun Q, Chao S, Yan C, Xu S, Fiedler J, Cai X. (2020) Partitioning and physical mapping of wheat chromosome 3B and its homoeologue 3E in *Thinopyrum elongatum* by inducing homoeologous recombination. *Theor Appl Genet* <https://doi.org/10.1007/s00122-020-03547-7>
- Zhang W, Cao Y, Zhang M, Zhu X, Ren S, Long Y, Gyawali Y, Chao S, Xu S, Cai X (2017) Meiotic homoeologous recombination-based alien gene introgression in the genomics era of wheat. *Crop Sci* 57:1189–1198
- Zhang W, Zhang M, Zhu X, Cao Y, Sun Q, Ma G, Chao S, Yan C, Xu S, Cai X (2018a) Molecular cytogenetic and genomic analyses reveal new insights into the origin of the wheat B genome. *Theor Appl Genet* 131:365–375

Zhang W, Zhu X, Zhang M, Chao S, Xu S, Cai X (2018b) Meiotic homoeologous recombination-based mapping of wheat chromosome 2B and its homoeologues in *Aegilops speltoides* and *Thinopyrum elongatum*. *Theor Appl Genet* 131:2381–2395

Zimin A, Puiu D, Hall R, Kingan S, Clavijo B, Salzberg S (2017) The first near-complete assembly of the hexaploid bread wheat genome, *Triticum aestivum*. *GigaScience* 6:1–7

CHAPTER 2. LITERATURE REVIEW

Wheat origin, evolution, and domestication

Taxonomy of wheat

Triticum L. genus belongs to Plantae kingdom, Monocots Clade, Poales Order, Poaceae Family, and Triticeae tribe. Wheat taxonomy had a long history, and the first classification of *Triticum* was estimated in 1753. There are two main wheat classifications, one is Mac Key's classification (Key, 1966, 1977, 2005) and another is Goncharov's classification (Goncharov, 2005). To simplify the understanding of wheat classification, *Triticum* species are classified into three sections based on ploidy: *Monococca* Flaksb. (*T. monococcum* and *T. urartu*), *Dicoccoidea* Flaksb. (*T. turgidum* and *T. timopheevii*), and *Triticum* (*T. aestivum* and *T. zhukovskyi*) (Table 2.1) (van Slageren, 1994; Goncharov, 2002; Goncharov et al., 2009).

Wheat is one of the essential crops for human consumption worldwide (Shewry, 2009). *T. aestivum* L. subsp. *aestivum* (common wheat, AABBDD, $2n = 6x = 42$) is the most widely grown species, producing 95% of wheat products, such as bread, noodles, cakes, and cookies. *T. turgidum* subsp. *durum* (durum wheat, AABB, $2n = 4x = 28$) is consumed as the other 5% of wheat products, such as pasta or other semolina products (Gill et al., 2004; Faris, 2014; Venske et al., 2019). *T. monococcum*, *T. urartu*, *T. timopheevii*, and *T. zhukovskyi* are not grown as major food sources for humans.

Aegilops is the closest related genus to *Triticum*, containing 11 diploids, 10 tetraploids, and 4 hexaploids. Most of them were found in Mediterranean climate areas (van Slageren, 1994; Schneider et al., 2008; Feldman and Levy, 2012). *Aegilops* genus has extremely diverse genomes including D, S, U, C, N, and M. Diploid *Ae. caudata* is the only species with the C genome and *Ae. tauschii* is the D genome donor of hexaploid wheat. *Ae. speltoides*, *Ae. bicornis*, *Ae.*

longissima, *Ae. searsii*, and *Ae. sharonensis* are all diploids of S genome. *Ae. comosa*, *Ae. uniaristata*, *Ae. mutica*, and *Ae. umbellulate* has genome M, N, T, and U, respectively. The genome of tetraploid or hexaploid wheat consists of two or more ancestral species under *Aegilops* (van Slageren, 1994; Zhang and Cai, 2019).

Table 2.1. The classification of *Triticum* genus

Section	Species ^a	Ploidy	Genome	
<i>Monococca</i> Flaksb.	<i>T. urartu</i> Tumanian ex Gandilyan	$2n = 2x = 14$	A ^u	
	<i>T. monococcum</i> L.			
	subsp. <i>aegilopoides</i> (Link) Thell.	$2n = 2x = 14$	A ^m	
	subsp. <i>monococcum</i>	$2n = 2x = 14$	A ^m	
<i>Dicoccoidea</i> Flaksb.	<i>T. turgidum</i>			
	subsp. <i>dicoccoides</i> (Körn.ex Asch. & Graebner) Thell.	$2n = 4x = 28$	BA ^u	
	subsp. <i>dicoccum</i> (Schrank ex Schübler) Thell.	$2n = 4x = 28$	BA ^u	
	subsp. <i>paleocolchicum</i> (Menabde) Á.Löve & D.Löve	$2n = 4x = 28$	BA ^u	
	subsp. <i>turgidum</i>	$2n = 4x = 28$	BA ^u	
	subsp. <i>durum</i> (Desf.) Husnot	$2n = 4x = 28$	BA ^u	
	subsp. <i>turanicum</i> (Jakubz.) Á.Löve & D.Löve	$2n = 4x = 28$	BA ^u	
	subsp. <i>polonicum</i> ((L.) Thell.	$2n = 4x = 28$	BA ^u	
	subsp. <i>carthlicum</i> (Nevski in Kom.) Á.Löve & D.Löve	$2n = 4x = 28$	BA ^u	
	<i>T. timopheevii</i> (Zhuk.) Zhuk.			
	subsp. <i>armeniicum</i> (Jakubz.) MacKey	$2n = 4x = 28$	GA ^{mu}	
	subsp. <i>timopheevii</i>	$2n = 4x = 28$	GA ^{mu}	
	<i>Triticum</i>	<i>T. aestivum</i> L.		
		subsp. <i>aestivum</i>	$2n = 6x = 42$	BA ^u D
subsp. <i>spelta</i> (L.) Thell.		$2n = 6x = 42$	BA ^u D	
subsp. <i>compactum</i> (Host) MacKey		$2n = 6x = 42$	BA ^u D	
subsp. <i>macha</i> (Dekapr. & Menabde) MacKey		$2n = 6x = 42$	BA ^u D	
subsp. <i>sphaerococcum</i> (Percival) MacKey		$2n = 6x = 42$	BA ^u D	
<i>T. zhukovski</i> Menabde & Ericzjan		$2n = 6x = 42$	GA ^u A ^m	

^aSpecies designation according to van Slageren (1994)

Origin and evolutionary of polyploid wheat

Wheat has a long and obscure evolutionary history. Taxa *Triticum* and *Aegilops* were given rise from a primary 7-chromosome common ancestor about 3 million years ago (MYA). *Aegilops* evolved and gave rise to D-genome and S-genome progenitor around 2.6 MYA (Dvorak et al., 1993; Dvorak and Akhunov, 2005; Faris, 2014; Middleton et al., 2014). The genus *Triticum* originated in Fertile Crescent of the Middle East, and two A-genome wild diploids were developed under this genus, *T. urartu* (A^uA^u , $2n = 2x = 14$) and *T. monococcum* (A^mA^m , $2n = 2x = 14$) (Faris, 2014). *Aegilops tauschii* (DD, $2n = 2x = 14$) and *Aegilops* Sitopsis section originated from a common ancestor and contain D and S genome, respectively. (Blake et al., 1999; Huang et al., 2002; Salamini et al., 2002; Chalupska et al., 2008; Salse et al., 2008; Feldman and Levy, 2009; Faris, 2014; Marcussen et al., 2014; El Baidouri et al., 2017; Pont et al., 2019; Venske et al., 2019). Diploid *T. urartu* is the A genome ancestor and *Ae. tauschii* is the D genome ancestor of wheat. Wheat B genome ancestor remains obscure and it might originate from multiple ancestors (Zhang et al., 2018a). *Aegilops speltoides*-related lineages are considered as the B genome donor.

Wheat originated from two times of hybridization and spontaneous chromosome doubling (Dvorak et al., 1993; Cai and Xu, 2007; Faris, 2014). The first hybridization occurred between *T. urartu* and *Ae. speltoides*-related lineages around 0.5 MYA. The wild tetraploid wheat (*T. turgidum* subsp. *dicoccoides*, AABB, $2n = 4x = 28$) had been developed in this polyploidization process. Hexaploid wheat (AABBDD, $2n = 6x = 42$) arose from the second hybridization between domesticated tetraploid wheat (*T. turgidum* subsp. *dicuccum*, AABB, $2n = 4x = 28$) and diploid *Ae. tauschii* about 8,000 years ago (Faris, 2014; Pont et al., 2019).

With the advances in genome sequencing technologies and sequence analysis tools, the genomes of common wheat, emmer wheat, and diploid ancestors have been sequenced and assembled [Choulet et al., 2014; Avni et al., 2017; Luo et al., 2017; International Wheat Genome Sequencing Consortium (IWGSC), 2018; Ling et al., 2018]. The genome sequence data led to the analysis of wheat classification and the ancient hybridization events at the genome level, and a new wheat evolutionary perspective has been proposed. Marcussen et al. (2014) annotated that wheat D genome originated from A and B genomes homoploid hybridization 5~6 million years ago by analyzing the genome-wide gene trees among common wheat and five diploid relatives. Glémin et al. (2019) gave a comprehensive transcriptome data analysis of all diploid species and proposed that more than half of the diploid species originated from an ancient hybridization. They confirmed that wheat D genome evolved from hybridization between the A and B genome ancestors.

Domestication of wheat

The only domesticated diploid wheat is einkorn (*T. monococcum* L. subsp. *monococcum*, $2n = 2x = 14$, A^mA^m) for acquisition of non-brittle rachis 10,000 years before the present (Heun et al., 1997). Meanwhile, tetraploid progenitor, *T. turgidum* ssp. *dicoccoides*, had been selected for non-brittle rachis (Salamini et al., 2002; Luo et al., 2007; Dvorak et al., 2011; Faris, 2014). The domesticated tetraploid wheat *T. turgidum* subsp. *dicoccum* ($2n = 2x = 28$, AABB) was developed in the southern Levant and southeastern Turkey 9,000-9,500 years ago (Faris, 2014). Then, the free-threshing tetraploid wheat appeared 8,000-9,000 years ago in the Prepottery Neolithic, which was known as *T. turgidum* ssp. *parvicoccum*. Hexaploid wheat originated from domesticated *T. dicoccum* and *Ae. tauschii* with non-brittle rachis and free-threshing spike traits about 8,000 years ago. Therefore, there was no wild hexaploid wheat in nature (Nesbitt, 2001;

Brown et al., 2009; Shewry, 2009; Dvorak et al., 2011, Peng et al., 2011; Faris, 2014; Avni et al., 2017; Pont et al., 2019; Venske et al., 2019).

Wheat had been spread and domesticated for the environment and agronomic adaptation by taking reproductive control and modification. The first and the most crucial trait modification was the acquisition of non-brittle rachis, allowing farmers to harvest the mature grain efficiently without spikelet premature dropping off. Meanwhile, some other traits were modified for human purposes, such as free-threshing spikes, loss of seed dormancy, larger seed, and high quality (Harlan et al., 1973; Faris, 2014). Many plants were domesticated sharing a set of traits, such as flowering time, plant height, grain yield, spike or kernel numbers, and growth habits. This scenario was known as domestication syndrome (Campbell et al., 2003; Peng et al., 2003; Meyer and Purugganan, 2013). More domestication genes remain to be discovered and utilized by computational analysis of the nucleotide diversity in wild diploid, tetraploid, and domesticated hexaploid wheat (Pont et al., 2019).

Wheat genome and chromosomes

Wheat genome

Wheat has a large, complex, and flexible genome. The estimated size of the wheat genome is 17 GB with 80% of repetitive transposable elements (TEs) (Eilam et al., 2007; Wicker et al., 2011; Zimin et al., 2017b; IWGSC, 2018). The wheat whole genome survey sequence was announced through isolating, sequencing, and the *de novo* assembly of each individual chromosome arm of the hexaploid wheat cultivar Chinese Spring (CS) (IWGSC, 2014). With an improved sequencing techniques and advanced assembly algorithms, wheat ancestors, *T. urartu* and *Ae. tauschii*, wild tetraploid, durum wheat, hexaploid, and other wheat relatives are

sequenced and available for wheat genome studies (Avni et al., 2017; IWGSC, 2018; Luo et al., 2017; Ling et al., 2018; Maccaferri et al., 2019; <https://wheat-urgi.versailles.inra.fr>).

The genome sequences of *Ae. tauschii* was assembled in the size of 4.48 Gb, and over 43,000 protein-coding genes has been predicted (Jia et al., 2013; Luo et al., 2013; Zimin et al., 2017a). Zimin et al. (2017b) reported that wheat D subgenome sequences were similar with *Ae. tauschii*, The difference of genome size between wheat D subgenome and *Ae. tauschii* appeared due to gene loss or gain during evolution (Brenchley et al., 2012; IWGSC, 2014). The A subgemone ancestor, *T. urartu*, was sequenced and assembled in the length of 4.86 Gb, closely to the estimated genome size (4.94 Gb). Over 40,000 protein-coding genes has been predicted for *T. urartu* (Ling et al., 2018). The genome sequences of wild tetraploid wheat (*T. turgidum* subsp. *dicoccoides*) and durum wheat cultivar Svevo were assembled in 10.10 Gb and 10.45 Gb, respectively (Avni et al., 2017; Maccaferri et al., 2019). IWGSC annotated hexaploid wheat [*T. aestivum* cv. Chinese Spring (CS)] reference sequence with 94% of the estimated genome coverage and over 100,000 high-confidence gene models. The assembled genome sequence for A, B, D subgenomes is 4.94 Gb, 5.18 Gb, and 3.95 Gb, respectively, with an average of 84.7% TEs. Wheat B subgenome had a higher number of gene loci and larger chromosomes assembled sequence size than A and D subgenomes (IWGSC, 2018). The genome assembly of CS was improved from whole genome shotgun PacBio SMRT (Single-molecule real-time) sequencing reads, and IWGSC RefSeq v2.0 assembly is available online (<https://wheat-urgi.versailles.inra.fr/Seq-Repository/Assemblies>). The genome resources of hexaploid, tetraploid, and its relatives are available to explore the wheat evolutionary history by comparative analysis and are used as genetic sources for wheat breeding improvement.

Wheat chromosomes

The diploids ($2n = 2x = 14$), tetraploids ($2n = 4x = 28$), and hexaploids ($2n = 6x = 42$) comprise a polyploid series based on $x = 7$. A complete wheat chromosome contains a short arm, long arm, centromere, and telomere. Some chromosomes have a satellite as well, such as wheat chromosomes 1B and 6B. The chromosome structure can be visualized clearly by an optical microscope during metaphase of mitosis and meiosis. The differences of chromosomes length can be distinguished at metaphase. The standardized B subgenome chromosome length is longer than A and D subgenomes, and D subgenome is the shortest (Dvorak et al., 1984).

Wheat chromosomes can be visualized and identified by chromosome landmarks by chemical treatment and subsequent chromosomes staining. There are several cytological techniques are used to generate specific chromosome transverse bands, i.e. chromosome banding, fluorescent *in situ* hybridization (FISH), genomic *in situ* hybridization (GISH), and CRISPR/Cas9-mediated fluorescent *in situ* hybridization (CASFISH) (Gill and Kimber, 1974; Gerlach, 1977; Schwarzacher et al., 1992; Jiang and Gill, 1993; Beliveau et al., 2012; Deng et al., 2015). Acetocarmine/N-banding and acetocarmine–Giemsa C-banding techniques are used to identify wheat chromosomes based on wheat chromosome heterochromatin distribution. N-banding differentiates 16 chromosomes of common wheat, and C-banding can distinguish all 21 wheat chromosomes from each other (Gill and Kimber, 1974; Endo and Gill, 1984a, 1984b; Endo, 1986). Moreover, wheat chromosomes can be visualized and differentiated by GISH and FISH using specific genomicDNA probes. FISH-painted wheat chromosomes exhibit different stains using repetitive DNAs, *pSC119.2* and *pASI*, labeled with multiple fluorochromes for wheat chromosome identification (Danilova et al., 2012; Zhang et al., 2017).

Chromosome engineering-based gene introgression in wheat

Wheat gene pools

The tribe Triticeae, containing more than 500 species, has been divided into three different gene pools based on the evolutionary distance and cross ability: primary gene pool, secondary gene pool, and tertiary gene pool (Jiang et al., 1994; Cai et al., 2005; Naranjo, 2019). Hexaploid wheat *T. aestivum* (AABBDD), tetraploid wheat *T. turgidum* (AABB), diploid wheat *Ae. tauschii* (DD) belong to the primary gene pool. Wheat ancestors and other closely related species consist of the secondary gene pool, such as the A genome carrier *T. monococcum* and *T. urartu*, B genome-related species *Ae. speltoides* ($2n = 2x = 14$, SS), the D genome cluster of other *Aegilops* species, and tetraploid wheat *T. timopheevii* ($2n = 4x = 28$, AAGG). The other Triticeae species carrying other than A, B, and D genomes constitute the tertiary gene pool, such as *Thinopyrum elongatum* ($2n = 2x = 14$, EE), *Secale cereale* ($2n = 2x = 14$, RR), and *Th. intermedium* ($2n = 6x = 42$, JJJ^{VS}J^{VS}StSt) (Qi et al., 2007).

Intraspecific or intragenomic chromosome recombination can occur between wheat species in the primary gene pool (Cox, 1991; Dvorak et al., 1993; Huang et al., 2002). Gene introgression from secondary gene pool into the primary has been accomplished through directly crossing and backcrossing to induce homologous or homoeologous recombination (Friebe et al., 1996; Qi et al., 1997; Zhang et al., 2015). It is generally difficult to achieve gene introgression from the tertiary gene pool into the wheat genome because of the low homology of their genomes. Specific physical or chemical treatment or gene-controlled homoeologous chromosome pairing and recombination can induce chromosome breakage and rearrangement, achieving gene introgression from the tertiary gene pool into the primary gene pool (Qi et al., 2007; Niu et al., 2011; Zhao et al., 2013; Zhang et al., 2017).

Chromosome engineering in wheat

Global wheat yield has increased by less than 1% in recent years, while the demand for wheat production is expected to increase 60% by 2050. Therefore, the global wheat yield must increase by ~1.6% annually to meet the global demand. The biotic threat causing 20% of wheat yield losses each year, is the substantial barriers for wheat yield improvement (Oerke, 2006). Wheat breeders strive to develop wheat cultivars with resistance to a broad range of biotic stresses [International Wheat Genome Sequencing Consortium (IWGSC), 2018]. A large number of resistance/tolerance genes in diploid and tetraploid ancestors are evolutionarily omitted in modern wheat. Utilization of the genomics-enabled chromosome engineering and genetic techniques can enhance alien introgression for wheat germplasm and variety development.

Chromosome engineering is a technology of manipulating chromosome number, ploidy, or structure of an organism for genetic improvement. It has been used for alien introgression from wheat relatives into the wheat genome for genetic enrichment and germplasm development by chromosome addition, substitution, or translocation. Alien chromosome addition and substitution incorporate one or more chromosomes into wheat. However, alien chromosomes from wheat relatives contain favorable as well as deleterious genes. Thus, the addition and substitution lines are used as the bridge materials to develop translocation lines. Chromosome translocations can involve distinct alien chromosome segments and minimize the linkage drag. Incorporation of small alien chromosomal segment with target genes from wheat relatives into wheat is the expectation of alien introgression and invaluable for germplasm development. Wheat-alien chromosome translocation can be induced by ionizing irradiation, gametocidal chromosomes, and homoeologous chromosome recombination (Sears, 1972; Endo, 1988; Chen et al., 1994; Bie et al., 2007; Chen et al., 2008).

Sears (1956) used X-ray irradiation to directly transfer a leaf rust resistance gene from wheat wild species into the wheat genome. This was the first case to achieve wheat chromosome engineering by irradiation. Ionizing irradiation causes random chromosome breakage and fusion to incorporate alien chromosome segment into the wheat genome. However, random chromosome segment rejoining can lead to genetic instability and sterility (Sears, 1972; Jiang et al., 1994). Gametocidal (*Gc*) genes induce chromosome breakages and subsequently chromosome rearrangement between wheat and alien chromosomes. *Gc* genes, also called selfish genes, have been identified on several wild species, such as *Ae. caudata* ($2n = 2x = 14$, CC) chromosome 3C, *Ae. triuncialis* ($2n = 2x = 14$, CC) chromosome 3C, *Ae. cylindrica* ($2n = 2x = 14$, CC) chromosome 2C, *Ae. speltoides* chromosomes 2S and 6S (Endo and Tsunewaki, 1975; Endo and Katayama, 1978; Tsujimoto and Tsunewaki, 1984, 1988; Endo, 1988; Zhang et al., 2019). *Gc* system induces random chromosome breakage and fusion resulting in a non-reciprocal recombination. Homoeologous chromosome recombination results in reciprocal translocations - an alien chromosome segment replaces a corresponding homoeologous chromosome segment of wheat. Reciprocal translocations with targeted small alien segment are genetically-friendly for wheat breeding (Sears, 1972; Qi et al., 2007, 2008; Niu et al., 2011).

Gene introgression in wheat and its relatives

Wheat has a narrow genetic variation due to the polyploid origin of the wheat genome. This has become a genetic bottleneck for wheat improvement (Haudry et al., 2007; Akunov et al., 2010; Feldman and Levy, 2012; Marcussen et al., 2014). “Polyploid diversity bottleneck” was first referred by Stebbins (1950) through the characterization of the formed allopolyploids by the limited genetic variation. The genetic diversification in polyploid wheat is much less than their diploid ancestors. The gene loss in D subgenome is more severe than A and B subgenomes

(Akhunov et al., 2010; He et al., 2019). Moreover, the allopolyploid had been isolated for reproduction immediately after it was formed. There was limited time for mutation accumulation during human selection and domestication (Feldman and Levy, 2012).

Gene introgression refers to the incorporation of genes from one species into the gene pool of another (gene flow) through repeated interspecific hybridization. Gene flow from wheat secondary and tertiary gene pools can expand wheat genetic diversity, improve wheat agronomic traits, and enhance wheat adaptation and quality (Qi et al., 2007). A large number of disease resistance genes from wheat relatives have been incorporated into wheat, and some of them have been cloned for further utilization, such as powdery mildew resistance gene *Pm21* from *Haynaldia villosa* ($2n = 2x = 14$, VV), yellow rust resistance gene *Yr15* from wild emmer wheat (Cao et al., 2011; Klymiuk et al., 2018; Xing et al., 2018).

By re-sequencing of 890 diverse accessions of hexaploid and tetraploid wheat, He et al. (2019) found a substantial level of gene flow from wild tetraploid relatives into wheat. Gene flow events mainly involved wheat chromosomes 1A, 4A, 4B, 5A, and 6A around the domestication-related genes (Simon et al., 2006; Nave et al., 2016; Avni et al., 2017; He et al., 2019). Wheat genome contains deleterious SNPs (dSNP) playing a negative effect on wheat agronomics. Wheat gene flow, environment adaptation, and breeding selection can reduce the dSNP burden and enhance the agronomic performance of modern wheat (He et al., 2019).

Meiotic homoeologous recombination-based alien introgression

Recombination between wheat chromosomes and its homoeologous counterparts in wild relatives results in alien gene introgression and enriches the gene pools of wheat breeding (Chen et al., 2012; Molnar-Lang et al., 2014; Winfield et al., 2016). However, incorporation of the alien chromosome segment with linkage drag would never be applied in wheat breeding because of the

reduced fitness or fertility caused by the deleterious genes (Nasuda et al., 1998; Qi et al., 2007). Repeated backcrossing and hybridization can shorten the alien introgression segments of interest and to minimize the linkage drag (Qi et al., 2007; Klindworth et al., 2013; Wulff and Moscou, 2014). The introgression line containing targeted genes with the minimum alien segment is preferred in the wheat breeding perspective (Ceoloni et al., 2017).

Homoeologous chromosome pairing and recombination frequency is low because of the existence of the *Ph* (homoeologous pairing) gene in wheat. *Ph* gene acts as a homoeologous pairing suppressor to maintain a diploid-like meiotic pairing in polyploid wheat. When removing the *Ph* gene, such as nullisomic of *Ph1* or *ph1b* mutant, homoeologous chromosomes can pair and recombine with each other, allowing for alien gene introgression (Sears, 1976, 1977). Hexaploid wheat [Chinese Spring (CS)] *ph1b* mutant was produced with a 70 Mb segment deletion at the *Ph1* locus on chromosome 5B by irradiation treatment (Sears, 1977; Dunford et al., 1995; Roberts et al., 1999). The CS *ph1b* mutant has been widely used in wheat homoeologous recombination research projects to incorporate favorable genes from wheat relatives (Friebe et al., 1996; Faris et al., 2008; Niu et al., 2011; Klindworth et al., 2012; Zhao et al., 2013; Zhang et al. 2018). The *ph1b* mutant-induced meiotic homoeologous recombination produces reciprocal wheat-alien chromosome translocations, which are genetically-friendly germplasm for variety development in wheat breeding (Ceoloni et al., 1996; Qi et al. 2007; Niu et al., 2014; Ceoloni et al., 2017; Danilova et al., 2017, Liu et al., 2017).

Fluorescence *in situ* hybridization (FISH) and genomic *in situ* hybridization (GISH) has been widely used to differentiate wheat and alien chromosomes (segments) directly. These technologies were developed around 40-year ago with various methodologies and modifications for DNA and RNA sequences detection (Levsky and Singer, 2003). Fluorescence-labeled

genomic DNAs of alien species or the specific repetitive DNA are used as probes for alien chromosome detection. Advances in the availability of genome sequences, sequence-specific genomic loci can be labeled with multicolor fluorescence to improve the visualization of the targeted genome regions (Beliveau et al., 2012; Deng et al., 2015).

The high-throughput genotyping platforms have been developed and applied for allelic polymorphism characterization, such as single nucleotide polymorphism (SNP). The wheat 9K and 90K Illumina iSelect® SNP arrays and Axiom® 35K and 820K SNP arrays can identify SNP polymorphisms among tetraploid and hexaploid accessions, and wheat wild relatives (Cavanagh et al., 2013; Wang et al., 2014; Winfield et al., 2016). The SNP-derived molecular markers, such as Kompetitive Allele Specific PCR (KASP) and Semi-Thermal Asymmetric Reverse PCR (STARP), have been used in wheat-alien recombinant detection and targeted genotype isolation (Semagn et al., 2014; Danilova et al., 2017; Klindworth et al., 2017; Long et al., 2017; Tan et al., 2017; Zhang et al., 2017; Zhang et al., 2018b). The integrative molecule marker and FISH/GISH analysis can detect wheat-alien recombinants for alien introgression and genome studies in a significantly improved efficacy and throughput.

References

- Akhunov E, Akhunova A, Anderson O, Anderson J, Blake N, Clegg M, Coleman-Derr D, Conley E, Crossman C, Deal K, Dubcovsky J, Gill B, Gu Y, Hadam J, Heo H, Huo N, Lazo G, Luo M, Ma Y, Matthews D, McGuire P, Morrell P, Qualset C, Renfro J, Tabanao D, Talbert L, Tian C, Toleno D, Warburton M, You F, Zhang W, Dvorak J (2010) Nucleotide diversity maps reveal variation in diversity among wheat genomes and chromosomes. *BMC Genomics* 11:702
- Avni R, Nave M, Barad O, Baruch K, Twardziok S, Gundlach H, Hale I, Mascher M, Spannagl M, Wiebe K, Jordan K, Golan G, Deek J, Ben-Zvi B, Ben-Zvi G, Himmelback A, MacLachlan R, Sharpe A, Fritz A, Ben-David R, Budak H, Fahima T, Korol A, Faris J, Hermamdes A, Mikel M, Levy A, Steffenson B, Maccaferri M, Tuberosa R, Vattavelli L, Faccioli P, Ceriotti A, Kashkush K, Pourkheirandish M, Komatsuda T, Eilam T, Sela H, Sharon A, Ohad N, Chamovitz D, Mayer K, Stein N, Ronen G, Peleg Z, Pozniak C, Akhunov E, Distelfeld A (2017) Wild emmer genome architecture and diversity elucidate wheat evolution and domestication. *Science* 357:93–97

- Beliveau BJ, Joyce EF, Apostolopoulos N, Yilmaz F, Fonseka CY, McCole RB, Chang Y, Li JB, Semaratne TN, Williams BR, Rouillard J, Wu C (2012) Versatile design and synthesis platform for visualizing genomes with Oligopaint FISH probes. *Proc Nat Acad Sci USA* 109:21301–21306
- Bie TD, Cao YP, Chen PD (2007) Mass production of intergeneric chromosomal translocations through pollen irradiation of *Triticum durum-Haynaldia villosa* amphiploid. *J Integr Plant Biol* 49:1619–1626
- Blake NK, Leffert BR, Lavin M, Talbert LE (1999) Phylogenetic reconstruction based on low copy DNA sequence data in an allopolyploid: The B genome of wheat. *Genome* 42:351–360
- Brenchley R, Spannag M, Pfeifer M, Barker G, D'Amore R, Allen A, McKenzie N, Kramer M, Kerhornou A, Bolser D, Kay S, Waite D, Trick M, Bancroft I, Gu Y, Huo N, Luo M–C, Sehgal S, Gill B, Kianian S, Anderson O, Kersey P, Dvorak J, McCombie W, Hall A, Mayer K, Edwards K, Bevan W, Hall N (2013) Analysis of the bread wheat genome using whole-genome shotgun sequencing. *Nature* 491:705–710
- Brown TA, Jones MK, Powell W, Allaby RG (2009) The complex origins of domesticated crops in the Fertile Crescent. *Trends in Ecology & Evolution* 24:103–109
- Cai X, Chen PD, Xu SS, Oliver RE, Chen X (2005) Utilization of alien genes to enhance Fusarium head blight resistance in wheat—a review. *Euphytica* 142:309–318
- Cai X, Xu SS (2007) Meiosis-driven genome variation in plants. *Curr Genomics* 8:151–161.
- Cao A, Xing L, Wang X, Yang X, Zhang W, Sun Y, Qian C, Ni J, Chen Y, Liu D, Wang X, Chen P (2011) Serine/threonine kinase gene *Stpk-V*, a key member of powdery mildew resistance gene *Pm21*, confers powdery mildew resistance in wheat. *Proc Nat Acad Sci USA* 108: 7727–7732
- Campbell B, Baenziger PS, Gill KS, Eskridge KM, Budak H, Erayman M, Dweikat I, Yen Y (2003) Identification of QTLs and environmental interactions associated with agronomic traits on chromosome 3A of wheat. *Crop Sci* 43:1493–1505
- Cavanagh CR, Chao S, Wang S, Huang BE, Stephen S, Kiani S, Forrest K, Saintenac C, Brown-Guedira GL, Akhunova A, See D, Bai G, Pumphrey M, Tomar L, Wong D, Kong S, Reynolds M, da Silva ML, Bockelman H, Talbert L, Anderson JA, Dreisigacker S, Baenziger S, Carter A, Korzun V, Morrell PL, Dubcovsky J, Morell MK, Sorrells ME, Hayden MJ, Akhunov E (2013) Genome-wide comparative diversity uncovers multiple targets of selection for improvement in hexaploid wheat landraces and cultivars. *Proc Natl Acad Sci USA* 110:8057–8062
- Ceoloni C, Biagetti M, Ciaffi M, Forte P, Pasquini M (1996) Wheat chromosome engineering at the 4x level: The potential of different alien gene transfers into durum wheat. *Euphytica* 89:87–97

- Ceoloni C, Kuzmanovic L, Ruggeri R, Rossini F, Forte P, Cuccurullo A, Bitti A (2017) Harnessing genetic diversity of wild gene pools to enhance wheat crop production and sustainability: challenges and opportunities. *Diversity* 9:55
- Chalupska D, LeeHY, Faris JD et al (2008) Acc homoeoloci and the evolution of the wheat genomes. *Proc Natl Acad Sci USA* 105:9691–9696
- Chen PD, Tsujimoto H, Gill BS (1994) Transfer of *Phl* genes promoting homoeologous pairing from *Triticum speltoides* to common wheat. *Theor Appl Genet* 88:97–101
- Chen G, Zheng Q, Liu S, Wang H, Li X (2012) Molecular cytogenetic identification of a novel dwarf wheat line with introgressed *Thinopyrum ponticum* chromatin. *J. Biosci.* 37:149–155
- Chen S, Chen P, Wang X (2008) Inducement of chromosome translocation with small alien segments by irradiating mature female gametes of the whole arm translocation line. *Sci China C Life Sci* 51:346–352
- Choulet F, Alberti A, Theil S, Glover N, Barbe V, Daron J, Pingault L, Sourdille P, Couloux A, Paux E, Leroy P, Mangenot S, Guilhot N, Gouis J, Balfourier F, Alaux M, Jamilloux V, Poulain J, Durand C, Bellec A, Gaspin C, Safar J, Dolezel J, Rogers J, Vandepoele K, Aury J, Mayer K, Berges H, Quesneville H, Wincker P, Feuillet C (2014) Structural and functional partitioning of bread wheat chromosome 3B. *Science* 345:1249721.
- Cox TS (1998) Deepening the wheat gene pool. *J Crop Prod Recent Advances* 1:1–25
- Danilova TV, Friebe B, Gill BS (2012) Single-copy gene fluorescence *in situ* hybridization and genome analysis: Acc-2 loci mark evolutionary chromosomal rearrangements in wheat. *Chromosoma* 121:597–611
- Danilova TV, Zhang G, Liu W, Friebe B, Gill BS (2017) Homoeologous recombination-based transfer and molecular cytogenetic mapping of a wheat streak mosaic virus and *Triticum* mosaic virus resistance gene *Wsm3* from *Thinopyrum intermedium*. *Theor Appl Genet* 130:549–555
- Deng W, Shi X, Tjian R, Lionnet T, Singer R (2015) CASFISH: CRISPR/Cas9-mediated *in situ* labeling of genomic loci in fixed cells. *Proc Nat Acad Sci USA* 112:11870–11875
- Dvorak J, McGuire PE, Mendlinger S (1984) Inferred chromosome morphology of the ancestral genome of *Triticum*. *Pl Syst Evol* 144:209–220
- Dvorak J, Terlizzi P, Zhang HB, Resta P (1993) The evolution of polyploidy wheats: Identification of the A genome donor species. *Genome* 36:21–31
- Dvorak J, Akhunov ED (2005) Tempos of gene locus deletions and duplications and their relationship to recombination rate during diploid and polyploid evolution in the *Aegilops-Triticum* alliance. *Genetics* 171:323–332

- Dvorak J, Luo MC, Akhunov ED (2011) N.I. Vavilov's theory of centers of diversity in light of current understanding of wheat diversity, domestication and evolution. *Czech J Genet Plant Breed* 24:20–27
- Eilam T, Anikster Y, Millet E, Manisterski J, Sagi-Assif O, Feldman M (2007) Genome size and genome evolution in diploid Triticeae species. *Genome* 50:1029–1037
- El Baidouri M, Murat F, Veysiere M, Molinier M, Flores R, Burlot L, Alaux M, Quesneville H, Pont C, Salse J (2017) Reconciling the evolutionary origin of bread wheat (*Triticum aestivum*). *New Phytol* 213:1477–1486
- Endo TR, Tsunewaki K (1975) Sterility of common wheat with *Aegilops triuncialis* cytoplasm. *J Hered* 66:13–18
- Endo TR, Katayama Y (1978) Finding of a selectively retained chromosome of *Aegilops caudata* L. in common wheat. *Wheat Inf Serv* 47:32–35
- Endo TR, GILL BS (1984a) Somatic karyotype, heterochromatin distribution, and nature of chromosome differentiation in common wheat, *Triticum aestivum* L. em Thell. *Chromosoma* 89:361–369
- Endo TR, GILL BS (1984b) The heterochromatin distribution and genome evolution in diploid species of *Elymus* and *Agropyron*. *Can J Genet Cytol* 26:669–678
- Endo TR (1986) Complete identification of common wheat chromosomes by means of the C-banding techniques. *Jpn J Genet* 61:89–93
- Endo TR (1988) Induction of chromosomal structural changes by a chromosome of *Aegilops cylindrica* L. in common wheat. *J Hered* 79:366–370
- Faris JD, Xu SS, Cai X, Friesen TL, Jin Y (2008) Molecular and cytogenetic characterization of a durum wheat–*Aegilops speltoides* chromosome translocation conferring resistance to stem rust. *Chromosom Res* 16:1097–1105
- Faris JD (2014) Wheat Domestication: Key to Agricultural Revolutions Past and Future. In: Tuberosa R, Graner A, Frison E (eds) *Genomics of plant genetic resources. Vol 1. Managing, sequencing and mining genetic resources*. Springer, Metherlands, pp439–464
- Feldman M, Levy AA (2012) Genome evolution due to allopolyploidization in wheat. *Genetics* 192: 763–774
- Friebe B, Jiang J, Raupp WJ, McIntosh RA, Gill BS (1996) Characterization of wheat-alien translocations conferring resistance to diseases and pests: current status. *Euphytica* 91:59–87
- Gerlach WL (1977) N-banded karyotypes of wheat species. *Chromosoma* 62:49–56
- Gill B, Kimber G (1974) Giemsa C-banding and the evolution of wheat. *Proc Nat Acad Sci USA* 71:4086-4090

Gill BS, Appels R, Botha–Oberholster AM, Buell CR, Bennetzen JL, Chalhoub B, Chumley F, Dvořák J, Iwanaga M, Keller B, Li W, McCombie WR, Ogihara Y, Quetier F, Sasaki T (2004) A workshop report on wheat genome sequencing: international genome research on wheat consortium. *Genetics* 168:1087–1096

Glémin S, Scornavacca C, Dainat J, Burgarella C, Viader V, Ardisson M, Sarah G, Santoni S, David J, Ranwez V (2019) Pervasive hybridizations in the history of wheat relatives. *Science Advances* 5:eaav9188

Goncharov NP (2002) Comparative genetics of wheats and their related species. Siberian Branch Press, Novosibirs, p 149

Goncharov NP (2005) Comparative-genetic analysis—a base for wheat taxonomy revision. *Czech J. Genet. Plant Breed* 41:52–55

Goncharov NP, Golovnina KA, Kondratenko EY (2009) Taxonomy and molecular phylogeny of natural and artificial wheat species. *Breeding Science* 59:492–498

Harlan JR, Wet MJ de, Price EG (1973) Comparative evolution of cereals. *Evolution* 27:3110–325

Haudry A, Cenci A, Ravel C, Bataillon T, Brunel D, Poncet C, Hochu I, Poirier S, Santoni S, Glémin S, David J (2007) Grinding up wheat: a massive loss of nucleotide diversity since domestication. *Mol Biol Evol* 24:1506–1517

He F, Pasam R, Shi F, Kant S, Keeble-Gagnere G, Kay P, Forrest K, Fritz A, Hucl P, Wiebe K, Knox R, Cuthbert R, Pozniak C, Akhunova A, Morrell P, Davies J, Webb S, Spangenberg G, Hayes B, Daetwyler H, Tibbits J, Hayden M, Akhunov E (2019) Exome sequencing highlights the role of wild-relative introgression in shaping the adaptive landscape of the wheat genome. *Nature Genetics* 51:894–904

Heun M, Schaefer-Pregl R, Klawan D et al (1997) Site of einkorn wheat domestication identified by DNA fingerprinting. *Science* 278:1312–1314

Huang S, Sirikhachornkit A, Su X, Faris J, Gill B, Haselkorn R, Gornicki P (2002) Genes encoding plastid acetyl-CoA carboxylase and 3-phosphoglycerate kinase of the *Triticum/Aegilops* complex and the evolutionary history of polyploid wheat. *Proc Natl Acad Sci USA* 99: 8133–8138.

International Wheat Genome Sequencing Consortium (2014) A chromosome-based draft sequence of the hexaploid bread wheat (*Triticum aestivum*) genome. *Science* 345:1251788

International Wheat Genome Sequencing Consortium (2018) Shifting the limits in wheat research and breeding using a fully annotated reference genome. *Science* 361:eaar7191

Jia J, Zhao S, Kong X, Li Y, Zhao G, He W, Appels R, Pfeifer M, Tao Y, Zhang X, Jing R, Zhang C, Ma Y, Gao L, Gao C, Spannagl M, Mayer K, Li D, Pan S, Zheng F, Hu Q, Xia X, Li J, Liang Q, Chen J, Wicher T, Gou C, Kuang H, He G, Luo Y, Keller B, Xia Q, Lu P, Wang J, Zou

- H, Zhang R, Xu J, Gao J, Middleton C, Quan Z, Liu G, Wang J, International Wheat Genome Sequencing Consortium, Yang H, Liu X, He Z, Mao L, Wang J (2012) *Aegilops tauschii* draft genome sequence reveals a gene repertoire for wheat adaptation. *Nature* 496:91–95
- Jiang J, Gill BS (1993) Sequential chromosome banding and in situ hybridization analysis. *Genome* 36:792–795
- Jiang J, Friebe B, Gill BS (1994) Recent advances in alien gene transfer in wheat. *Euphytica*. 73:199–212
- Klindworth DL, Niu ZX, Chao SM, Friesen TL, Jin Y, Faris JD, Cai XW, Xu SS (2012) Introgression and characterization of a goatgrass gene for a high level of resistance to Ug99 stem rust in tetraploid wheat. *G3* 2:665–673
- Klindworth DL, Hareland GA, Elias EM, Xu SS (2013) Attempted compensation for linkage drag affecting agronomic characteristics of durum wheat 1AS/1DL translocation lines. *Crop Sci* 53:422–429
- Klindworth DL, Saini J, Long Y, Rouse MN, Faris JD, Jin Y, Xu SS (2017) Physical mapping of DNA markers linked to stem rust resistance gene *Sr47* in durum wheat. *Theor Appl Genet* 130:1135–1154
- Klymiuk V, Yaniv E, Huang L, Raats D, Fatiukha A, Chen S, Feng L, Frenkel Z, Krugman T, Lidzbarsky G, Chang W, Jääskeläinen M, Schudoma C, Paulin L, Laine P, Bariana H, Sela H, Saleem K, Sørensen C, Hovmøller M, Distelfeld A, Chalhoub B, Dubcovsky J, Korol A, Schulman A, Fahima T (2018) Cloning of the wheat *Yr15* resistance gene sheds light on the plant tandem kinase-pseudokinase family. *Nature Communications* 9:3735
- Levsky JM, Singer RH (2003) Fluorescence in situ hybridization: Past, present and future. *J Cell Sci* 116:2833–2838
- Li G, Chen P, Zhang S, Wang X, He Z, Zhang Y, Zhao H, Huang H, Zhou X (2006) Effects of the 6VS.6AL translocation on agronomic traits and dough properties of wheat. *Euphytica* 155:305–313
- Ling H, Ma B, Shi X, Liu H, Dong L, Sun H, Cao Y, Gao Q, Zheng S, Li Y, Yu Y, Du H, Qi M, Li Y, Lu H, Yu H, Cui Y, Wang N, Chen C, Wu H, Zhao Y, Zhang J, Li Y, Zhou W, Zhang B, Hu W, van Eijk M, Tang J, Witsenboer H, Zhao S, Li Z, Zhang A, Wang D, Liang C (2018) Genome sequence of the progenitor of wheat A subgenome *Triticum urartu*. *Nature* 557:424–428
- Ling HQ, Ma B, Shi XL, Liu H, Dong LL, Sun H, Cao YH, Gao Q, Zheng SS, Li Y, Yu Y, Du HL, Qi M, Li Y, Lu HW, Yu H, Cui Y, Wang N, Chen CL, Wu HL, Zhao Y, Zhang JC, Li YW, Zhou WJ, Zhang BR, Hu WJ, Eijk MJT, Tang JF, Witsenboer HMA, Zhao SC, Li ZS, Zhang AM, Wang DW, Liang CZ (2018) Genome sequence of the progenitor of wheat A subgenome *Triticum urartu*. *Nature* 557:424–428

- Liu W, Koo DH, Xia Q, Li C, Bai F, Song Y, Friebe B, Gill BS (2017) Homoeologous recombination-based transfer and molecular cytogenetic mapping of powdery mildew-resistant gene *Pm57* from *Aegilops searsii* into wheat. *Theor Appl Genet* 130:841–848
- Long Y, Chao WS, Ma G, Xu SS, Qi, L (2017) An innovative SNP genotyping method adapting to multiple platforms and throughputs. *Theor Appl Genet* 130:597–607
- Luo MC, Yang ZL, You FM, Kawahara T, Waines JG, Dvorak J (2007) The structure of wild and domesticated emmer wheat populations, gene flow between them, and the site of emmer domestication. *Theor Appl Genet* 114:947–959
- Luo MC, Gu YQ, You FM, Deal KR, Ma Y, Hu Y, Huo N, Wang Y, Wang J, Chen S, Jorgensen CM, Zhang Y, McGuire PE, Pasternak S, Stein JC, Ware D, Kramer M, McCombie WR, Kianian SF, Martis MM, Mayer KFX, Sehgal SK, Li W, Gill BS, Bevan MW, Šimková H, Doležel J, Weining S, Lazo GR, Anderson OD, Dvorak J (2013) A 4-gigabase physical map unlocks the structure and evolution of the complex genome of *Aegilops tauschii*, the wheat D-genome progenitor. *Proc Natl Acad Sci USA* 110:7940–7945
- Luo MC, Gu YQ, Puiu D, Wang H, Twardziok SO, Deal KR, Huo N, Zhu T, Wang L, Wang Y, McGuire PE, Liu S, Long H, Ramasamy RK, Rodriguez JC, Van SL, Yuan L, Wang Z, Xia Z, Xiao L, Anderson OD, Ouyang S, Liang Y, Zimin AV, Peretea G, Qi P, Bennetzen JL, Dai X, Dawson MW, Müller H, Kugler K, Rivarola-Duarte L, Spannagl M, Mayer KFX, Lu FH, Becan MW, Lerou P, Li P, You FM, Sun Q, Liu Z, Lyons E, Wicher T, Zalzberg SL, Devos KM, Dvořák J (2017) Genome sequence of the progenitor of the wheat D genome *Aegilops tauschii*. *Nature* 551:498–502
- Mac Key J (1966) Species relationship in *Triticum*. In: MacKey J (ed) Proceedings of the 2nd International Wheat Genetics Symposium, 1963. *Hereditas Suppl* 2:237–275
- Mac Key J (1977) Sec. *Dicccocoides* Flaksb. of wheat, its phylogeny, diversification and subdivision. In: Proceedings of the Symposium on Extended Availability of Wheat Genetics Resources. Bari 5–46
- Mac KJ (2005) Wheat: its concept, evolution and taxonomy. In: Royo C et al. (eds) Durum wheat breeding. Current approaches and future strategies, vol. 1. CRC Press. Boca Raton, pp3–61
- Maccaferri M, Harris N, Twardziok S, Pasam R, Gundlach H, Spannagl M, Ormanbekova D, Lux T, Prade V, Milner S, Himmelbach A, Mascher M, Bagnaresi P, Faccioli P, Cozzi P, Lauria M, Lazzari B, Stella A, Manconi A, Gnocchi M, Moscatelli M, Avni R, Deek J, Biyiklioglu S, Frascaroli E, Corneti S, Salvi S, Sonnante G, Desiderio F, Marè C, Crosatti C, Mica E, Özkan H, Kilian B, De Vita P, Marone D, Joukhadar R, Mazzucotelli E, Nigro D, Gadaleta A, Chao S, Faris J, Melo A, Pumphrey M, Pecchioni N, Milanesi L, Wiebe K, Ens J, MacLachlan R, Clarke J, Sharpe A, Shin Koh C, Liang K, Taylor G, Knox R, Budak H, Mastrangelo A, Xu S, Stein N, Hale I, Distelfeld A, Hayden M, Tuberosa R, Walkowiak S, Mayer K, Ceriotti A, Pozniak C, Cattivelli L (2019) Durum wheat genome highlights past domestication signatures and future improvement targets. *Nature Genetics* 51: 885–895

- Marcussen T, Sandve SR, Heier L, Spannagl M, Pfeifer M, Jakobsen KS, Wulff BBH, Steuernagel B, Mayer KFX, Olsen O (2014) Ancient hybridizations among the ancestral genomes of bread wheat. *Science* 345:1250092
- Meyer RS, Purugganan MD (2013) Evolution of crop species: genetics of domestication and diversification. *Nature Rev Genet* 14:840–852
- Middleton CP, Senerchia N, Stein N, Akhunov ED, Keller B, Wicker T, Kilian B (2014) Sequencing of chloroplast genomes from wheat, barley, rye and their relatives provides a detailed insight into the evolution of the Triticeae tribe. *PLoS One* 9:e85761
- Molnar-Lang M, Line G, Szakacs E (2014) Wheat-barley hybridization: the last 40 years. *Euphytica* 195:315–329
- Naranjo T (2019) The effect of chromosome structure upon meiotic homologous and homoeologous recombinations in *Triticeae*. *Agronomy* 9:552. doi:10.3390/agronomy9090552
- Nasuda S, Friebe B, Busch W, Kynast RG, Gill BS (1998) Structural rearrangement in chromosome 2M of *Aegilops comosa* has prevented the utilization of the compair and related wheat–*Ae. comosa* translocations in wheat improvement. *Theor Appl Genet* 96: 780–785
- Nave M, Avni R, Ben-Zvi B, Hale I, Distelfeld A (2016) QTLs for uniform grain dimensions and germination selected during wheat domestication are co-located on chromosome 4B. *Theor Appl Genet* 129:1303–1315
- Nesbitt M (2001) Wheat evolution: integrating archaeological and biological evidence. In: Caligari PDS, Brandham PE (eds) *Wheat taxonomy: the legacy of John Percival*. Linnean Society, London, pp 37–59 (Linnean Special Issue 3)
- Niu Z, Klindworth DL, Friesen TL, Chao S, Jin Y, Cai X, Xu SS (2011) Targeted introgression of a wheat stem rust resistance gene by DNA marker–assisted chromosome engineering. *Genetics* 187:1011–1021
- Niu Z, Klindworth DL, Friesen TL, Chao S, Ohm JB, Xu SS (2014) Development and characterization of wheat lines carrying stem rust resistance gene *Sr43* derived from *Thinopyrum ponticum*. *Theor Appl Genet* 127:969–980
- Peng JH, Ronnin Y, Fahima T, Roder MS, Li YC, Nevo E, Korol A (2003) Domestication quantitative trait loci in *Triticum dicoccoides*, the progenitor of wheat. *Proc Natl Acad Sci USA* 100:2489–2494
- Peng JH, Sun D, Nevo E (2011) Domestication evolution, genetics and genomics in wheat. *Mol Breeding* 28:281–301
- Pont C, Leroy T, Seidel M, Tondelli A, Duchemin W, Armisen D, Lang D, Bustos-Korts D, Goué N, Balfourier F, Molnar-Lang M, Lage J, Kilian B, Ozkan H, Waite D, Dyer S, Alaux M, Letellier T, Russell J, Keller B, Eeuwijk F, Spannagl M, Mayer K, Waugh R, Stein N, Cattivelli

- L, Haberer G, Charmet G, Salse J (2019) Tracing the Ancestry of Modern Bread Wheats. *Nature Genetics* 51:905–911
- Qi LL, Wang SL, Chen PD, Liu DJ, Friebe B, Gill BS (1997) Molecular cytogenetic analysis of *Leymus recemosus* chromosomes added to wheat. *Theor Appl Genet* 95:1084–1091
- Qi LL, Friebe B, Zhang P, Gill BS (2007) Homoeologous recombination, chromosome engineering and crop improvement. *Chromosome Res* 15:3–19
- Qi LL, Pumphrey MO, Friebe B, Chen PD, Gill BS (2008) Molecular cytogenetic characterization of alien introgressions with gene *Fhb3* for resistance to Fusarium head blight disease of wheat. *Theor Appl Genet* 117:1155–1166
- Roberts MA, Reader SM, Dalgliesh C, Miller TE, Foote TN, Fish LJ, Snape JW, Moore G (1999) Induction and characterization of *Ph1* wheat mutants. *Genetics* 153: 1909–1918
- Salamini F, Özkan H, Brandolini A, Schäfer-Pregl R, Martin W (2002) Genetics and geography of wild cereal domestication in the near east. *Nature Reviews Genetics* 3:429–441
- Salse J, Chague V, Bolot S, Magdelenat G, Huneau C, Pont C, Belcram H, Couloux A, Gardais S, Evrard A, Segurens B, Charles M, Ravel C, Samain S, Charmet G, Boudet N, Chalhoub B (2008) New insights into the origin of the B genome of hexaploid wheat: evolutionary relationships at the *SPA* genomic region with the S genome of the diploid relative *Aegilops speltoides*. *BMC Genomics* 9:555
- Schneider A, Molnár I, Molnár-Láng M (2008). Utilisation of *Aegilops* (goatgrass) species to widen the genetic diversity of cultivated wheat. *Euphytica* 163:1–19
- Schwarzacher T, Anamthawat-Jónsson K, Harrison G, Islam A, Jia J, King I, Leitch A, Miller T, Reader S, Rogers W, Shi M, Heslop-Harrison J (1992) Genomic in situ hybridization to identify alien chromosomes and chromosome segments in wheat. *Theor Appl Genet* 84:778–786
- Sears ER (1956) The transfer of leaf rust resistance from *Aegilops umbellulata* to wheat. *Brookhaven Symp Biol* 9:1–22
- Sears ER (1972) Chromosome Engineering in wheat. *Stadler Symposia* 4:23–38
- Sears ER (1976) Genetic control of chromosome pairing in wheat. *Ann Rev Genet* 10:31–51
- Sears ER (1977) An induced mutant with homoeologous pairing in common wheat. *Can J Genet Cytol* 19:585–593
- Semagn K, Babu R, Hearne S, Olse M (2014) Single nucleotide polymorphism genotyping using Kompetitive Allele Specific PCR (KASP): overview of the technology and its application in crop improvement. *Mol Breed* 33:1–14
- Shewry PR (2009). Wheat. *Journal of Experimental Botany* 60:1537–1553

- Simons KJ, Fellers JP, Trick HN, Zhang Z, Tai Y, Gill BS, Faris JD (2006) Molecular characterization of the major wheat domestication gene Q. *Genetics* 172: 547–555
- Stebbins GL (1950) *Variation and Evolution in Plants*. Columbia University Press, New York.
- Tan CT, Assanga A, Zhang G, Rudd JC, Haley SD, Xue Q, Ibrahim A, Bai G, Zhang X, Byrne P, Fuentealba MP, Liu S (2017) Development and validation of KASP markers for wheat streak mosaic virus resistance gene *Wsm2*. *Crop Sci* 57:1–10
- Tsujimoto H, Tsunewaki K (1984) Gametocidal genes in wheat and its relatives. I. Genetic analyses in common wheat of a gametocidal gene derived from *Aegilops speltoides*. *Can J Genet Cytol* 26:78–84
- Tsujimoto H, Tsunewaki K (1988) Gametocidal genes in wheat and its relatives. III. Chromosome location and effects of two *Aegilops speltoides*-derived gametocidal genes in common wheat. *Genome* 30:239–244
- van Slageren MW (1994). *Wild Wheats: A Monograph of Aegilops L. and Amblyopyrum (Jaub. and Spach) Eig (Poaceae)*. Wageningen. Wageningen Agricultural University.
- Venske E, dos Santos RS, Busanello C, Gustafson P, de Oliveira AC (2019) Bread wheat: a role model for plant domestication and breeding. Venske et al. *Hereditas* 156. <https://doi.org/10.1186/s41065-019-0093-9>
- Wang S, Wong D, Forrest K, Allen A, Huang BE, Maccaferri M, Salvi S, Milner SG, Cattivelli L, Mastrangelo AM, Whan A, Stephen S, Barker G, Wieseke R, Plieske J, International Wheat Genome Sequencing Consortium, Lillemo M, Mather D, Appels R, Dolferus R, Brown–Guedira G, Korol A, Akhunova AR, Feuillet C, Salse J, Morgante M, Pozniak C, Luo MC, Dvorak J, Morell M, Dubcovsky J, Ganal M, Tuberosa R, Lawley C, Mikoulitch I, Cavanagh C, Edwards KJ, Hayden M, Akhunov E (2014) Characterization of polyploid wheat genomic diversity using a high–density 90,000 single nucleotide polymorphism array. *Plant Biotechnol J* 12:787–796
- Wicker T, Mayer K, Gundlach H, Martis M, Steuernagel B, Scholz U, Simkova H, Kubalaková M, Choulet F, Taudien S, Platzer M, Feuillet C, Fahima T, Budak H, Dolezel J, Keller B, Stein N (2011) Frequent gene movement and pseudogene evolution is common to the large and complex genomes of wheat, barley, and their relatives. *Plant Cell* 23:1706–1718
- Winfield MO, Allen AM, BurrIDGE AJ, Barker GLA, Benbow HR, Wilkinson PA, Coghill J, Waterfall C, Davassi A, Scopes G, Pirani A, Webster T, Brew F, Bloor C, King J, West C, Griffiths S, King I, Bentley AR, Edwards KJ (2016) High–density SNP genotyping array for hexaploid wheat and its secondary and tertiary gene pool. *Plant Biotech J* 14:1195–1206
- Wulff BBH, Moscou MJ (2014) Strategies for transferring resistance into wheat: from wide crosses to GM cassettes. *Front Plant Sci* 5:692
- Xing L, Hu P, Liu J, Witek K, Zhou S, Xu J, Zhou W, Gao L, Huang Z, Zhang R, Wang X, Chen P, Wang H, Jones J, Karafiatova M, Vrana J, Bartos J, Dolezel J, Tian Y, Wu Y, Cao A (2018)

Pm21 from *Haynaldia villosa* encodes a CC-NBS-LRR protein conferring powdery mildew resistance in Wheat. *Molecular Plant* 11:874–878

Zhang P, Dundas IS, McIntosh RA, Xu SS, Park RF, Gill BS, Friebe B (2015) Wheat–*Aegilops* introgressions. In: Molnár–Láng M, Ceoloni C, Doležel J (eds) *Alien introgression in wheat*. Springer International Publishing, Switzerland, pp 221–244

Zhang W, Cao Y, Zhang M, Zhu X, Ren S, Long Y, Gyawali Y, Chao S, Xu S, Cai X (2017) Meiotic homoeologous recombination-based alien gene introgression in the genomics era of wheat. *Crop Sci* 57:1189–1198

Zhang W, Zhang M, Zhu X, Cao Y, Sun Q, Ma G, Chao S, Yan C, Xu S, Cai X (2018a) Molecular cytogenetic and genomic analyses reveal new insights into the origin of the wheat B genome. *Theor Appl Genet* 131:365–375

Zhang W, Zhu X, Zhang M, Chao S, Xu S, Cai X (2018b) Meiotic homoeologous recombination-based mapping of wheat chromosome 2B and its homoeologues in *Aegilops speltoides* and *Thinopyrum elongatum*. *Theor Appl Genet* 131:2381–2395

Zhang W, Cai X (2019) Alien introgression and breeding of synthetic wheat. In: Ordon F, Friedt W (eds) *Advances in breeding techniques for cereal crops*. Burleigh Dodds, Sawston, pp3–54

Zhao R, Wang H, Xiao J, Bie T, Cheng S, Jia Q, Yuan C, Zhang R, Cao A, Chen P, Wang X (2013) Induction of 4VS chromosome recombinants using the CS *ph1b* mutant and mapping of the wheat yellow mosaic virus resistance gene from *Haynaldia villosa*. *Theor Appl Genet* 126:2921–2930

Zimin A, Puiu D, Luo M, Zhu T, Koren S, Marçais G, Yorke J, Dvořák J, Salzberg S (2017a) Hybrid assembly of the large and highly repetitive genome of *Aegilops tauschii*, a progenitor of bread wheat, with the MaSuRCA mega-reads algorithm. *Genome Res* 27: 787–792

Zimin A, Puiu D, Hall R, Kingan S, Clavijo B, Salzberg S (2017b) The first near-complete assembly of the hexaploid bread wheat genome, *Triticum aestivum*. *GigaScience* 6:1–7

**CHAPTER 3. PARTITIONING AND PHYSICAL MAPPING OF WHEAT
CHROMOSOME 3B AND ITS HOMOELOGUE 3E IN *THINOPYRUM ELONGATUM*
BY INDUCING HOMOELOGOUS RECOMBINATION**

Abstract

The wheat (*Triticum aestivum*, $2n = 6x = 42$, AABBDD) and *Thinopyrum elongatum* ($2n = 2x = 14$, EE) genomes can be differentiated from each other by fluorescent genomic *in situ* hybridization (FGISH) as well as molecular markers. This has facilitated homoeologous recombination-based partitioning and engineering of their genomes for physical mapping and alien introgression. Here, we isolated a special wheat genotype, which was double monosomic for wheat chromosome 3B and *Th. elongatum* chromosome 3E and homozygous for the *ph1b* mutant, to induce 3B-3E homoeologous recombination. Totally, 81 3B-3E recombinants were recovered and detected in the primary, secondary, and tertiary homoeologous recombination cycles by FGISH. Comparing to the primary recombination, the secondary and tertiary recombination shifted toward the proximal regions due to the increase of homology between the pairing partners. The 3B-3E recombinants were genotyped by high-throughput wheat 90K single nucleotide polymorphism (SNP) arrays and their recombination breakpoints physically mapped based on the FGISH patterns and SNP results. The 3B-3E recombination physically partitioned chromosome 3B into 38 bins, and 429 SNPs were assigned to the distinct bins. Integrative analysis of FGISH and SNP results led to the construction of a composite bin map for chromosome 3B. Additionally, we developed 22 SNP-derived semi-thermal asymmetric reverse PCR (STARP) markers specific for chromosome 3E and constructed a comparative map of homoeologous chromosomes 3E, 3B, 3A, and 3D. In summary, this work provides a unique

physical framework for further studies of the 3B-3E homoeologous pair and diversifies the wheat genome for wheat improvement.

Introduction

Common wheat (*T. aestivum*, $2n = 6x = 42$, AABBDD), one of the most important food crops worldwide, offers approximately 20% of calories for human consumption. Two spontaneous interspecific hybridization involving three diploid ancestors and subsequent chromosome doubling led to hexaploid wheat (McFadden and Sears, 1946; Dvorak et al., 1993; Cai et al., 2010; Marcussen et al., 2014; Zhang et al., 2018a; Pont et al., 2019). The polyploid origin of wheat resulted in a narrow genetic variability in the wheat genome. Tremendous genetic variation was left in the ancestors and relatives of wheat during polyploidization. This has increasingly become a bottleneck in wheat improvement. It is time to restore the evolutionarily-omitted genetic diversity to enrich and diversify the wheat genome by chromosome engineering due to rapid advances in genomics. In recent years, the efficacy and throughput of homoeologous recombination-based chromosome engineering have been dramatically improved in alien introgression and genome studies by taking advantage of the newly-developed genomics resources and technologies in wheat and its relatives (Qi et al., 2007; Faris et al., 2008; Niu et al., 2011; Klindworth et al., 2012; Zhao et al., 2013; Danilova et al., 2017; Zhang et al., 2017, 2018a, b, 2019).

Meiotic homoeologous recombination is inhibited by *Ph* (pairing homoeologous) gene. *Ph* gene ensures meiotic pairing and recombination to occur between homologous chromosomes, not between homoeologous chromosomes. It functions as a defense system to prevent homoeologous chromosomes from exchanging genetic material and maintains the integrity and stability of the wheat genome. The absence of *Ph* gene, such as nullisomy for *Ph1* and *ph1b*

mutant, enhances homoeologous pairing and recombination (Riley and Chapman, 1958; Riley et al., 1959; Sears, 1977; Qi et al., 2007). The *ph1b*-induced homoeologous recombination partitions the wheat genome for physical mapping and results in genetically-compensated recombinants for alien introgression and germplasm development (Jiang et al., 1994; Friebe et al., 1996; Qi et al., 2008; Niu et al., 2011; Patokar et al., 2016; Rey et al., 2018; Zhang et al., 2017, 2018a, 2019). Thus, *ph1b*-induced homoeologous recombination provides a unique approach to the physical studies of the wheat genome and creates an effective pipeline of gene flow from wild species into wheat. Homoeologous recombination-based chromosome engineering diversifies the wheat genome and facilitates understanding of the complex polyploid genome.

Wheat has large chromosomes and a complex polyploid genome. Partitioning and dissection of wheat chromosomes enhance understanding and manipulation of the genome for wheat improvement. Wheat aneuploid and deletion stocks have been widely used to partition and dissect the wheat genome and individual chromosomes based on morphological, cytological, and molecular markers (Sears, 1954, 1966; Gill et al., 1991; Endo and Gill, 1996; Qi et al., 2003). In addition, wheat has many relatives that contain the genomes homoeologous with its genome. The homoeologous genomes/chromosomes of wheat and its relatives can be physically differentiated from each other by genomic *in situ* hybridization (GISH) (Liu et al., 2013; Zhang et al., 2018b) and fluorescent *in situ* hybridization (FISH) (Zhao et al., 2013; Danilova et al., 2014; Niu et al., 2014; Zhang et al., 2017; Dai et al., 2019). Furthermore, homoeologous genomes/chromosomes are highly polymorphic, offering a great opportunity to integrative physical and genetic mapping of the wheat genome. Therefore, inducing meiotic homoeologous recombination between wheat and its relatives leads to partitioning and dissection of wheat chromosomes, generating unique

physical frameworks useful in wheat genome studies (Anderson et al., 1992; Chen et al., 1995, 2013; Qi et al., 2003, 2004, 2008; Kalavacharla et al., 2006; Niu et al., 2011; Zhao et al., 2013; Zhang et al., 2018b).

Advances in high-throughput genotyping, such as wheat 90K SNP arrays (Wang et al., 2014), and availability of wheat reference genome sequences [Choulet et al., 2014; Avni et al., 2017; Luo et al., 2017; Ling et al., 2018; The International Wheat Genome Sequencing Consortium (IWGSC), 2018], have dramatically enhanced homoeologous recombination-based genome studies and chromosome engineering in wheat and its relatives (Zhang et al., 2017, 2018a, b, 2019; Danilova et al., 2019; Dai et al., 2019; Li et al., 2019). Recently, wheat chromosome 2B was physically partitioned and characterized by meiotic recombination with its homoeologous counterparts in wheat-related wild species. Homoeologous recombinants involving different regions of chromosome 2B were delineated by FGISH and wheat 90K SNP arrays, leading to the construction of a composite bin map of 2B (Zhang et al., 2018b). Two wild species-derived disease resistance genes were mapped and introduced into wheat by homoeologous recombination (Zhang et al., 2019). Therefore, inducing meiotic recombination of wheat chromosomes with their homoeologues in the relatives dissects chromosomes for a better understanding of the wheat genome, and reshapes the wheat genome to boost its genetic potential in wheat improvement. Here, we report our studies on the partitioning and physical mapping of wheat chromosome 3B by *ph1b*-induced meiotic homoeologous recombination with *Th. elongatum* ($2n = 2x = 14$, EE) chromosome 3E. The 3B-3E recombinants were physically characterized by FGISH and genotyped by high-throughput 90K SNP assay and SNP-derived STARP markers, leading to a unique physical framework of wheat chromosome 3B and *Th. elongatum* chromosome 3E for further genome studies.

Material and methods

Plant materials

Common wheat ‘Chinese Spring’ (CS) *ph1b* mutant was supplied by the Wheat Genetics Resource Center at Kansas State University, USA. The CS-*Th. elongatum* disomic substitution line 3E(3B) [DS 3E(3B)] was provided by J. Dvorak at University of California, Davis, USA.

Homoeologous recombination population development

DS 3E(3B) (*Ph1Ph1*) and CS *ph1b* mutant (*ph1bph1b*) were used to develop the special genotype that was double monosomic for wheat chromosomes 3B and *Th. elongatum* chromosome 3E and homozygous for the *ph1b* mutant (i.e. *ph1bph1b*) in the CS background (Figure 3.1). Sequence-tagged site (STS) markers specific for *Ph1/ph1b* and for chromosomes 3B and 3E were used to select the special genotype, which was subsequently verified by FGISH (Cai et al., 1998). Meiotic homoeologous recombination between chromosomes 3B and 3E was induced by *ph1b* mutant in the special genotype. 3B-3E recombinants were recovered in the backcross population of the special genotype × DS 3E(3B) (Figure 3.1). We expected a higher homoeologous recombinant recovery rate in the backcross population than the self-pollinating population of the special genotype (Zhang et al., 2017). In addition, the backcross introduced *Ph1* into the recombinants to ensure their genetic stability. Secondary or tertiary recombination were induced with the primary 3B-3E recombinants to further partition the recombination segments following the same procedure as the primary recombination cycle (Figure 3.1).

Molecular cytogenetic analysis

Mitotic chromosomes were prepared from root tip cells at metaphase as described by Chen et al. (1995). Meiotic chromosomes were prepared from the meiocytes [pollen mother cells (PMCs)] at metaphase I (MI) of the special genotypes with and without *Ph1* following the

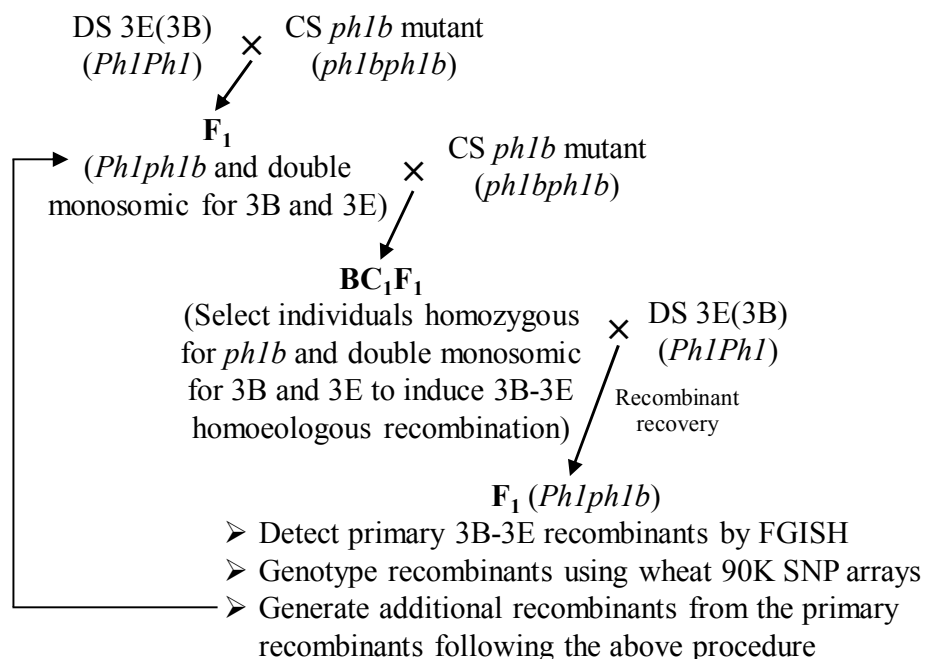


Figure 3.1. Induction, recovery, detection, and characterization of 3B-3E homoeologous recombinants. CS: Chinese Spring; DS 3E(3B): CS wheat-*Th. elongatum* disomic substitution line 3E(3B).

procedure of Cai and Jones (1997). Over 100 PMCs were analyzed for meiotic homoeologous pairing between wheat chromosome 3B and *Th. elongatum* chromosome 3E in each genotype. FGISH was performed to differentiate *Th. elongatum* chromatin from wheat chromatin in both mitotic and meiotic cells following the procedure of Cai et al. (1998). Biotin-16-dUTP (Enzo Life Sciences, Inc., USA) was used to label *Th. elongatum* total genomic DNA as probe by nick translation. Total genomic DNA of CS was used as blocking after being sheared by boiling in 0.4 M NaOH for 40-50 minutes. *Th. elongatum* chromatin was painted in yellow-green with fluorescein isothiocyanate-conjugated avidin (FITC-avidin) (Vector Laboratories, Inc., USA) and wheat chromatin was counterstained in red by propidium iodide (PI). FGISH patterns of mitotic and meiotic chromosomes were observed and captured under a fluorescence microscope (BX51, Olympus, Japan) installed with a CCD camera (DP72, Olympus, Japan) and Olympus

CellSens Software. The absolute length of the chromosome 3E and 3B segments in each 3B-3E recombinant chromosome were measured in 2-7 FGISH-painted mitotic cells using Olympus CellSens Software.

Molecular marker analyses

Two *Ph1*-specific STS markers, *PSR128* and *PSR574* (Roberts et al., 1999), were used to select individuals homozygous for *ph1b* mutant in the construction of the special genotype. The chromosome 3B/3E-specific STS marker *STS3B-83* (Liu and Anderson, 2003) was used to select the individuals double monosomic for chromosome 3B and 3E in the special genotype development. The PCR products were separated using a non-denatured polyacrylamide gel system as described by Zhang et al. (2018a). Wheat 90K SNP genotyping assay was performed by the Illumina BeadStation and iScan instruments according to the manufacturer's protocols (Illumina Inc., San Diego, CA, USA). GenomeStudio 2.0 software (Illumina Inc.) was used for SNP allele clustering and genotype calling (Wang et al. 2014). The SNP genotypes of the 3B-3E recombinants were analyzed following the procedure of Zhang et al. (2018b).

Semi-thermal asymmetric reverse PCR (STARP) markers were developed from chromosome 3E-specific SNPs based on the context sequences of the SNPs (Luo et al., 2017). PCR was performed as described by Long et al. (2017). PCR products of the STARP markers were sorted in an IR² 4200 DNA Analyzer with denaturing polyacrylamide gel electrophoresis (LI-COR, Lincoln, NE, USA).

Results

Induction and recovery of 3B-3E recombinants and aberrations

We developed a genotype that was double monosomic for wheat chromosome 3B and *Th. elongatum* chromosome 3E, but hemizygous for *Ph1* (i.e. *Ph1ph1b*) by crossing DS 3E(3B) to

CS *ph1b* mutant (Figure 3.1). Wheat chromosome 3B was observed to pair with *Th. elongatum* chromosome 3E in a frequency of 2.17% (3 out of 138 PMCs) in the hemizygous genotype (*Ph1ph1b*) with *Ph1* present (Zhang et al., 2018a). After that, a special genotype that was double monosomic for 3B and 3E and homozygous for *ph1b* was generated by backcrossing the F₁ hybrid to CS *ph1b* mutant and selected from the backcrossing population (BC₁F₁) by molecular marker analysis and FGISH (Figure 3.1). Homoeologous 3B-3E pairing (17 out of 139 PMCs; 12.23%) was significantly increased in the absence of *Ph1* (Zhang et al., 2018a), indicating induction of *ph1b* mutant for 3B-3E pairing and recombination (Figure 3.2). In addition, we induced secondary and tertiary recombination with the primary or secondary 3B-3E recombinants having a large chromosome 3E segment by *ph1b* mutant (Figure 3.1).

The BC₁F₁ individuals selected as double monosomics (3B'+3E') and *ph1b* homozygous (*ph1bph1b*) were crossed to DS 3E(3B) (*Ph1Ph1*) to recover 3B-3E recombinant gametes (Figure 3.1). DS 3E(3B) was used in the recombinant recovery cross because it introduced a *Ph1* allele and *Th. elongatum* chromosome 3E into the recombinants. The presence of *Ph1* in the recombinants stabilized their genome and subsequently improved their fertility. Introduction of *Th. elongatum* chromosome 3E into the recombinants was helpful for the differentiation of recombinant chromosome segments by high-throughput 90K SNP genotyping because wheat 90K SNPs mostly exhibited a dominant pattern for the 3B-3E homoeologous pair with an allele present on 3B and absence on 3E. For this reason, DS 3E(3B) played the role of a tester (recessive homozygote) in this testcross-like cross for genotypic analysis. In addition, we found that this testcross-like procedure recovered homoeologous recombinants more efficiently than self-pollination (Zhang et al., 2017; see data below). Also, the secondary and tertiary 3B-3E recombinant gametes were recovered through this testcross-like cross (Figure 3.1).

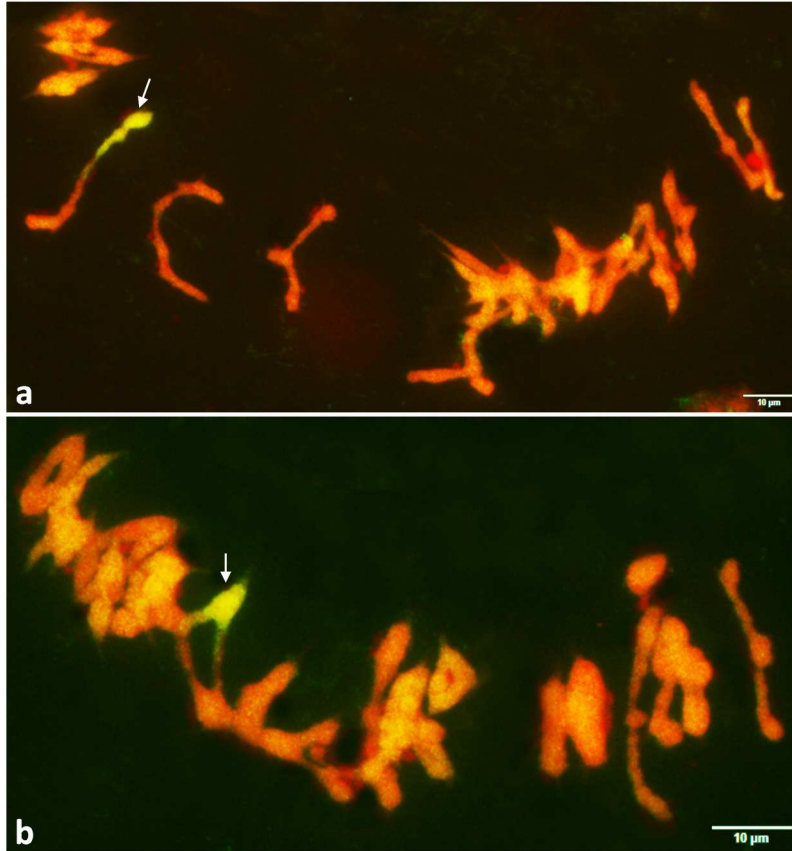


Figure 3.2. FGISH patterns of *ph1b* mutant-induced 3B-3E homoeologous pairing as a rod bivalent (a) and a ring bivalent (b) in the special genotype that was double monosomic for 3B and 3E, and homozygous for *ph1b*. Wheat chromosomes were painted in red, while chromosome 3E was painted in yellow-green. Arrows point to 3B-3E rod (a) and ring (b) bivalents.

Detection and delineation of 3B-3E recombinants and aberrations by FGISH

Total *Th. elongatum* genomic DNA-probed FGISH specifically paints *Th. elongatum* chromatin, and consequently differentiates *Th. elongatum* chromosomes or chromosomal segments from those in the wheat genome. We screened 267 individuals from the progeny of the primary recombination recovery cross [i.e. special genotype \times DS 3E(3B)] by FGISH and detected 43 3B-3E recombinants with a recombination rate of 16.10%. Meanwhile, we screened 30 individuals from the self-pollinated progeny of the special genotype and detected two 3B-3E recombinants with a recombination rate of 6.67%. These results indicated that the testcross-like procedure was more efficient than self-pollination for 3B-3E recombinant recovery. All 3B-3E

recombinants and aberrations were grouped into seven categories (I, II, III, IV, V, VI, and VII) according to their compositions (Figure 3.3). A total of 45 3B-3E recombinants were obtained from the primary recombination cycle with an overall recombination rate of 15.15% (Table 3.1 and APPENDIX A). Most of the primary recombination events occurred in the terminal regions of the 3B-3E homoeologous pair. Thus, the majority of the primary recombinants fell into Category I and II (Figure 3.3, 3.4). One of the primary recombinants was found to contain two terminal recombinant chromosomes (i.e. V-1 and V-2 in Figure 3.3), called a double recombinant. According to their FGISH patterns, V-1 seemed to be a 3B-3E recombinant (3ES·3EL-3BL), while V-2 might be a 3D-3E recombinant (3DS·3DL-3EL) according to its morphology. Only two of the primary recombinants involved the interstitial regions [III-1 (3BS-3ES·3EL-3BL) and IV-I (3ES-3BS·3BL-3EL)]. They should be derived from a double crossover between chromosomes 3B and 3E. In addition, two Robertsonian translocations [VI-1 (3ES·3BL) and VI-2 (3BS·3EL)] and two telocentric chromosomes of 3E (VII-1 and VII-2) were detected from the primary recombination population (Figure 3.3 and APPENDIX A). Both Robertsonian translocations and telocentric chromosomes probably resulted from misdivision of the univalent chromosomes 3B and 3E, instead of meiotic crossover-derived recombination (Zhang et al., 2018b).

Secondary recombination was induced with six primary 3B-3E recombinants (I-1, I-2, I-8, I-12, I-13, and I-22) containing a large 3E segment and chromosome 3B using *ph1b* mutant as illustrated in Figure 3.5 (APPENDIX A). Out of 253 individuals screened in the secondary recombination population, 29 new 3B-3E recombinants (11.46%) were identified by FGISH (Table 3.1). Over 50% of the secondary recombinants involved interstitial regions and fell into Category III and IV. Most of the other secondary recombinants involved a terminal region on

one arm under Category II (Figure 3.3, 3.4 and APPENDIX A). Overall, the secondary recombination shifted toward the proximal regions and enhanced partitioning of the chromosome regions with low recombination frequency.

Table 3.1. 3B-3E homoeologous recombinants detected in the primary, secondary, and tertiary recombination populations

Populations	No. plants screened	No. recombinants	Recombination rate
Primary	297	45	15.15%
Secondary	253	29	11.46%
Tertiary	95	7	7.37%
Total	645	81	n.a.^a

^aThe chromosomes involved in 3B-3E homoeologous recombination in each of the three populations were different. Thus, an overall 3B-3E homoeologous recombination rate could not be calculated by combining the three populations.

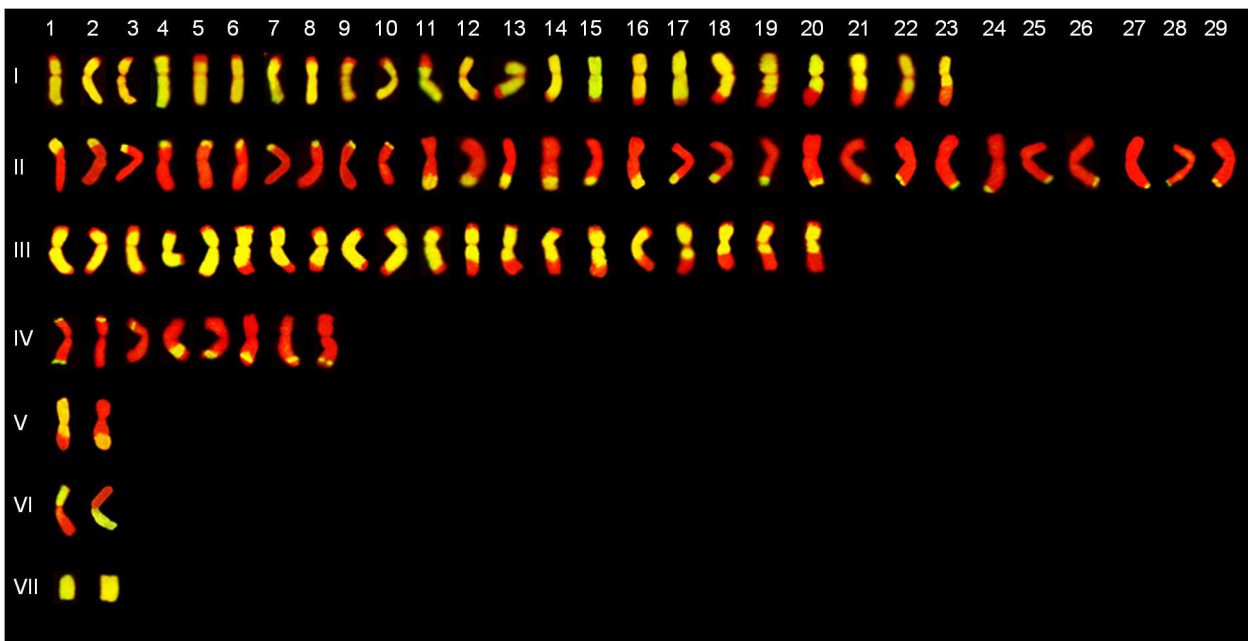


Figure 3.3. FGISH-painted 3B-3E recombinant chromosomes and aberrations in the seven categories. *I*-Terminal recombinants with a large 3E segment; *II*-Terminal recombinants with a large 3B segment; *III*- Interstitial recombinants with a large 3E pericentromeric region flanked by 3B terminal segments; *IV*-Interstitial recombinants with a small 3E segment within one or both arms; *V*-Double recombinant [V1 (3ES·3EL-3BL) + V2 (3DS·3DL(?)·3EL)]; *VI*-Robertsonian translocations (3ES·3BL and 3BS·3EL); *VII*-Telocentric chromosomes of 3E. Wheat chromosome 3B segments were painted in red, while chromosome 3E segments were painted in yellow-green.

To further enhance homoeologous recombination in the pericentromeric region of the 3B-3E homoeologous pair, tertiary recombination was induced between the interstitial secondary recombinant containing a large 3E pericentromeric region flanked by a terminal 3B segment on both arms (III-11) and chromosome 3B using *ph1b* mutant (Figure 3.5). Chromosome 3B had higher homology with III-11 than with chromosome 3E because 3B and III-11 shared the terminal regions on both arms. This led to a significant shift of tertiary recombination toward the centromeric regions. Seven new 3B-3E recombinants were detected by FGISH from 95 individuals with a recombination rate of 7.37% in the tertiary recombination population (Table 1). They were all interstitial recombinants under Category III and IV (Figure 3.3, 3.4, 3.5 and APPENDIX A).

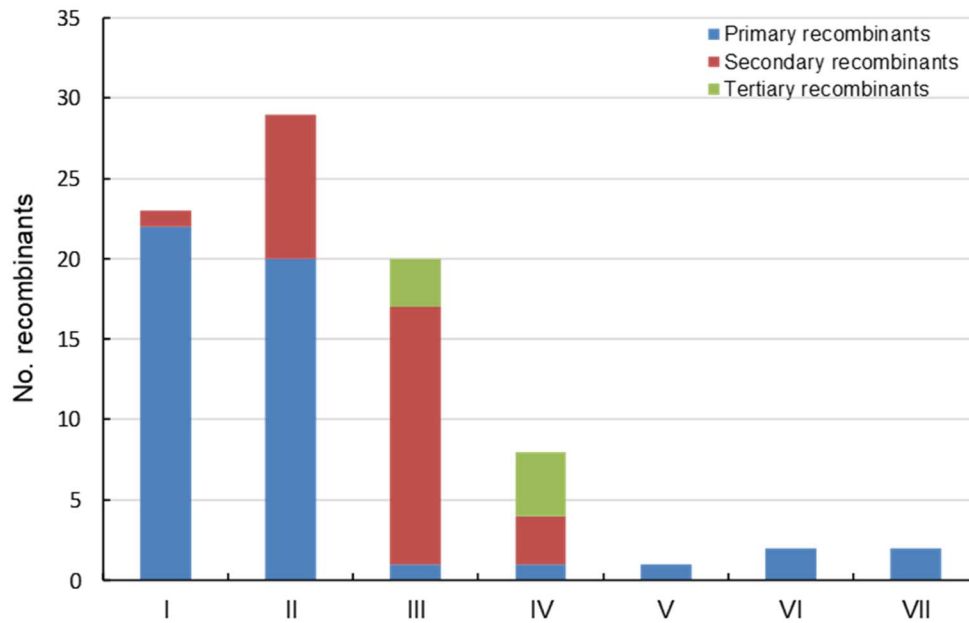


Figure 3.4. Distribution of primary, secondary, and tertiary 3B-3E recombinants and aberrations in the following seven categories: *I*-Terminal recombinants with a large 3E segment; *II*-Terminal recombinants with a large 3B segment; *III*- Interstitial recombinants with a large 3E pericentromeric region flanked by 3B terminal segments; *IV*-Interstitial recombinants with a small 3E segment within one or both arms; *V*-Double recombinant [V1 (3ES·3EL-3BL) + V2 (3DS·3DL(?)·3EL)]; *VI*-Robertsonian translocations (3ES·3BL and 3BS·3EL); *VII*-Telocentric chromosomes of 3E; *VII*-Telocentric chromosomes of 3E.

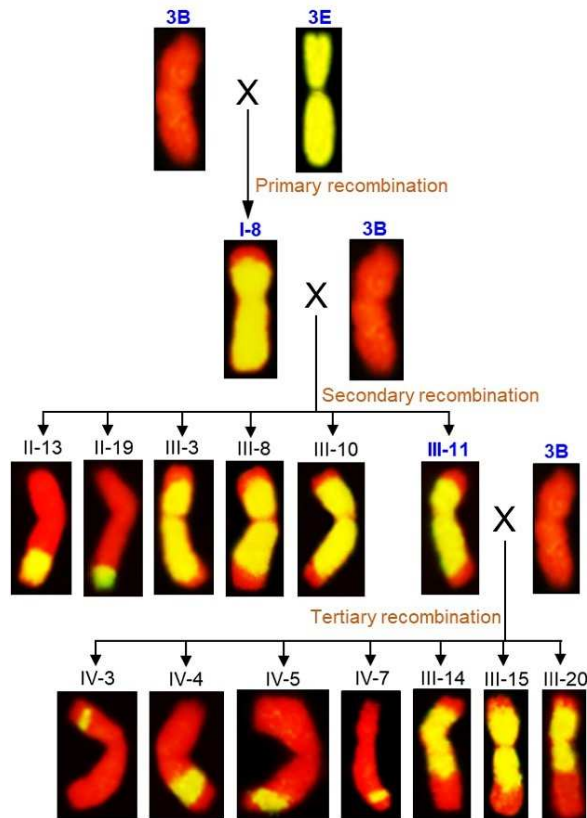


Figure 3.5. FGISH images illustrating three cycles (primary, secondary, and tertiary) of *ph1b*-induced 3B-3E homoeologous recombination and resultant recombinants. The secondary recombinants were derived from the primary recombinant I-8, and the tertiary recombinants from the secondary recombinant III-11. Wheat chromosomes and segments were painted in red, while chromosome 3E and its segments were painted in yellow-green.

A total of 81 3B-3E meiotic recombinants and 4 aberrations under seven categories were identified from 645 individuals in the primary, secondary, and tertiary recombination populations (Figure 3.3 and APPENDIX A). Fifty-two of the recombinants (61.18%) resulted from recombination involving terminal segments on the short or long arms of the 3B-3E homoeologous pair and were placed under Category I and II (Figure 3.3). They were the major type of 3B-3E recombinants recovered and identified in this work. Most of the terminal recombinants were derived from primary recombination (Figure 3.4). Out of 81 meiotic recombinants, 28 involved an interstitial pericentromeric region or an interstitial segment within an arm. They were grouped under Category III and IV, representing the second largest group of

3B-3E recombinants in this study (Figure 3.3 and APPENDIX A). Twenty-six of the interstitial recombinants (92.86%) were generated from the secondary and tertiary recombination cycles (Figure 3.4).

FGISH-based physical analysis of 3B-3E recombination breakpoints

Each of the recombinant chromosome arms were evenly partitioned into 10 intervals with each representing 10% of the arm as illustrated in Figure 3.6. The 3B-3E recombination breakpoints were assigned to respective intervals according to their physical positions on the recombinant chromosomes. The physical position of a recombination breakpoint was determined based on the relative length of the proximal recombination segment (3B or 3E) over the total length of the entire recombinant arm, which was calculated as “length of the proximal recombination segment/total length of the entire recombinant arm” (APPENDIX B). The secondary and tertiary 3B-3E recombinants were categorized into two groups based on the origin of the recombinant chromosomes. The first group contained a new recombinant chromosome resulting from a secondary or tertiary recombination event, such as the secondary recombinants II-13 and II-19 (Figure 3.5). The second group contained a recombinant chromosome with a newly-formed secondary or tertiary recombinant in addition to the initial primary or secondary recombinant, such as the secondary recombinants III-3, III-8, III-10, and III-11, and all tertiary recombinants (Figure 3.5). The origin of the recombinants was determined according to the physical measurements and wheat 90K SNP analysis of the recombinant chromosomes (APPENDIX B).

The primary 3B-3E recombination breakpoints mostly clustered within the three distal intervals (0.61-0.70, 0.71-0.80, and 0.81-0.90) on the short arm and four distal intervals (0.51-0.60, 0.61-0.70, 0.71-0.80, and 0.81-0.90) on the long arm. The homoeologous recombination

hotspots were located at the 0.71-0.80 and 0.81-0.90 intervals on the short and long arm, respectively (Figure 3.6). Overall, the primary recombination breakpoints were positioned mostly to the distal regions on both arms, but there were more breakpoints toward the proximal region on the long arm than the short arm (Figure 3.6). Comparing to the primary recombination, the secondary and tertiary recombination breakpoints shifted toward the proximal regions on both arms, especially the tertiary breakpoints on the long arm (Figure 3.6). Apparently, increased homology between the homoeologous partners in the secondary and tertiary recombination enhanced 3B-3E recombination toward the proximal regions (Figure 3.5, 3.6).

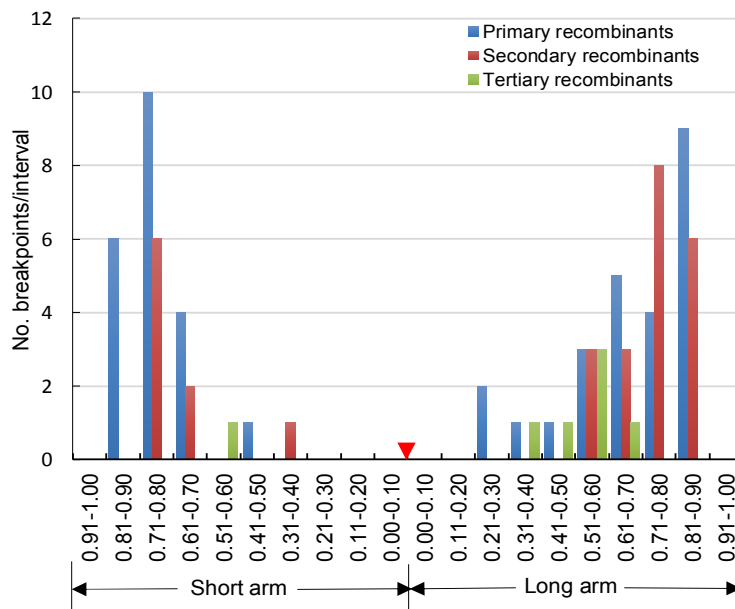


Figure 3.6. Distribution of the three rounds (primary, secondary, and tertiary) of 3B-3E recombination breakpoints on the centromere-telomere axis. Each interval on the x-axis represents 10% length of the entire short or long arm. The red triangle points to the centromere.

Homoeologous recombination-based physical mapping of wheat chromosome 3B

We assigned 505 polymorphic SNPs to the 3B-3E homoeologous pair by genotyping DS 3E(3B) and CS using wheat 90K SNP arrays. Out of the polymorphic SNPs, 429 had significant hits on wheat chromosome 3B by BLASTn against the IWGSC RefSeq v2.0 and physically mapped to chromosome 3B (Zhang et al., 2018b; <https://wheat-urgi.versailles.inra.fr/>;

APPENDIX C). The physical locations of these SNPs were plotted against their genetic positions (Wang et al., 2014), leading to a S-shape distribution of the SNPs (Figure 3.7). The SNPs mapped to the linkage block of 62.57-82.16 cM, which traverses the centromere, spanned a wide physical region of 91.73-748.85 Mb on chromosome 3B (Figure 3.7 and Wang et al., 2014). The average cM/Mb ratio along the entire chromosome was 0.169, while the cM/Mb ratio of the pericentromeric region (91.73-748.85 Mb) was 0.030. Thus, the proximal regions had significantly lower meiotic recombination than the distal regions for the 3B-3E homoeologous pair.

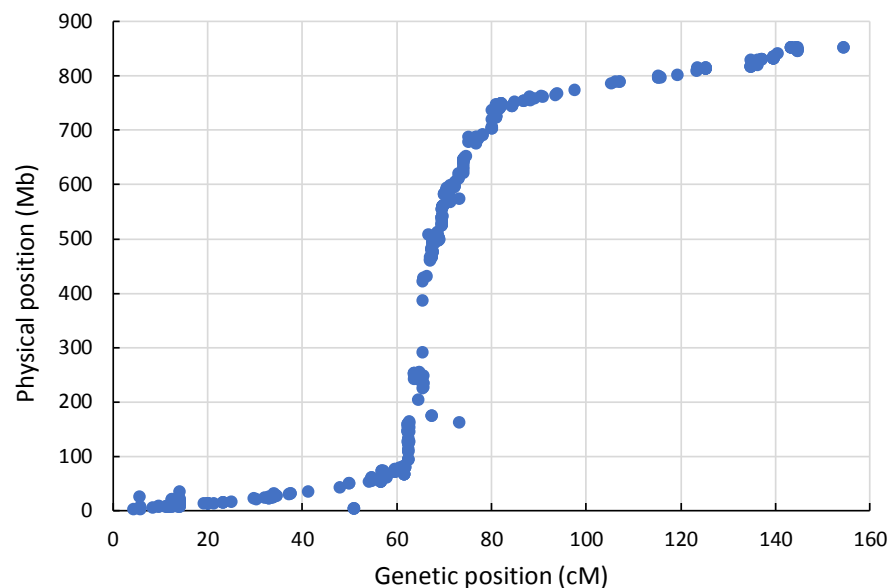


Figure 3.7. The genetic and physical positions of 3B-3E polymorphic SNPs on chromosome 3B.

All 79 3B-3E meiotic recombinants identified through the testcross-like procedure were delineated by the high-throughput wheat 90K SNP assay in addition to FGISH. Some of the 3B-3E recombinant chromosomes had a similar composition, which could not be precisely distinguished from each other by FGISH and SNP analysis. Under this circumstance, only one of the similar recombinants was used in the construction of the bin map. Thus, 46 critical 3B-3E recombinants were included in the homoeologous recombination-based physical mapping of

chromosome 3B. As a result, wheat chromosome 3B was partitioned into 38 distinct bins with 17 on the short arm and 21 on the long arm based on the FGISH and SNP delineation results (Figure 3.8b). The 3B-3E polymorphic SNPs with unambiguous physical positions ($n = 429$) were assigned to the respective bins of chromosome 3B. The genotypes of the 46 recombinants at 429 SNP loci are graphically illustrated in Figure 3.8a. The physical size of chromosome 3B and 3E segments in a recombinant was estimated according to the physical location of the middle point between the SNPs immediately flanking the recombination breakpoint in the IWGSC RefSeq

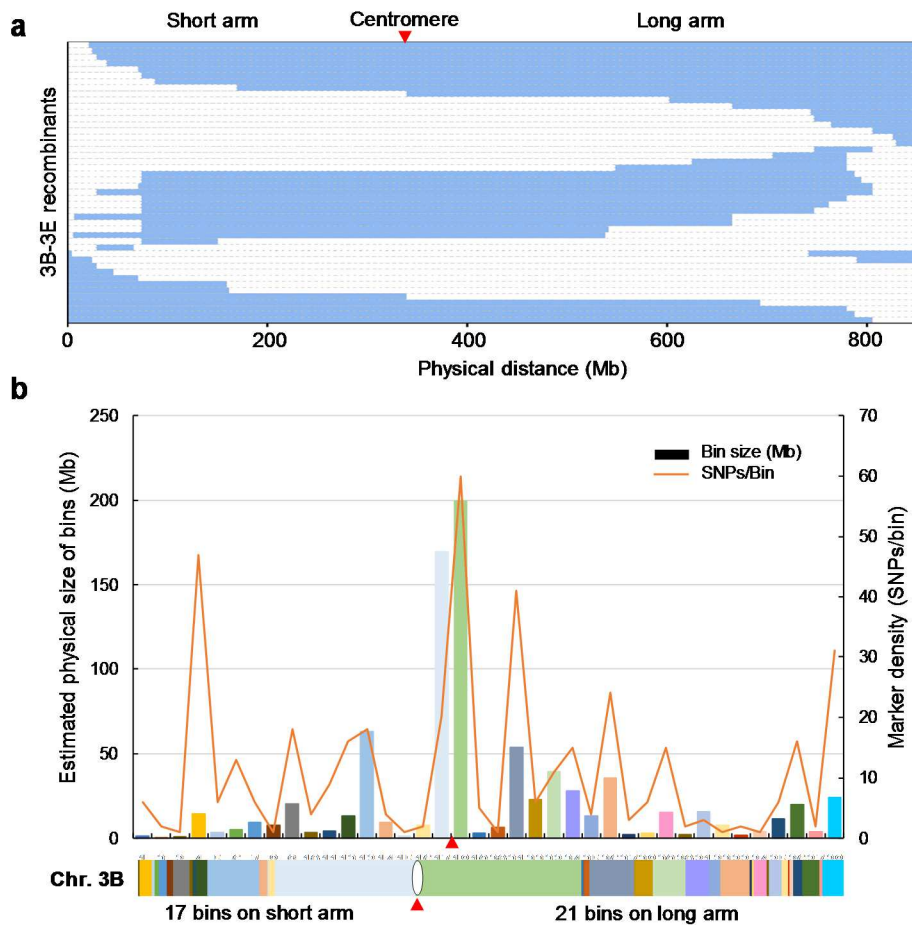


Figure 3.8. Integrative SNP genotyping and FGISH analysis of 3B-3E recombinants. *a* Graphical representation of the wheat 90K SNP genotypes for the 46 3B-3E recombinants. Blue and white bars represent chromosome 3E and 3B segments, respectively. The red triangle points to the centromere position. *b* Composite bin map of wheat chromosome 3B. Vertical bars indicate physical size of the bins, and curved lines indicate SNP density within each bin. All bins were color-coded according to their physical size and locations in the horizontal ideogram of chromosome 3B (*bottom*).

v2.0 (<https://wheat-urgi.versailles.inra.fr/>). Subsequently, the recombination breakpoints of the 46 critical 3B-3E recombinants were determined on chromosome 3B (APPENDIX D). Overall, the SNP-resolved recombinant chromosome compositions were consistent with their FGISH patterns in terms of size and location of the recombinant segments. Minor discrepancy was observed with the 3B-3E recombinants I-19, I-23, II-18, and III-1 in their FGISH and SNP results. A small chromosome 3B fragment was detected at the end of 3ES by SNP assay in I-19 (~4.85 Mb) and I-23 (~3.74 Mb), but they were not detected by FGISH. In II-18, a small chromosome 3E segment (~3.32 Mb) was detected at the end of 3BS by the SNP assay, but not by FGISH. On the other hand, FGISH detected a small chromosome 3B segment at both ends of the recombinant III-1, but the 3B segment on the long arm was not resolved by the SNP assay due probably to the lack of diagnostic SNP markers within that region (Figure 3.8 and APPENDIX D).



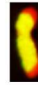

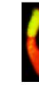
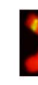







A composite bin map was constructed for chromosome 3B based on the SNP and FGISH delineation results of the recombinants, indicating the bin size and number of SNPs in each bin (Figure 3.8b). The physical size of the chromosomal bins ranged from 0.42 Mb to 199.76 Mb. The SNP density within a bin ranged from 1 to 60 SNPs/bin. The two bins located in the pericentromeric region were significantly larger than others toward the distal regions on both arms, indicating lower homoeologous recombination near the centromere than in other chromosomal regions (Figure 3.8b).

Development of chromosome 3E-specific STARP markers and construction of a comparative physical map for chromosomes 3E, 3B, 3A, and 3D

We developed 22 PCR-based STARP markers from 33 chromosome 3E-specific SNPs identified by Luo et al. (2017) (APPENDIX E). They were used to genotype 13 representative

3B-3E recombinants involving different regions of chromosome 3E. Subsequently, these STARP markers were physically assigned to 10 bins of chromosome 3E (i.e. A-J) (Table 3.2 and Figure 3.9).

Table 3.2. Chromosome 3E-specific STARP markers spanning distinct regions along the entire chromosome^a

STARP Markers	III-1	III-3	III-11	III-14	VI-1	IV-3	IV-1	II-23	II-21	IV-8	II-13	IV-4	I-11	Chromosome 3E bins
														
<i>Xwgc2200</i>	-	-	-	-	+	-	+	-	-	-	-	-	-	A
<i>Xwgc2201</i>	+	-	-	-	+	-	-	-	-	-	-	-	-	B
<i>Xwgc2202</i>	+	+	+	+	+	+	-	-	-	-	-	-	-	C
<i>Xwgc2203</i>	+	+	+	+	+	+	-	-	-	-	-	-	-	C
<i>Xwgc2204</i>	+	+	+	+	+	-	-	-	-	-	-	-	+	D
<i>Xwgc2205</i>	+	+	+	+	+	-	-	-	-	-	-	-	+	D
<i>Xwgc2206</i>	+	+	+	+	+	-	-	-	-	-	-	-	+	D
<i>Xwgc2207</i>	+	+	+	+	-	-	-	-	-	-	-	-	+	E
<i>Xwgc2208</i>	+	+	+	+	-	-	-	-	-	-	-	-	+	E
<i>Xwgc2209</i>	+	+	+	+	-	-	-	-	-	-	-	-	+	E
<i>Xwgc2210</i>	+	+	+	+	-	-	-	-	-	-	-	-	+	E
<i>Xwgc2211</i>	+	+	+	+	-	-	-	-	-	-	-	-	+	E
<i>Xwgc2212</i>	+	+	+	+	-	-	-	-	-	-	-	-	+	E
<i>Xwgc2213</i>	+	+	+	+	-	-	-	-	-	-	-	-	+	E
<i>Xwgc2214</i>	+	+	+	+	-	-	-	-	-	-	-	-	+	E
<i>Xwgc2215</i>	+	+	+	+	-	-	-	-	-	-	-	-	+	E
<i>Xwgc2216</i>	+	+	+	+	-	-	-	-	-	-	-	-	+	E
<i>Xwgc2217</i>	+	+	+	+	-	-	-	-	-	-	-	+	+	F
<i>Xwgc2218</i>	+	+	+	-	-	-	-	-	-	+	+	+	+	G
<i>Xwgc2219</i>	+	+	-	-	-	-	-	-	+	+	+	-	+	H
<i>Xwgc2220</i>	-	-	-	-	-	-	+	+	+	+	+	-	+	I
<i>Xwgc2221</i>	-	-	-	-	-	-	+	+	+	-	+	-	+	J

^a “+” and “-” indicate the presence and absence of chromosome 3E-specific marker allele, respectively. Letters “A-J” refer to the chromosome bins harboring the marker loci. The critical 3B-3E recombinants with chromosome 3E segments FGISH-painted in yellow-green and chromosome 3B segments in red were used to resolve the markers.

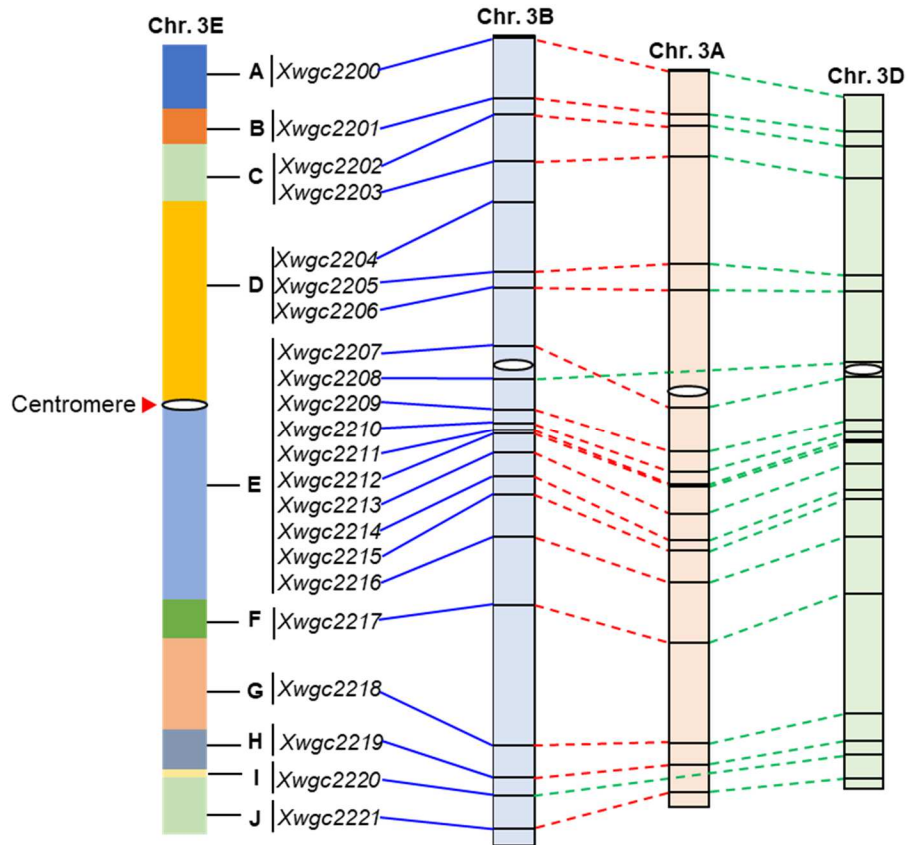


Figure 3.9. Comparative physical map of *Th. elongatum* chromosome 3E and wheat chromosomes 3A, 3B, and 3D at 22 chromosome 3E-specific STARP (i.e. SNP) marker loci. The 3B-3E recombinant-resolved bins of chromosome 3E were color-coded as illustrated in the ideogram of chromosome 3E (left). The collinear marker loci between chromosomes 3E and 3B were connected by solid blue lines, and those among chromosomes 3B, 3A, and 3D by red and green dashed lines.

All 22 chromosome 3E-specific STARP markers were aligned to wheat chromosome 3B by BLASTn against the IWGSC RefSeq v2.0 (<https://wheat-urgi.versailles.inra.fr/>). The STARP marker loci within each of the bins C, D, and E on chromosome 3E were ordered according to their physical locations on chromosome 3B. Also, the homoeologous alleles of the STARP markers on wheat chromosomes 3A and 3D were identified by BLASTn against the IWGSC RefSeq v2.0 (<https://wheat-urgi.versailles.inra.fr/>). The physical locations of the homoeologous SNP loci for the STARP markers on chromosomes 3A, 3B, and 3D were listed in APPENDIX E. A comparative physical map was constructed for chromosomes 3E, 3A, 3B, and 3D based on the

FGISH patterns of the 3B-3E recombinants and physical locations of the wheat homoeologous loci of the chromosome 3E-specific SNPs (Figure 3.9). *Xwgc2204* had a homoeologous allele on chromosome 3B, but not on 3A and 3D. *Xwgc2208* and *Xwgc2220* had a homoeologous allele on chromosome 3B and 3D, but not on 3A. Also, a pericentromeric inversion was observed between *Xwgc2207* and *Xwgc2208* (Figure 3.9). Overall, these chromosome 3E-specific STARP (SNP) markers had a good collinearity with their homoeologous counterparts on wheat chromosomes 3A, 3B, and 3D. They are useful for the detection of chromosome 3E introgression in wheat and will dramatically improve the throughput and efficacy of homoeologous recombination-based chromosome engineering in wheat improvement.

Discussion

The wheat genome is homoeologous with the genomes of many wild grass species. This has made the wild grasses usable as a gene pool for wheat improvement by meiotic homoeologous recombination-based alien introgression. In addition, inducing homoeologous recombination between wheat and wild grass chromosomes provides a unique approach to physically dissect and map the complex polyploid genome of wheat as well as the genomes of the wild grasses. In this study, we inactivated the *Ph1* system of wheat to promote homoeologous pairing/recombination of wheat chromosome 3B with *Th. elongatum* chromosome 3E using *ph1b* mutant (Riley and Chapman, 1958; Riley et al., 1959; Sears, 1977). The 3B-3E meiotic pairing and recombination were significantly increased by *ph1b* mutant, but the primary recombination between these two homoeologous chromosomes occurred mostly in the distal regions.

Homologous chromosomes remained to pair and recombine preferentially under *ph1b* mutant condition although homoeologous pairing/recombination were induced. So, we used the primary or secondary 3B-3E recombinants to enhance homoeologous recombination of their 3E

segments with wheat chromosome 3B in the secondary and tertiary recombination cycles under *ph1b* mutant. In the successive *ph1b*-induced recombination cycles, the meiotic pairing/recombination partners (i.e. 3B-3E recombinant and 3B) shared a higher level of homology than the initial 3B-3E homoeologous pair. An elevated homology level enhanced meiotic pairing between the partners, and consequently promoted 3B-3E homoeologous recombination toward the proximal regions of these two homoeologous chromosomes. A clear shift of 3B-3E recombination breakpoints from the distal to proximal regions was observed in the order of the primary, secondary, and tertiary recombinants for this homoeologous pair. Thus, this strategy may potentially make the homoeologous recombination-coldspots, such as pericentromeric regions, more accessible for genome mapping and alien introgression. In addition, specific chromosomal regions of interest can be further partitioned and dissected in the properly-designed successive homoeologous recombination cycles. This will improve the resolution of homoeologous recombination-based molecular mapping for specific chromosomal regions and reduce the linkage drag in alien introgression as well.

Homoeologous chromosomes 3B and 3E paired in a frequency of 12.23% under *ph1b* mutant condition (Zhang et al., 2018a). We observed a recombination rate of 15.15% in the primary 3B-3E recombination cycle. Generally, a 3B-3E crossover should generate two recombinant gametes with each containing one of the reciprocal recombinant chromosomes. Thus, a 12.23% 3B-3E pairing frequency could lead to up to 24.46% (i.e. $2 \times 12.23\%$) 3B-3E recombinant gametes. The discrepancy between the expected and actual 3B-3E recombination rates (i.e. 24.46% vs. 15.15%) might result from the failure of recovering some of the recombinants, especially those involving small 3E or 3B segments, due to the limitation of FGISH in detecting small recombination segments.

Homology between pairing partners (i.e. 3B-3E recombinant and 3B) increased over the successive recombination cycles, subsequently leading to increased pairing frequency between the partners. The overall recombination rates between the pairing partners, including both homologous and homoeologous recombination, increased in the secondary and tertiary recombination cycles although the 3B-3E homoeologous recombination rates decreased from the primary (15.15%) to the secondary (11.46%) and tertiary (7.37%) recombination cycles. Lower 3B-3E homoeologous recombination rates were expected in the secondary and tertiary recombination cycles because 3B-3E recombination was forced to occur toward the proximal regions with a low recombination rate. Those regions were generally not reached in the previous recombination cycle. Therefore, homology increase of the secondary and tertiary pairing partners enhances the accessibility of the proximal chromosome regions for homoeologous recombination.

Interstitial 3B-3E recombinants were recovered in the primary, secondary, and tertiary recombination cycles in this study. The primary interstitial recombinants (III-1 and IV-1) should result from a double crossover on both arms of chromosomes 3B and 3E. This was consistent with the observation of 3B-3E ring bivalents in the special parental genotype of the primary recombination population. However, the 3B-3E interstitial recombinants identified in the secondary and tertiary recombination populations mostly resulted from two single crossovers occurring in the different recombination cycles (i.e. primary and secondary or tertiary). In addition, we recovered a double recombinant that contained two 3E-derived terminal recombinant chromosomes (V-1 and V-2) from the primary recombination population in this study. Presumably, it might result from a double crossover of chromosome 3E with chromosome 3B and 3D or 3A that paired in a trivalent or other multivalent pairing configuration involving

these homoeologous chromosomes. Under this circumstance, two 3E-involved recombinant chromosomes segregated into the same daughter cell at meiosis I, resulting in the gametes with two recombinant chromosomes involving 3E and two wheat homoeologous.

Homoeologous recombination can be recovered and delineated by molecular markers as well as FGISH. Molecular markers are useful landmarks for chromosome mapping and engineering. Advances in high-throughput molecular marker assays have dramatically improved the efficacy of homoeologous recombination-based genome study and alien introgression. However, the utility of molecular markers in chromosome research could be limited due to the lack of diagnostic markers in some chromosome regions. For instance, we detected a 3B-3E recombination breakpoint on the long arm of recombinant III-1 by FGISH. However, that recombination was not resolved by SNP markers because there were no diagnostic SNPs within that region. On the other hand, FGISH may be limited in its ability to differentiate small homoeologous chromosome segments although it provides direct visualization of homoeologous recombination. In this study, we resolved extra 3B-3E recombination events in several recombinants (I-19, I-23, and II-18) by SNP assays, which were not detected by FGISH. Evidently, both molecular markers and FGISH demonstrate their uniqueness and advantages in the recovery and delineation of homoeologous recombination for genome mapping and alien introgression. Integrative application of these two technologies in homoeologous recombination studies will enhance understanding of the genomes in wheat and its relatives, and diversify the wheat genome by harnessing the genetic variation of wild grasses.

Both wheat chromosome 3B and *Th. elongatum* chromosome 3E were physically partitioned into distinct bins by *ph1b*-induced 3B-3E homoeologous recombination. A total of 429 SNPs were assigned to 38 bins of chromosome 3B, generating a composite bin map for this

chromosome. In addition, 22 SNP-based STARP markers were developed and used to resolve 10 bins for chromosome 3E. A comparative physical map was constructed for all four homoeologous chromosomes, i.e. 3E, 3A, 3B, and 3D. Also, the 3B-3E recombination breakpoints mapped to different chromosome intervals along the entire homoeologous pair based on the FGISH patterns of the recombinants. The primary 3B-3E homoeologous recombination distributed in a pattern similar to homologous recombination on both arms (Saintenac et al., 2009). The majority of primary 3B-3E recombination clustered in the distal regions, although secondary and tertiary recombination shifted toward the proximal regions. In summary, this genomics-enabled homoeologous recombination-based mapping work provides a unique physical framework for further study of the 3B-3E homoeologous pair as well as the genomes of wheat and *Th. elongatum*.

References

- Anderson J, Ogihara Y, Sorrells M, Tanksley S (1992) Development of a chromosomal arm map for wheat based on RFLP markers. *Theor Appl Genet* 83:1035–1043
- Avni R, Nave M, Barad O, Baruch K, Twardziok SO, Gundlach H, Hale L, Mascher M, Spannagl M, Wiebe K, Jordan KW, Golan G, Deek J, Ben-Zvi G, Himmelbach A, MacLachlan RP, Sharpe AG, Fritz A, Ben-David R, Budak H, Fahima T, Korol A, Faris JD, Hernandez A, Mikel MA, Levy AA, Steffenson B, Maccaferri M, Tuberosa R, Cattivelli L, Faccioli P, Ceriotti A, Kashkush K, Pourkheirandish M, Komatsuda T, Eilam T, Sela H, Sharon A, Ohad N, Chamovitz DA, Mayer KFX, Stein N, Ronon G, Peleg Z, Pozniak CJ, Akhunov ED, Distelfeld A (2017) Wild emmer genome architecture and diversity elucidate wheat evolution and domestication. *Science* 357:93–97
- Cai X, Jones S (1997) Direct evidence for high level of autosyndetic pairing in hybrids of *Thinopyrum intermedium* and *Th. ponticum* with *Triticum aestivum*. *Theor Appl Genet* 95:568–572
- Cai X, Jones S, Murray T (1998) Molecular cytogenetic characterization of *Thinopyrum* and wheat–*Thinopyrum* translocated chromosomes in a wheat *Thinopyrum* amphiploid. *Chromosome Res* 6:185–189
- Cai X, Xu SS, Zhu X (2010) Mechanism of haploidy-dependent unreductional meiotic cell division in polyploid wheat. *Chromosoma* 119:295–285

Chen PD, Qi LL, Zhou B, Zhang SZ, Liu DJ (1995) Development and molecular cytogenetic analysis of wheat-*Haynaldia villosa* 6VS/6AL translocation lines specifying resistance to powdery mildew. *Theor Appl Genet* 91:1125–1128

Chen PD, You CF, Hu Y, Chen SW, Zhou B, Cao AZ, Wang XE (2013) Radiation-induced translocations with reduced *Haynaldia villosa* chromatin at the *Pm21* locus for powdery mildew resistance in wheat. *Molecular Breeding* 31:477–484

Choulet F, Alberti A, Theil S, Glover N, Barbe V, Daron J, Pingault L, Sourdille P, Couloux A, Paux E, Leroy P, Mangenot S, Guilhot N, Gouis J, Balfourier F, Alaux M, Jamilloux V, Poulain J, Durand C, Bellec A, Gaspin C, Safar J, Dolezel J, Rogers J, Vandepoele K, Aury J, Mayer K, Berges H, Quesneville H, Wincker P, Feuillet C (2014) Structural and functional partitioning of bread wheat chromosome 3B. *Science* 6194:1249721

Dai K, Zhao R, Shi M, Xiao J, Yu Z, Jia Q, Wang Z, Yuan C, Sun H, Cao A, Zhang R, Chen P, Li Y, Wang H, Wang X (2019) Dissection and cytological mapping of chromosome arm 4VS by the development of wheat-*Haynaldia villosa* structural aberration library. *Theor Appl Genet* <https://doi.org/10.1007/s00122-019-03452-8>

Danilova TV, Friebe B, Gill BS (2014) Development of a wheat single gene FISH map for analyzing homoeologous relationship and chromosomal rearrangements within the Triticeae. *Theor Appl Genet* 127:715–730

Danilova TV, Zhang G, Liu W, Friebe B, Gill BS (2017) Homoeologous recombination-based transfer and molecular cytogenetic mapping of a wheat streak mosaic virus and *Triticum* mosaic virus resistance gene *Wsm3* from *Thinopyrum intermedium* to wheat. *Theor Appl Genet* 130:549–556

Danilova TV, Friebe B, Gill BS (2019) Production of a complete set of wheat–barley group-7 chromosome recombinants with increased grain β -glucan content. *Theor Appl Genet* 132:3129–3141

Dvorak J, Terlizzi P, Zhang H, Resta P (1993) The evolution of polyploidy wheats: Identification of the A genome donor species. *Genome* 36:21–31

Endo TR, Gill BS (1996) The deletion stocks of common wheat. *J Hered* 87:295–307

Faris JD, Xu SS, Cai X, Friesen TL, Jin Y (2008) Molecular and cytogenetic characterization of a durum wheat-*Aegilops speltoides* chromosome translocation conferring resistance to stem rust. *Chromosome Res* 16:1097–1105

Friebe B, Jiang J, Raupp WJ, McIntosh RA, Gill BS (1996) Characterization of wheat–alien translocations conferring resistance to diseases and pests: current status. *Euphytica* 91:59–87

Gill BS, Friebe B, Endo TR (1991) Standard karyotype and nomenclature system for description of chromosome bands and structural aberrations in wheat (*Triticum aestivum*). *Genome* 34:830–839

- Jiang J, Friebe B, Gill BS (1994) Recent advances in alien gene transfer in wheat. *Euphytica* 73:199–212
- Kalavacharla V, Hossain K, Gu Y, Riera-Lizarazu O, Vales MI, Bhamidimarri S, Gonzalez-Hernandez JL, Maan SS, Kianian SF (2006) High-resolution radiation hybrid map of wheat chromosome 1D. *Genetics* 173:1089–1099
- Klindworth DL, Niu Z, Chao S, Friesen TL, Jin Y, Faris JD, Cai X, Xu SS (2012) Introgression and characterization of a goatgrass gene for a high level of resistance to Ug99 stem rust in tetraploid wheat. *G3* 2:665–673
- Li H, Dong Z, Ma C, Tian X, Qi Z, Wu N, Friebe B, Xiang Z, Xia Q, Liu W, Li T (2019) Physical mapping of stem rust resistance gene *Sr52* from *Dasypyrum villosum* based on *ph1b*-induced homoeologous recombination. *Int J Mol Sci* 20:4887
- Ling HQ, Ma B, Shi XL, Liu H, Dong LL, Sun H, Cao YH, Gao Q, Zheng SS, Li Y, Yu Y, Du HL, Qi M, Li Y, Lu HW, Yu H, Cui Y, Wang N, Chen CL, Wu HL, Zhao Y, Zhang JC, Li YW, Zhou WJ, Zhang BR, Hu WJ, Eijk MJT, Tang JF, Witsenboer HMA, Zhao SC, Li ZS, Zhang AM, Wang DW, Liang CZ (2018) Genome sequence of the progenitor of wheat A subgenome *Triticum urartu*. *Nature* 557:424–428
- Liu S, Anderson JA (2003) Targeted molecular mapping of a major wheat QTL for Fusarium head blight resistance using wheat ESTs and synteny with rice. *Genome* 46:817–823
- Liu W, Danilova TV, Rouse MN, Bowden RL, Friebe B, Gill BG (2013) Development and characterization of a compensating wheat-*Thinopyrum intermedium* Robertsonian translocation with *Sr44* resistance to stem rust (Ug99) *Theor Appl Genet* 126:1167–1177
- Long Y, Chao WS, Ma G, Xu SS, Qi L (2017) An innovative SNP genotyping method adapting to multiple platforms and throughputs. *Theor Appl Genet* 130:597–607
- Luo H, Dong L, Zhang K, Wang D, Zhao M, Li Y, Rong C, Qin H, Zhang A, Dong Z, Wang D (2017) High-throughput mining of E-genome-specific SNPs for characterizing *Thinopyrum elongatum* introgressions in common wheat. *Mol Ecol Res* 17:1318–1329
- Luo MC, Gu YQ, Puiu D, Wang H, Twardziok SO, Deal KR, Huo N, Zhu T, Wang L, Wang Y, McGuire PE, Liu S, Long H, Ramasamy RK, Rodriguez JC, Van SL, Yuan L, Wang Z, Xia Z, Xiao L, Anderson OD, Ouyang S, Liang Y, Zimin AV, Perrea G, Qi P, Bennetzen JL, Dai X, Dawson MW, Müller H, Kugler K, Rivarola-Duarte L, Spannagl M, Mayer KFX, Lu FH, Becan MW, Lerou P, Li P, You FM, Sun Q, Liu Z, Lyons E, Wicher T, Zalzberg SL, Devos KM, Dvořák J (2017) Genome sequence of the progenitor of the wheat D genome *Aegilops tauschii*. *Nature* 551:498–502
- Marcussen T, Sandve SR, Heier L, Spannagl M, Pfeifer M, IWGSC, Jakobsen KS, Wulff BBH, Steuernagel B, Mayer KFX, Olsen OA (2014) Ancient hybridizations among the ancestral genomes of bread wheat. *Science* 345:1250092

- McFadden ES, Sears ER (1946) The origin of *Triticum spelta* and its free-threshing hexaploid relatives. *J Hered* 37:107–116
- Niu Z, Klindworth DL, Friesen TL, Chao S, Jin Y, Cai X, Xu SS (2011) Targeted introgression of a wheat stem rust resistance gene by DNA marker-assisted chromosome engineering. *Genetics* 187:1011–1021
- Niu Z, Klindworth DL, Yu G, Friesen TL, Chao S, Jin Y, Cai X, Ohm J-B, Rasmussen JB, Xu SS (2014) Development and characterization of wheat lines carrying stem rust resistance gene *Sr43* derived from *Thinopyrum ponticum*. *Theor Appl Genet* 129:969–980
- Patokar C, Sepsi A, Schwarzacher T, Kishii M, Heslop-Harrison JS (2016) Molecular cytogenetic characterization of novel wheat-*Thinopyrum bessarabicum* recombinant lines carrying intercalary translocations. *Chromosoma* 125:163–172
- Pont C, Leroy T, Seidel M, Tondelli A, Duchemin W, Armisen D, Lang D, Bustos-Korts D, Goué N, Balfourier F, Molnar-Lang M, Lage J, Kilian B, Ozkan H, Waite D, Dyer S, Alaux M, Letellier T, Russell J, Keller B, Eeuwijk F, Spannagl M, Mayer K, Waugh R, Stein N, Cattivelli L, Haberer G, Charvet G, Salse J (2019) Tracing the Ancestry of Modern Bread Wheats. *Nature Genetics* 51:905–911
- Qi L, Echalié B, Friebe B, Gill B (2003) Molecular characterization of a set of wheat deletion stocks for use in chromosome bin mapping of ESTs. *Funct Integr Genomics* 3:39–55
- Qi LL, Echalié B, Chao S, Lazo GR, Butler GE, Anderson OD, Akhunov ED, Dvorak J, Linkiewicz AM, Ratnasiri A, Dubcovsky J, Bermudez-Kandianis CE, Greene RA, Kantety R, La Rota CM, Munkvold JD, Sorrells SF, Sorrells ME, Dilbirligi M, Sidhu D, Erayman M, Randhawa HS, Sandhu D, Bondareva SN, Gill KS, Mahmoud AA, Ma XF, Miftahudin Gustafson JP, Conley EJ, Nduati V, Gonzalez-Hernandez JL, Anderson JA, Peng JH, Lapitan NLV, Hossain KG, Kalavacharla V, Kianian SF, Pathan MS, Zhang DS, Nguyen HT, Choi DW, Fenton RD, Close TJ, McGuire PE, Qualset CO, Gill BS (2004) A chromosome bin map of 16,000 expressed sequence tag loci and distribution of genes among the three genomes of polyploid wheat. *Genetics* 168:701–712
- Qi LL, Friebe B, Zhang P, Gill BS (2007) Homoeologous recombination, chromosome engineering and crop improvement. *Chromosome Res* 15:3–19
- Qi LL, Pumphrey MO, Friebe B, Chen PD, Gill BS (2008) Molecular cytogenetic characterization of alien introgressions with gene *Fhb3* for resistance to Fusarium head blight disease of wheat. *Theor Appl Genet* 117:1155–1166
- Rey M, Martín AC, Smedley M, Hayta S, Harwood W, Shaw P, Moore G (2018) Magnesium increases homoeologous crossover frequency during meiosis in *ZIP4* (*Ph1* gene) mutant wheat-wild relative hybrids. *Front Plant Sci* 9:509
- Riley R, Chapman V (1958) Genetic control of the cytologically diploid behaviour of hexaploid wheat. *Nature* 182:713–715

- Riley R, Chapman V, Kimber G (1959) Genetic control of chromosome pairing in intergeneric hybrids with wheat. *Nature* 185:1244–1246
- Roberts MA, Reader SM, Dalgliesh C, Miller TE, Foote TN, Fish LJ, Snape JW, Moore G (1999) Induction and characterization of *Ph1* wheat mutants. *Genetics* 153:1909–1918
- Saintenac C, Falque M, Martin OC, Paux E, Feuillet C, Sourdille P (2009) Detailed recombination studies along chromosome 3B provide new insights on crossover distribution in wheat (*Triticum aestivum* L.). *Genetics* 181:393–403
- Sears ER (1954) The aneuploids of common wheat. *Mo Agric Exp Stn Res Bull* 572:1–59
- Sears ER (1966) Nullisomic-tetrasomic combinations in hexaploid wheat. In: Riley R, Lewis KR (eds) *Chromosome manipulation and plant genetics*. Oliver and Boyd, Edinburgh, pp 29–45
- Sears ER (1977) An induced mutant with homoeologous pairing in common wheat. *Can J Genet Cytol* 19:585–593
- International Wheat Genome Sequencing Consortium (IWGSC) (2018) Shifting the limits in wheat research and breeding using a fully annotated reference genome. *Science* 361:6403
- Wang S, Wong D, Forrest K, Allen A, Huang BE, Maccaferri M, Salvi S, Milner SG, Cattivelli L, Mastrangelo AM, Whan A, Stephen S, Barker G, Wieseke R, Plieske J, International Wheat Genome Sequencing Consortium, Lillemo M, Mather D, Appels R, Dolferus R, Brown–Guedira G, Korol A, Akhunova AR, Feuillet C, Salse J, Morgante M, Pozniak C, Luo MC, Dvorak J, Morell M, Dubcovsky J, Ganai M, Tuberosa R, Lawley C, Mikoulitch I, Cavanagh C, Edwards KJ, Hayden M, Akhunov E (2014) Characterization of polyploid wheat genomic diversity using a high-density 90,000 single nucleotide polymorphism array. *Plant Biotechnol J* 12:787–796
- Zhang R, Yao R, Sun D, Sun B, Feng Y, Zhang W, Zhang M (2017) Development of V chromosome alterations and physical mapping of molecular markers specific to *Dasypyrum villosum*. *Mol Breeding* 37:67
- Zhang W, Cao Y, Zhang M, Zhu X, Ren S, Long Y, Gyawali Y, Chao S, Xu S, and Cai X (2017) Meiotic homoeologous recombination-based alien gene introgression in the genomics era of wheat. *Crop Sci* 57:1189–1198
- Zhang W, Zhang M, Zhu X, Cao Y, Sun Q, Ma G, Chao S, Yan C, Xu S, Cai X (2018a) Molecular cytogenetic and genomic analyses reveal new insights into the origin of the wheat B genome. *Theor Appl Genet* 131:365–375
- Zhang W, Zhu X, Zhang M, Chao S, Xu S, Cai X (2018b) Meiotic homoeologous recombination-based mapping of wheat chromosome 2B and its homoeologues in *Aegilops speltoides* and *Thinopyrum elongatum*. *Theor Appl Genet* 131:2381–2395
- Zhang W, Zhu X, Zhang M, Shi G, Liu Z, Cai X (2019) Chromosome engineering-mediated introgression and molecular mapping of novel *Aegilops speltoides*-derived resistance genes for tan spot and Septoria nodorum blotch diseases in wheat. *Theor Appl Genet* 132:2605–2614

Zhao R, Wang H, Xiao J, Bie T, Cheng S, Jia Q, Yuan C, Zhang R, Cao A, Chen P, Wang X (2013) Induction of 4VS chromosome recombinants using the CS *ph1b* mutant and mapping of the wheat yellow mosaic virus resistance gene from *Haynaldia villosa*. Theor Appl Genet 126:2921–2930

**CHAPTER 4. DISSECTION AND PHYSICAL MAPPING OF WHEAT CHROMOSOME
7B BY INDUCING MEIOTIC RECOMBINATION WITH ITS HOMOEOLOGUES IN
AEGILOPS SPELTOIDES AND *THINOPYRUM ELONGATUM***

Abstract

Recombination-based chromosome engineering of wheat chromosomes and its homoeologous counterparts from wild species produces reciprocal translocations, diversifying and enrichment of evolutionary-omitted wheat genetic variation. Available of high-throughput genotyping tools and wheat-related genome sequences data advance cytogenetic studies. Genomics-enabled cytogenetic analysis of homoeologous recombinants in a throughput scale and improved efficacy. In this study, we exploited meiotic recombination of wheat chromosome 7B and its homoeologous chromosomes 7E in *Thinopyrum elongatum* and 7S in *Aegilops speltoides* using *ph1b*-induced system to characterize wheat chromosome 7B, 7E, and 7S. We developed four diagnostic semi-thermal asymmetric reverse PCR (STARP) markers for homoeologous pair 7B-7E and eleven for 7B-7S to pre-screen their recombination populations. The possible recombinants detected by STARP markers were verified by fluorescent genomic *in situ* hybridization (FGISH). A total of 29 7B-7E recombinants and 61 7B-7S recombinants were identified for wheat 90K SNP genotyping analysis. Combination of the FGISH patterns and SNPs genotype data of 7B-7E and 7B-7S recombinants and the wheat genome reference sequence data, chromosome 7B was physically partitioned into 44 bins with 523 polymorphic SNPs. A composite bin map of chromosome 7B was constructed, illustrating the estimated bins size and SNPs density. The unique physical framework of chromosome 7B is potentially benefit genome studies of wheat and its relatives. The genetic-enabled chromosome engineering

accelerates the process of wheat genome enrichment and gene introgression for wheat improvement.

Introduction

Common wheat (*Triticum aestivum* L., $2n=6x=42$), one of the most important food crops for humans worldwide, originated from two rounds of spontaneous hybridization of three diploid ancestors and subsequent chromosome doubling (Feldman and Levy, 2012; Faris, 2014; Pont et al., 2019). Domestication and targeted breeding efforts have led to production and selection of adaptable and productive wheat genotypes. The polyploid origin of the wheat genome and extensive breeding practices have narrowed down the genetic variability of the wheat genome, which has become a genetic bottleneck for modern wheat improvement (Venske et al., 2019). The wild relatives of wheat maintain considerable genetic diversity, including numerous favorable genes for agronomically-important traits of wheat. Many of them contain a genome homoeologous with the wheat genome. They represent an invaluable gene source for wheat improvement and can be utilized to expand genetic variability of wheat by diversifying and enriching the wheat genome (Qi et al., 2007).

Meiotic homoeologous recombination-based chromosome engineering shuffles the genetic material of related genomes and leads to gene introgression from one genome to another. It has been widely used in alien introgression and genome studies of wheat and its relatives (Liu et al., 2013; Zhao et al., 2013; Niu et al., 2014; Danilova et al., 2017; Zhang et al., 2018a, b, 2019; Dai et al., 2019; Li et al., 2019). Wheat has a diploidization system, called *Ph* (pairing homoeologous) genes. *Ph* genes ensure homologous pairing and recombination by preventing homoeologous chromosomes from pairing and recombination in meiosis (Riley and Chapman, 1958; Riley et al., 1959). So, eliminating or inactivating *Ph* genes enhances homoeologous

pairing and recombination. Wheat *ph1b* mutant, a large deletion at the *Ph1* locus (Riley and Chapman, 1958; Riley et al., 1959; Sears, 1977; Gyawali et al., 2019), has been used to induce meiotic homoeologous recombination for chromosome mapping and alien introgression (Lukaszewski et al., 2004; Niu et al., 2011; Zhao et al., 2013; Patokar et al., 2016; Danilova et al., 2017; Zhang et al., 2018b). Through this approach, wheat chromosomes 2B and 3B was partitioned and physically mapped (Zhang et al., 2018b; Zhang et al., 2020). Two wild species-derived disease resistance genes were identified, mapped, and introgressed into wheat by homoeologous recombination (Zhang et al., 2019).

Wheat has a complex polyploid genome with three homoeologous subgenomes (i.e. A, B, and D). Homoeologous recombination-based partitioning and dissection of individual chromosomes provide a unique approach for genome study in wheat and its relatives. Wheat aneuploids and genome-wide deletion stocks have been developed and employed to physically dissect the wheat genome and individual chromosomes (Sears, 1954, 1966; Gill et al., 1991; Endo and Gill, 1996; Qi et al., 2003). In addition, various wheat-alien species chromosome translocations have been produced and applied in chromosome dissection and mapping (Chen et al., 1995, 2005; Friebe et al., 1996; Rabinovich, 1998; Crasta et al., 2000). Generally, meiotic homoeologous recombination-derived translocations or recombinants are genetically more stable than non-compensating translocations, and more useful for alien introgression in germplasm development. Also, meiotic homoeologous recombinants are invaluable resources for genome and chromosome studies, including physical mapping, gene identification, and genome evolution, etc. (Riley et al., 1968; Mago et al., 2002; Chen et al., 2005; Niu et al., 2011; Zhao et al., 2013; Zhang et al., 2018a,b, 2019; Dai et al., 2019).

The availability of wheat reference genome sequences and high-throughput genotyping technologies have dramatically improved the efficacy and throughput of homoeologous recombination-based chromosome engineering for alien introgression and genome studies in wheat and its relatives (Wang et al., 2014; Avni et al., 2017; Luo et al. 2017; The International Wheat Genome Sequencing Consortium (IWGSC), 2018; Ling et al., 2018; Tatiana et al., 2014, 2017; Zhang et al., 2017, 2018a,b, 2019; Dai et al., 2019). Wheat chromosomes can be painted differentially from those in the homoeologous genomes of wheat-related species by fluorescence genomic *in situ* hybridization (FGISH), allowing for visual detection of chromosomal segments with different genomic origin in homoeologous recombinants (Schwarzacher et al., 1992; Cai et al., 1998; Zhao et al., 2013; Niu et al., 2014; Zhang et al., 2018b, 2019; Li et al., 2019; Zhang et al., 2020). Recently, the high-throughput SNP genotyping technology and SNP-derived PCR marker systems, including kompetitive allele specific PCR (KASP) (Neelam et al., 2013) and semi-thermal asymmetric reverse PCR (STARP) (Long et al., 2017; Zhang et al., 2017), have permitted the homoeologous recombination-based genome study and alien introgression in a significantly improved throughput (Tatiana et al., 2017, 2019; Zhang et al., 2017, 2018a,b, 2019). FGISH and SNP markers demarcate wheat and alien chromosomal segments in the homoeologous recombinants cytogenetically and molecularly, respectively. Integrative FGISH and marker analysis of homoeologous recombination leads to the construction of unique physical frameworks useful for genome studies in wheat and its relatives (Zhang et al., 2018b; Zhang et al., 2020). In this study, we aimed to cytogenetically dissect wheat chromosome 7B by inducing meiotic recombination with its homoeologous counterparts 7E from *Th. elongatum* ($2n = 2x = 14$, EE) and 7S from *Ae. speltoides* ($2n = 2x = 14$, SS), and to physically map chromosome 7B by delineating the 7B-7E and 7B-7S recombinants with SNP markers and FGISH.

Materials and methods

Plant materials

Common wheat ‘Chinese Spring’ (CS) -*Ae. speltoides* disomic substitution line 7S(7B) [DS 7S(7B)] (Friebe et al., 2011) and CS *ph1b* mutant were supplied by the wheat Genetics Resource Center at Kansas State University, USA. The CS-*Th. elongatum* disomic substitution line 7E(7B) [DS 7E(7B)] was provided by J. Dvorak at University of California, Davis, USA.

Construction of the *ph1b*-induced homoeologous recombination populations

The disomic substitution lines [DS 7E(7B) and DS 7S(7B)] and CS *ph1b* mutant were employed to construct the special genotype that was double monosomic for chromosomes 7E and 7B or 7S and 7B, and homozygous for *ph1b* mutant following the procedure illustrated in Figure 4.1. The *Ph1*-specific molecular marker *PSR574* or *PSR128* (Roberts et al., 1999) were used to select homozygous *ph1b* mutant for inducing homoeologous 7E-7B and 7S-7B recombination. Chromosome 7E-specific marker *Xgpw1164* and 7S-specific marker *Xgpw7518* were used to select the individuals double monosomic for chromosome 7E and 7B, and chromosomes 7S and 7B, respectively (Sourdille et al., 2004). Meiotic homoeologous recombination of wheat chromosome 7B with *Th. elongatum* chromosome 7E and *Ae. speltoides* chromosome 7S were induced by the *ph1b* mutant in the newly-constructed special genotypes. 7B-7E and 7B-7S recombinant gametes were recovered by backcrossing to the respective substitution line as described by Zhang et al. (2017) and Zhang et al. (2020).

Molecular markers analysis

Chromosome-specific STARP markers were developed within the pericentromeric and distal regions on both arms for the homoeologous pairs 7B-7E and 7B-7S (Long et al., 2017; Zhang et al., 2017). They were used to screen the recombination populations for 7B-7E and 7B-

7S recombinants and chromosome aberrations involving the pericentromeric and distal regions of both homoeologous pairs as illustrated in Figure 4.2. PCR was performed as described by Long et al. (2017). STARP amplicons were sorted using IR² 4200 DNA Analyzer with denaturing polyacrylamide gel electrophoresis (LI-COR, Lincoln, NE, USA).

Wheat 90K SNP assay was performed on the Illumina BeadStation and iScan instruments following the manufacturer's protocols. GenomeStudio v2.0.4 software was used to analyze and call SNP clusters (Illumina Inc., San Diego, CA, USA) following the procedure of Zhang et al. (2018b).

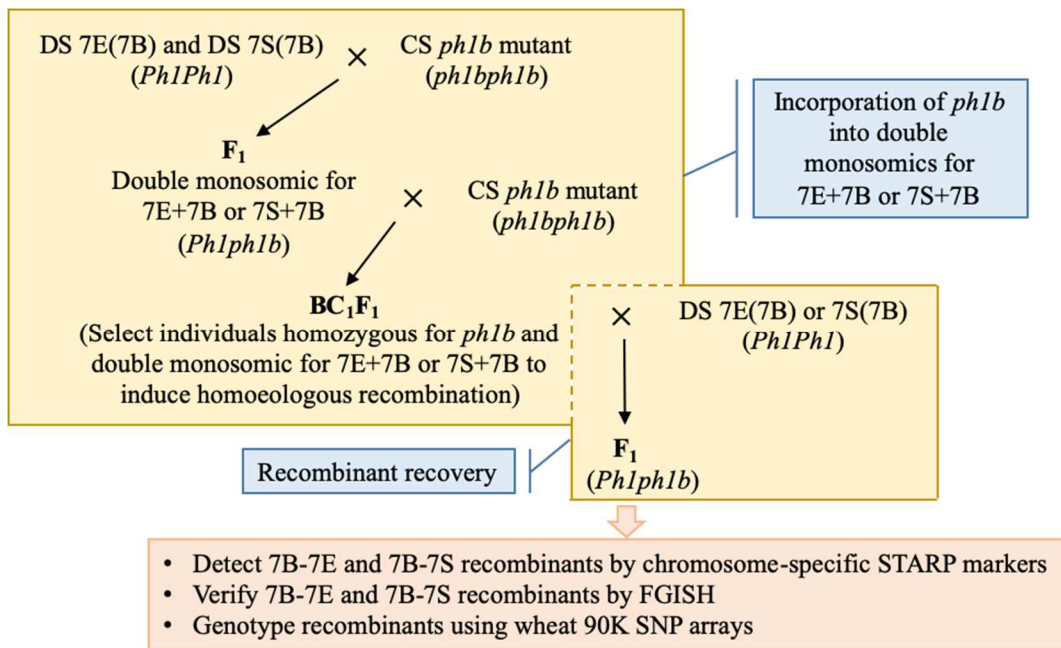


Figure 4.1. Diagram showing induction, recovery, detection, and characterization of 7B-7E and 7B-7S homoeologous recombinants.

Cytogenetic analysis

Fluorescent genomic *in situ* hybridization (FGISH) was performed to differentiate *Ae. speltoides* and *Th. elongatum* chromatin from wheat chromatin as described by Cai et al. (1998).

Total genomic DNA of *Ae. speltoides* and *Th. elongatum* were used to prepare FGISH probes

with Bio-16-dUTP by nick translation (Enzo Life Science, Inc., USA). Total CS genomic DNA was used as blocking after being sheered in boiling 0.4M NaOH for 40-50 mins. Hybridization signals on *Ae. speltoides* and *Th. elongatum* chromatin were detected with fluorescein isothiocyanate-conjugated avidin (FITC-avidin) (Vector Laboratories, Inc., USA) as green-yellow and wheat chromatin was counter-stained with propidium iodide (PI) as red color.

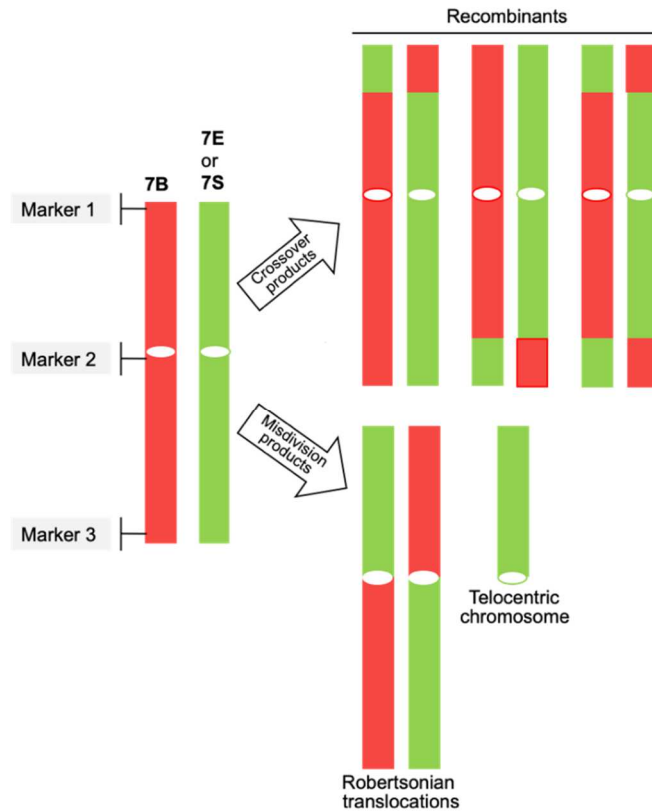


Figure 4.2. Ideogram of wheat chromosome 7B (red), *Th. elongatum* chromosome 7E (green), and *Ae. speltoides* chromosome 7S (green) illustrating chromosome-specific molecular markers for the detection of meiotic homoeologous recombinants and chromosome aberrations.

Microscopy

Fluorescence microscope (BX51, Olympus, Japan) with a CCD camera (DP72, Olympus, Japan) was used to visualize the FGISH signals and chromosomes. FGISH images were captured by Olympus CellSens software.

Results

Development and validation of chromosome-specific STARP markers for the detection of 7B-7E and 7B-7S recombinants

Wheat 90K SNP assay mapped 2,347 SNPs to wheat chromosome 7B (Wang et al., 2014). Out of these mapped SNPs, we identified 1,018 polymorphic for the homoeologous pair 7B-7S (Zhang et al., 2018) and 1,055 polymorphic for 7B-7E. Initially, the polymorphic SNPs, physically mapped to the pericentromeric and distal regions on both arms of chromosome 7B, were used as queries to search against the IWGSC RefSeq v2.0 and the genome sequences *Ae. speltoides* (<https://wheat-urgi.versailles.inra.fr/>), and *Th. elongatum* genome sequences (<http://blast.ncbi.nlm.nih.gov/blast/Blast.cgi>) by BLASTn. The SNPs polymorphic between 7B and 7E or 7B and 7S, and also polymorphic between 7B/7S/7E and 7A/7D were ideal for the development of STARP markers diagnostic for the homoeologous pairs 7B-7E and 7B-7S. However, most of the 90K SNPs within the targeted regions were found to be polymorphic for the homoeologous pair 7B-7E or 7B-7S, but not polymorphic between 7B/7S/7E and 7A/7D. Under this circumstance, we searched for new SNPs nearby those 90K SNP loci within the targeted region on chromosome 7B by BLASTn and sequence alignment analysis to identify the SNPs diagnostic for the homoeologous pair 7B-7E or 7B-7S in the CS wheat background.

Four diagnostic STARP markers were developed for the homoeologous pair 7B-7E and eleven for 7B-7S (Table 4.1). They were located either within the pericentromeric region on the long arm or the terminal region on the short or long arm. Three 7B-7E specific markers (*Xwgc2300*, *Xwgc2301*, and *Xwgc2303*) and three 7B-7S specific markers (*Xwgc2304*, *Xwgc2307*, and *Xwgc2313*) were selected to pre-screen the homoeologous recombination population for 7B-7E or 7B-7S recombinants. They resided within the terminal region of the

short arm, pericentromeric region on the long arm, and terminal region of the long arm in each of these two homoeologous pairs (Table 4.1 and Figure 4.3a). *Xwgc2304* and *Xwgc2307* are codominant markers and *Xwgc2313* is dominant for the homoeologous pair 7B-7S. *Xwgc2300*, *Xwgc2301*, and *Xwgc2303* are dominant markers for the homoeologous pair 7B-7E (Figure 4.3a).

Table 4.1. SNP-derived STARP markers specific for the 7B-7E and 7B-7S homoeologous pairs

Marker	SNP alleles	SNP location ^a	Forward and reverse primers ^b	Polymorphism
<i>Xwgc2300</i>	[A/G]	7BS(603,689bp)	F1: [Tail 2]-5' GACGATGACAGCTCCGCA 3' F2: [Tail 1]-5' GACGATGACAGATCCTCG 3' R: 5' CCAAGTTTGCAGAGGCAGAAG 3'	7B-7E
<i>Xwgc2301</i>	[T/C]	7BL(379,299,483bp)	F1: [Tail 2]-5' AAAGCTGTCCGGTTTACTCTT 3' F2: [Tail 1]-5' AAAGCTGTCCGATTTGCCATC 3' R: 5' CGCATGCATGTGCGTGTA 3'	7B-7E
<i>Xwgc2302</i>	[A/G]	7BL(386,081,398bp)	F1: [Tail 2]-5' CATTCTACCCTACGCACGTA 3' F2: [Tail 1]-5' CATTCTACCCTACGCATACG 3' R: 5' CCATTTCATTCCATTGAGGACAA	7B-7E
<i>Xwgc2303</i>	[T/G]	7BL(758,280,973bp)	F1: [Tail 2]-5' CCAGGAGTCAACACAAAAT 3' F2: [Tail 1]-5' CCAGGAGTCAACACAAGAG 3' R: 5' GCACTCCGCTCTGTATGC 3'	7B-7E
<i>Xwgc2304</i>	[C/A]	7BS(3,695,566bp)	F1: [Tail 1]-5' TATGCTCTTATTCGCGACC 3' F2: [Tail 2]-5' TATGCTCTTATTCGCGGTA 3' R: 5' GCGTACGTCAATCACGGATCAG 3'	7B-7S
<i>Xwgc2305</i>	[A/G]	7BS(4,121,716bp)	F1: [Tail 2]-5' CGTAAGCAATGTAGTTTATATGA 3' F2: [Tail 1]-5' CGTAAGCAATGTAGTTTATACCGG 3' R: 5' GAGAGTGGTCCCTGTCTGATG 3'	7B-7S
<i>Xwgc2306</i>	[A/G]	7BS(244,368,635bp)	F1: [Tail 1]-5' GCAATAAAATATAACAATCAACAAAATAAA 3' F2: [Tail 2]-5' GCAATAAAATATAACAATCAACAAAACCAG 3' R: 5' GGTTTGCCGTCTATCATATCAGC 3'	7B-7S
<i>Xwgc2307</i>	[T/C]	7BL(379,299,435bp)	F1: [Tail 2]-5' GTCCATGGCATCACAACGT 3' F2: [Tail 1]-5' GTCCTTGGCATCACACAGC 3' R: 5' CAGCTTTGTTGCCACATTTC 3'	7B-7S
<i>Xwgc2308</i>	[A/G]	7BL(396,962,870bp)	F1: [Tail 1]-5' TCATTCATTTTCATACAGAGACG 3' F2: [Tail 2]-5' TCATTCATTTTCATACAGAAGCA 3' R: 5' CCAATGATGTTACTTTGATGCTGC 3'	7B-7S
<i>Xwgc2309</i>	[A/G]	7BL(465,240,318bp)	F1: [Tail 1]-5' ACAAGGTGACAAGACTTCTCA 3' F2: [Tail 2]-5' ACAAGGTGACAAGACTTTCCG 3' R: 5' GGTTTGCCGTCTATCATATCAGC 3'	7B-7S
<i>Xwgc2310</i>	[A/G]	7BL(654,629,105bp)	F1: [Tail 2]-5' CCATATCGTAGCACATGAACGTA 3' F2: [Tail 1]-5' CCATATCGTAGCACATGAATATG 3' R: 5' TCTTCACTGTGGGTCGGCA 3'	7B-7S
<i>Xwgc2311</i>	[G/T]	7BL(655,975,979bp)	F1: [Tail 1]-5' GACCACCTGTGTGTGTACATG 3' F2: [Tail 2]-5' GACCACCTGTGTGTGTAACCT 3' R: 5' CCCTACAACAACAAAAGAACAT 3'	7B-7S
<i>Xwgc2312</i>	[A/G]	7BL(754,572,320bp)	F1: [Tail 1]-5' TGACATGGGAGCCCTAGG 3' F2: [Tail 2]-5' TGACATGGGAGCCCGGA 3' R: 5' CCCCAGGCAGACAATTCATTTT 3'	7B-7S
<i>Xwgc2313</i>	[A/G]	7BL(754,572,989bp)	F1: [Tail 2]-5' ACTAAGACCCTGAACAAGCAAA 3' F2: [Tail 1]-5' ACTGAGACCCTGAACAAGTCAG 3' R: 5' CTGAATTCCACAGGAGATACCATTAA 3'	7B-7S
<i>Xwgc2314</i>	[C/G]	7BL(754,570,889bp)	F1: [Tail 1]-5' AGAGGAAACGGGGCCAC 3' F2: [Tail 2]-5' GGCCTCGTCAGTGTACCTG 3' R: 5' GCTAAAGTATTTATCTCTGCCCA 3'	7B-7S

^aSNP locations in the IWGSC Reference Sequence v2.0 assembly (IWGSC RefSeq v2.0)

^b[Tail1] = GCAACAGGAACCAGCTATGAC; [Tail2] = GACGCAAGTGAGCAGTATGAC

Meanwhile, we identified six 7B-7E and eighteen 7B-7S recombinants by FGISH to verify the utility of the chromosome-specific STARP markers in recombinant detection. Marker analysis of the FGISH-delineated 7B-7E and 7B-7S recombinants provided clear genotyping results consistent with their FGISH patterns in terms of recombination breakpoints and sizes of the recombinant segments (Figure 4.3). Therefore, these STARP markers were diagnostic for differentiating wheat chromosome 7B from *Th. elongatum* chromosome 7E and *Ae. speltoides* chromosome 7S in the targeted regions, and useful in detecting the recombinants of 7B with 7E and 7S.

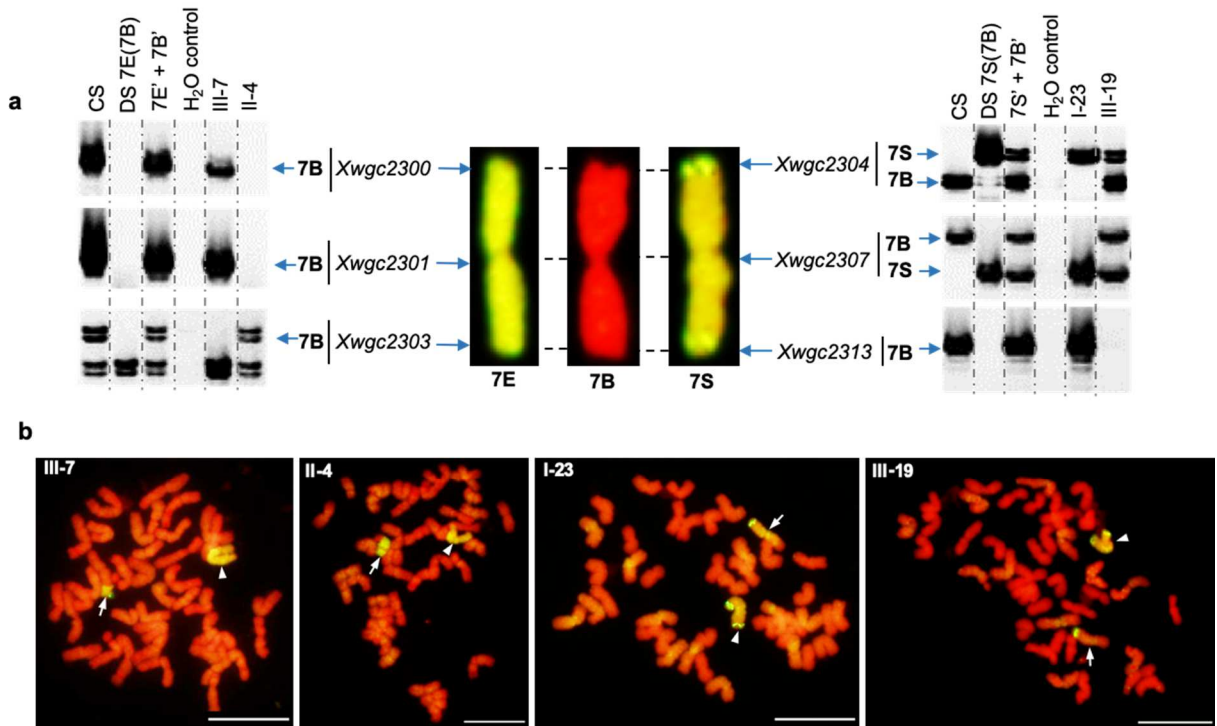


Figure 4.3. Detection of 7B-7E and 7B-7S recombinants by chromosome-specific STARP markers (a) and verification of the recombinants by FGISH (b). FGISH painted wheat chromosomes/segments in red, and chromosome 7E and 7S and their segments in yellow-green. Arrows point to 7B-7E or 7B-7S recombinant chromosomes and arrowheads to chromosome 7E or 7S. III-7 and II-4 are 7B-7E recombinants, designated 7BS·7BL-7EL and 7ES·7EL-7BL, respectively. I-23 and III-19 are 7B-7S recombinants, designated 7SS·7SL-7BL and 7BS·7BL-7SL, respectively. Scale bar = 10µm.

Pre-screening and verification of 7B-7E and 7B-7S recombinants and aberrations by STARP markers and FGISH

The chromosome-specific STARP markers we developed for the homoeologous pairs 7B-7E and 7B-7S enabled us to pre-screen large recombination populations for recombinants involving these two homoeologous pairs in a timely manner. We pre-screened 578 individuals from the 7B-7E recombination population using the three STARP markers diagnostic for 7B-7E (i.e. *Xwgc2300*, *Xwgc2301*, and *Xwgc2303*) and found that 116 of them possibly contained a 7B-7E recombinant chromosome or other structural aberration involving chromosome 7B. Similarly, 288 individuals from the 7B-7S recombination population were pre-screened by the STARP markers diagnostic for 7B-7S (i.e. *Xwgc2304*, *Xwgc2307*, and *Xwgc2313*). Seventy-nine of them were found to contain a 7B-7S recombinant chromosome or other structural aberration involving chromosome 7B.

The *ph1b* mutant induces homoeologous recombination of wheat chromosome 7B with *Th. elongatum* chromosome 7E and *Ae. speltoides* 7S, as well as with its wheat homoeologues 7A and 7D in the special genotypes. In addition, other chromosome aberrations, including Robertsonian translocations, telocentric chromosomes, and chromosome deletions, could occur in the special genotypes. So, we expected to see those chromosome aberrations in addition to 7B-7E or 7B-7S recombinants among the STARP marker-based selections. FGISH was performed to all selected individuals. Out of 116 individuals selected from the 7B-7E recombination population, we detected 23 7B-7E recombinants, seven Robertsonian translocations, and one telocentric chromosome of 7E. One or two copies of chromosome 7E were visualized in the rest of 116 individuals (n=85). Similarly, FGISH analysis detected 43 7B-7S recombinants, four Robertsonian translocations, and three deletions of chromosome 7S from the 79 individuals

selected from the 7B-7S recombination population. In addition, FGISH detected two extra interstitial 7B-7S recombination events (V-10 and V-11 in Figure 4.4), which regions were not covered by the STARP markers. The other 29 selected individuals contained one or two copies of chromosome 7S.

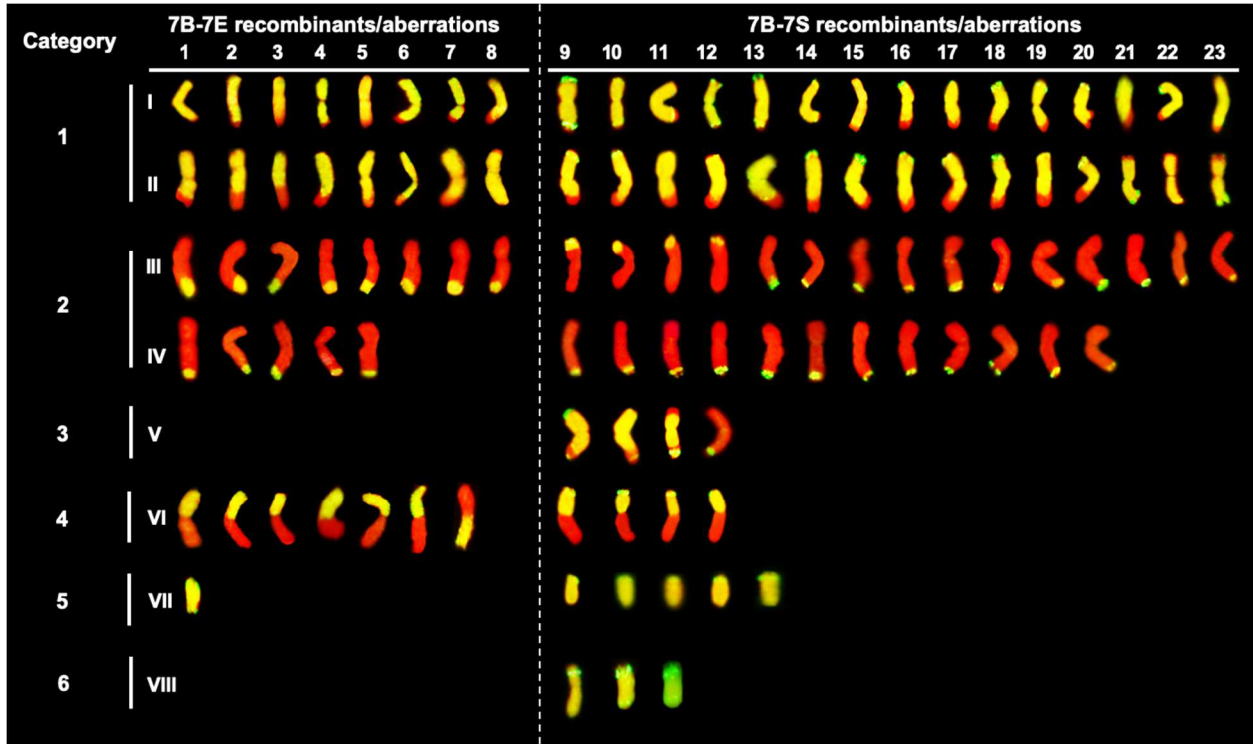


Figure 4.4. FGISH-painted 7B-7E and 7B-7S recombinant chromosomes and aberrations in six categories, including Category 1 (I & II) - terminal recombinants with a small 7B segment, Category 2 (III & IV) - terminal recombinants with a small 7E or 7S segment, Category 3 (V) - interstitial recombinants, Category 4 (VI) - Robertsonian translocation, Category 5 (VII) - telocentric 7E or 7S chromosomes, and Category 6 (VIII) - chromosome 7E or 7S deletions. Chromosome 7B segments were painted in red, and 7E and 7S chromosome segments in yellow-green.

All 7B-7E and 7B-7S recombinants and chromosome aberrations are categorized into six categories according to their structural compositions and their FGISH patterns are displayed in Figure 4.4. A total of 29 7B-7E and 61 7B-7S recombinants were detected and verified by chromosome-specific markers and FGISH (Table 4.2). The number of single crossover-derived

Table 4.2. Six categories of 7B-7E and 7B-7S recombinants and aberrations

Homoeologous pairs	No. individuals screened	Crossover-derived			Misdivision products		Deletion
		Category 1	Category 2	Category 3	Category 4	Category 5	Category 6*
7B-7E	644	16	13	0	7	1	0
		2.48%	2.02%	0.00%	1.09%	0.16%	0.00%
7B-7S	436	30	27	4	4	5	3
		6.88%	6.19%	0.92%	0.92%	1.14%	0.69%

*See Figure 4 for detailed description of these six categories of recombinants and aberrations.

7B-7S terminal recombinants with a small 7B segment (Category 1) and with small 7S segment (Category 2) were 30 and 27, with a recombination rate of 6.88% and 6.19%, respectively (Figure 4.4 and Table 4.2). The single crossover-derived 7B-7E recombination rates for Category 1 and Category 2 were 2.48% and 2.02%, respectively, which were much lower than 7B-7S. Two double crossover-derived (V-9 and V-12) and two multiple crossover-derived (V-10 and V-11) interstitial recombinants were detected for the homoeologous pair 7B-7S, but not for 7B-7E. In addition, we identified seven 7B-7E Robertsonian translocations (1.09%) and one 7E telocentric chromosome (0.16%) from the 7B-7E recombination population, and four 7B-7S Robertsonian translocations (0.92%) and five 7S telocentric chromosomes (1.15%) from the 7B-7S recombination population. Also, three long arm deletions of chromosome 7S (0.69%) were identified from the 7B-7S recombination population, including VIII-9, VIII-10, and VIII-11 (Figure 4.4). Most of the 7B-7E and 7B-7S recombinants involved their long arms. Only one recombination event was recovered in the short arm of the homoeologous pair 7B-7E and eight in the short arm of 7B-7S (APPENDIX F). The detailed compositions and pedigree of all 7B-7E and 7B-7S recombinants and aberrations are provided in APPENDIX F.

Homoeologous recombination-based delineation and dissection of wheat chromosome 7B

The 7B-7E and 7B-7S recombinants were genotyped together with several controls, including CS, DS 7E(7B), DS 7S(7B), and double monosomics 7E'+7B' and 7S'+7B', using wheat 90K SNP arrays. Out of 2,347 SNPs mapped to wheat chromosome 7B (Wang et al., 2014), we identified 430 SNPs polymorphic for the homoeologous pair 7B-7E and 352 for 7B-7S. Both 7B-7E and 7B-7S shared 241 polymorphic SNPs. So, a total of 541 wheat 90K SNPs were polymorphic for the homoeologous pairs 7B-7E and 7B-7S, with 189 specifically for 7B-

7E and 111 for 7B-7S (Figure 4.5a). Overall, the homoeologous pair 7B-7E had a high level of polymorphism than 7B-7S at the 90K SNP loci.

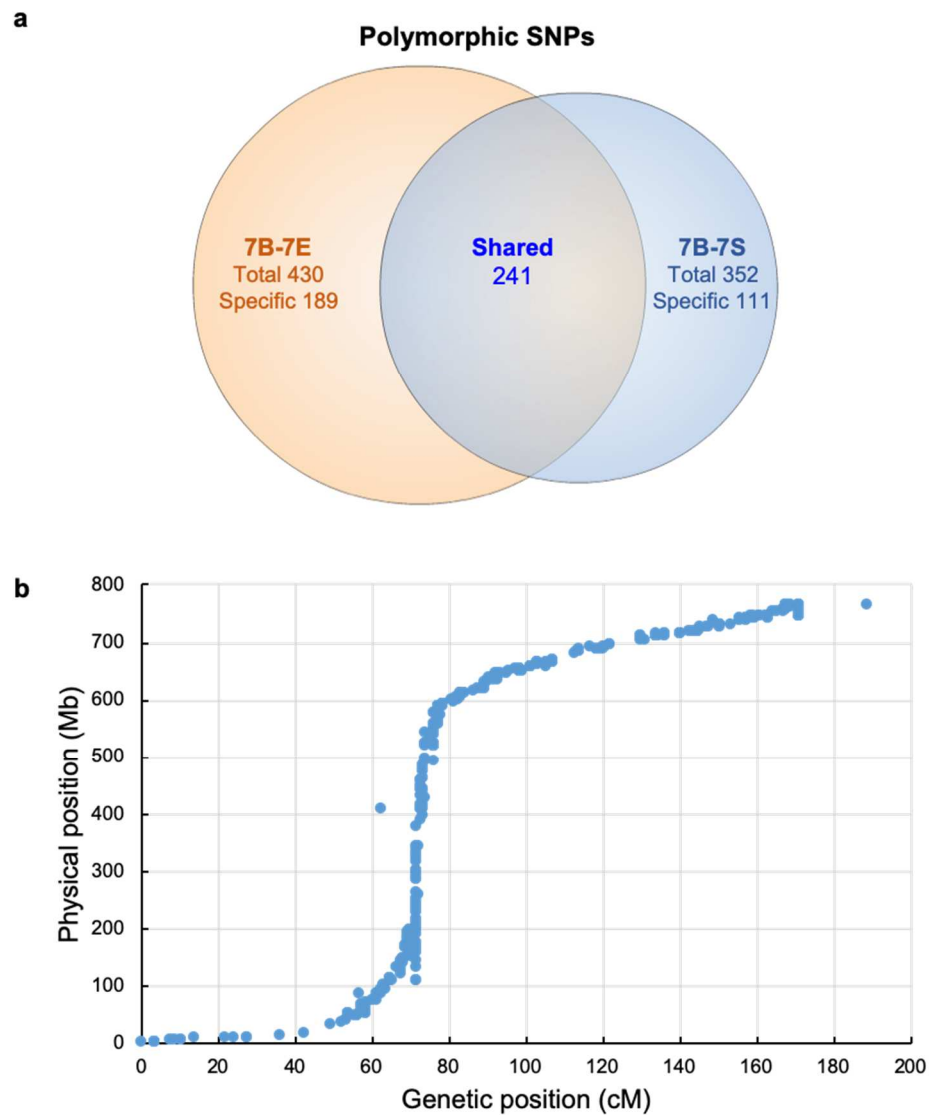


Figure 4.5. Polymorphic SNPs of the homoeologous pair 7B-7E and 7B-7S (*a*) and their genetic and physical positions on chromosome 7B (*b*).

The SNPs polymorphic for the homoeologous pair 7B-7E and 7B-7S genetically mapped to chromosome 7B (Wang et al. 2014). We physically aligned the SNP loci onto chromosome 7B by BLASTn against the IWGSC RefSeq v2.0 (<https://wheat-urgi.versailles.inra.fr/>) (APPENDIX G). The sequenced wheat 7B chromosome size in the RefSeq v2.0 was 763.71 Mb, which

covered 85.91% of the entire chromosome 7B (889 Mb) (<https://wheat-urgi.versailles.inra.fr/>; Šafář et al. 2010). The genetic and physical positions of the SNPs were plotted as an “S” curve distribution in Figure 4.5b. The average cM/Mb ratio along the entire chromosome was 0.25. The SNPs within the linkage block of 67.47-78.44 cM, which traverses the centromere, span the physical region of 118.71-589.04 Mb, with an average cM/Mb ratio of 0.023. Thus, the homoeologous recombination rate in the proximal region was significantly lower than the distal region for the homoeologous pairs 7B-7E and 7B-7S.

Overall, the wheat 90K SNP genotyping results of the 7B-7E and 7B-7S recombinants were consistent with their FGISH patterns except a few discrepancies. Wheat 90K SNP genotyping identified IV-20 as an interstitial 7B-7S recombinant with a small 7S segment proximal to a 7BL terminal segment on the long arm. However, the 7BL terminal segment in IV-20 was not detected by FGISH (Figure 4.4; APPENDIX H). IV-1 was initially identified as a 7B-7E terminal recombinant with a small 7E segment at the end of the long arm by FGISH. But, wheat 90K SNP genotyping detected a terminal 7B segment distal to the 7E segment on the long arm, identifying it as an interstitial 7B-7E recombinant (Figure 4.4; APPENDIX H). Some of the 7B-7E and 7B-7S recombinants had similar FGISH patterns and could not be resolved by SNPs. Only one of the recombinants with the same SNP genotype was used for delineation and dissection analysis. Thus, we selected 26 representative 7B-7E recombinants involving 23 unique recombination breakpoints and 38 representative 7B-7S recombinants involving 31 unique breakpoints to partition wheat chromosome 7B. The integrative SNP and FGISH analysis of the 7B-7E and 7B-7S recombinants resolved their recombination breakpoints and segment sizes. Consequently, wheat chromosome 7B was physically partitioned and dissected by these homoeologous recombination events. The overall results about 7B-7E and 7B-7S recombination-

based partition and dissection of wheat chromosome 7B are graphically illustrated in Figure 4.6. The physical locations of the recombination breakpoints were estimated as the middle point between the SNP loci immediately flanking the breakpoint (APPENDIX H). Most of the 7B-7E and 7B-7S recombination breakpoints clustered in the distal regions of the long arm (Figure 4.6).

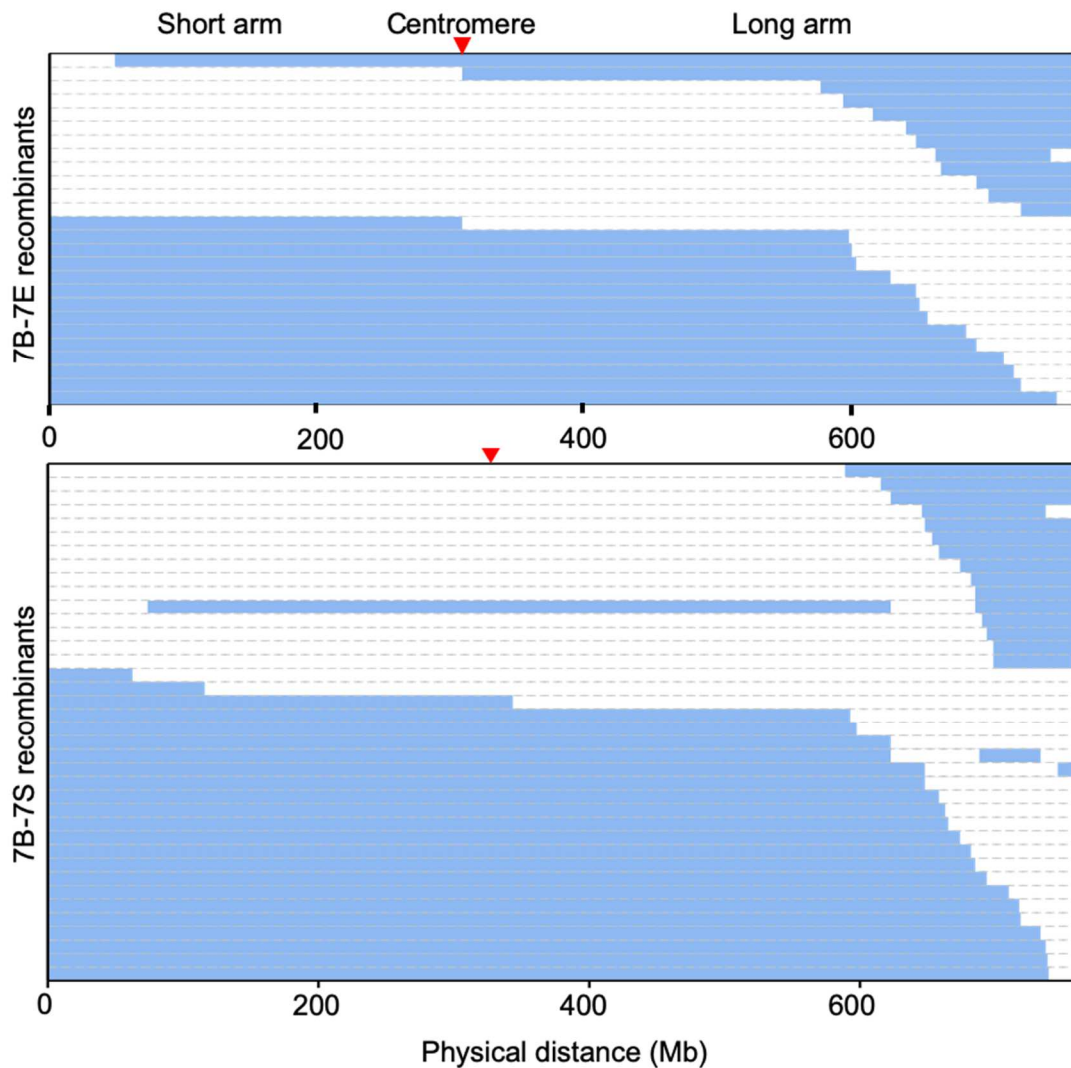


Figure 4.6. Graphical representation of the 26 7B-7E recombinants (*top*) and 38 7B-7S recombinants (*bottom*), showing their SNP genotypes and FGISH patterns. Blue bars represent chromosome 7E or 7S segments and open bars for 7B segments. Red triangles point to the centromere positions.

Construction of the composite bin map for wheat chromosome 7B

Chromosome 7B was partitioned into 24 bins with 430 SNPs assigned in based on the FGISH patterns and SNP genotyping data of the 26 representative 7B-7E recombinants. Likewise, chromosome 7B was partitioned into 32 bins with 352 SNPs assigned in based on the SNP data and FGISH patterns of the 38 representative 7B-7S recombinants. A composite bin map was constructed for chromosome 7B individually based on the 7B-7E and 7B-7S recombination, respectively (APPENDIX I). In addition, we integrated the SNP data and FGISH patterns of all representative 7B-7E and 7B-7S recombinants to construct a more informative composite bin map for wheat chromosome 7B. The integrative genetic and physical analysis with the reference genome sequence of the IWGSC RefSeq v2.0 (<https://wheat-urgi.versailles.inra.fr/>) led to the informative composite bin map containing 44 distinct bins and 523 SNPs (Figure 4.7). The estimated bin size ranged from 0.84 Mb to 266.74 Mb and the SNP density within each of the bins ranged from 1 to 107 (APPENDIX J). Two pericentromeric bins were significantly larger than others toward the distal regions on both arms, indicating fewer homoeologous recombination near the centromere region than other chromosomal region for the homoeologous pairs 7B-7E and 7B-7S.

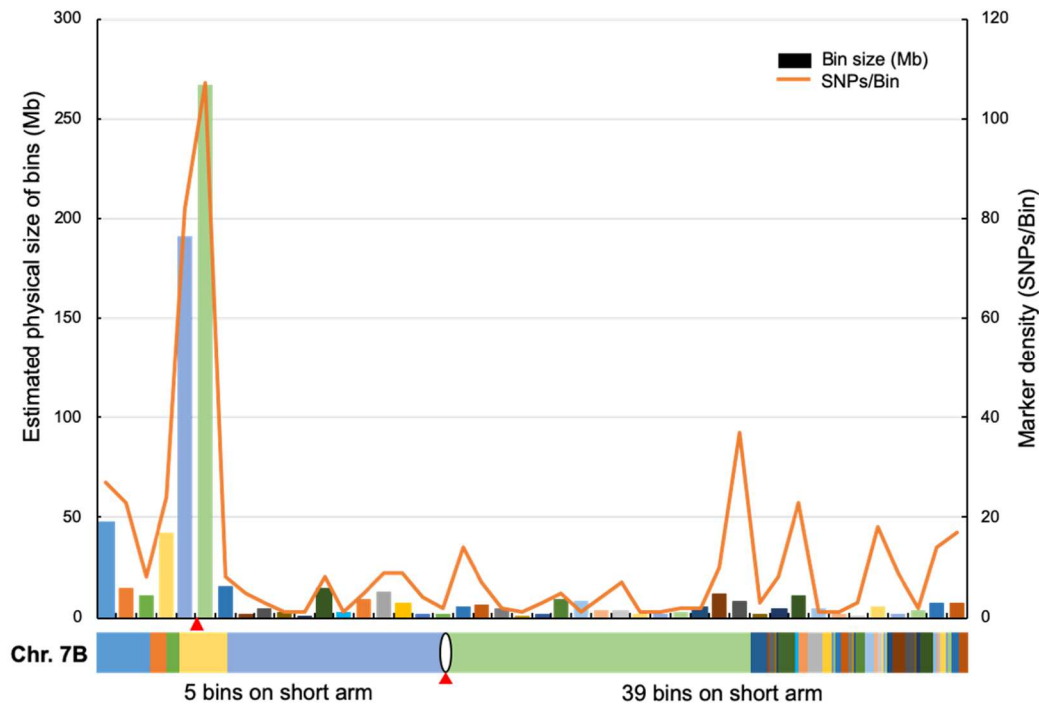


Figure 4.7. Composite bin map of wheat chromosome 7B and corresponding partitioned chromosome 7B. Vertical bars indicate physical size of the bins, and curved lines indicate SNP numbers within each bin. All bins were color-coded according to their physical size and locations in the horizontal ideogram of chromosome 7B (*bottom*). Red triangles point to the centromere.

Discussion

Meiotic homoeologous recombination-based chromosome engineering generates genetically compensating recombinants for genome studies and genetic diversification of wheat and its relatives. Over the recent years, rapid advances in genomics and associated technologies have dramatically increased the efficacy and throughput of homoeologous recombination-based chromosome engineering in alien introgression and provided a unique approach of investigating the complex polyploid genome of wheat (Zhang et al., 2017, 2018a,b, 2019; Zhang et al., 2020). The availability of the wheat reference genome sequence IWGSC RefSeq v2.0 (<https://wheat-urgi.versailles.inra.fr/>) and the genome sequences of *Ae. speltoides* and *Th. elongatum* permitted us to survey the polymorphisms of wheat chromosome 7B with its homoeologous counterparts 7S in *Ae. speltoides* and 7E in *Th. elongatum* for chromosome-specific marker development.

Through that approach, we identified homoeoalleles at multiple SNP loci diagnostic for the pericentromeric regions and distal regions on both arms of the homoeologous pairs 7B-7E and 7B-7S. The chromosome-specific STARP markers developed from the diagnostic SNPs tagged the critical homoeologous regions of chromosomes 7B, 7E, and 7S, allowing for pre-screening of large recombination populations for 7B-7E and 7B-7S recombinants. Thus, chromosome-specific DNA markers enable homoeologous recombination-based chromosome engineering in a large scale and improved efficacy. We induced and recovered a total of 29 7B-7E and 61 7B-7S recombinants using this genomics-enabled chromosome engineering technology. Integrative SNP genotyping and FGISH analysis of the recombinants partitioned wheat chromosome 7B into 44 distinct bins with 523 SNPs assigned in, providing a unique homoeologous recombination-based physical framework to wheat genome study. Overall, the homoeologous pair 7B-7S had a significantly higher recombination rate than 7B-7E. Also, multiple crossover-derived recombinants were recovered for 7B-7S, but not for 7B-7E. In addition, SNP analysis indicated that the homoeologous pair 7B-7S had lower polymorphism than 7B-7E. All these results suggest that *Ae. speltoides* chromosome 7S has a higher homology level with wheat chromosome 7B than *Th. elongatum* chromosome 7E.

The majority of 7B-7E and 7B-7S recombination events clustered in the distal and sub-distal regions of these two homoeologous pairs. No 7B-7E and 7B-7S recombination events were recovered within the large pericentromeric region (>1/2 physical length of entire chromosome 7B) (Figure 4.7). Also, we observed extremely low recombination with the short arms of both homoeologous pairs, especially for 7B-7E. This might result from the 4AL/7BS translocation involved in chromosome 7B, where the terminal 7BS segment was replaced by a 4AL segment (Devos et al., 1995; Miftahudin et al., 2004). Apparently, absence of the terminal region on 7BS

limited its recombination with the homoeologous regions on 7E and 7S. This was probably why 7B-7E and 7B-7S recombination was so low on the short arms.

Meiotic homoeologous recombination could occur between wheat and alien chromosomes, but also between wheat homoeologous chromosomes from different wheat subgenomes (A, B, and D) under the *ph1b* mutant condition. In this study, we used the *ph1b* mutant to induce 7B-7E and 7B-7S recombination under the double monosomic conditions (i.e. 7B'+7E' and 7B'+7S'). This should prioritize homoeologous recombination of chromosome 7B with 7E and 7S as expected. However, chromosome 7B under a monosomic condition (i.e. 7B') might occasionally recombine with 7A or 7D by forming a heteromorphic trivalent during meiotic pairing. Similarly, chromosome 7E or 7S could occasionally recombine with chromosome 7A or 7D. Also, chromosome aberrations, including Robertsonian translocation, telocentric chromosomes, and deletions, occurred in the special genotypes. These untargeted homoeologous recombination and chromosome aberrations complicated the marker-based pre-screening for recombinants and led to false pre-selection of the recombinants. We identified 23 7B-7E recombinants from 116 individuals pre-selected by STARP markers and 43 7B-7S recombinants from 79 pre-selected individuals. The rest of the pre-selected individuals were verified as non-crossover-derived 7B-7E or 7B-7S recombinants by FGISH, including chromosome aberrations and possibly the recombinants of chromosome 7B with 7A or 7D.

Both homologous and homoeologous recombination can be resolved by DNA markers. But, only homoeologous recombination can be visualized by FGISH, making it unique for genome study. We took this advantage of homoeologous recombination to partition wheat chromosome 7B for physical mapping by performing integrative marker and FGISH analysis of the 7B-7E and 7B-7S recombinants. The composite bin map of chromosome 7B constructed

through this approach provided a unique physical framework to wheat genome study. However, this homoeologous recombination-based chromosome mapping may confront limitations imposed by the physical coverage of markers on the targeted chromosomes and resolution of FGISH in chromatin detection. In this study, we identified a total of 29 7B-7E and 61 7B-7S recombinants. Some of the recombinants with close recombination breakpoints could not be distinguished from each other by FGISH. Also, they could not be resolved by the wheat 90K SNP genotyping assay due to the lack of diagnostic SNPs within the chromosomal regions between the breakpoints. So, we used only one of those recombinants for chromosome mapping. Thus, increasing marker coverage on the recombination chromosomes can make the similar recombinants resolvable and consequently improve the resolution of homoeologous recombination-based chromosome mapping. On the other hand, small recombination segments, which cannot be visualized by FGISH, may be detectable by the diagnostic markers tagging the segments. For instance, wheat 90K SNP genotyping assay detected a tiny 7BL terminal segment in the 7B-7S recombinant chromosome of IV-20 and a tiny 7EL terminal segment in the 7B-7E recombinant chromosome of IV-1. But both terminal segments were too small to be visualized by FGISH (Figure 4.4; APPENDIX H). In the same manner, FGISH might be able to detect the recombination segments that are not resolvable by markers due to the lack of diagnostic markers within the chromosomal region involved in the recombination, such as the interstitial recombination segments in the 7B-7S recombinants V-10 and V-11 (Figure 4.4) and the homoeologous recombination reported by Zhang et al. (2020).

In summary, we physically dissected wheat chromosome 7B by homoeologous recombination-based chromosome engineering and developed a unique physical framework of chromosome 7B useful for wheat genome study. In addition, the 7B-7E and 7B-7S recombinants

diversify and enrich the wheat genome and represent a useful gene source for wheat improvement. The genomics-enabled chromosome engineering pipeline we developed in this study will further facilitate homoeologous recombination-based genome studies and alien introgression in wheat improvement.

References

- Avni R, Nave M, Barad O, Baruch K, Twardziok SO, Gundlach H, Hale L, Mascher M, Spannagl M, Wiebe K, Jordan KW, Golan G, Deek J, Ben-Zvi G, Himmelbach A, MacLachlan RP, Sharpe AG, Fritz A, Ben-David R, Budak H, Fahima T, Korol A, Faris JD, Hernandez A, Mikel MA, Levy AA, Steffenson B, Maccaferri M, Tuberosa R, Cattivelli L, Faccioli P, Ceriotti A, Kashkush K, Pourkheirandish M, Komatsuda T, Eilam T, Sela H, Sharon A, Ohad N, Chamovitz DA, Mayer KFX, Stein N, Ronon G, Peleg Z, Pozniak CJ, Akhunov ED, Distelfeld A (2017) Wild emmer genome architecture and diversity elucidate wheat evolution and domestication. *Science* 357:93–97
- Cai X, Jones S, Murray T (1998) Molecular cytogenetic characterization of *Thinopyrum* and wheat–*Thinopyrum* translocated chromosomes in a wheat *Thinopyrum* amphiploid. *Chromosome Res* 6:185–189
- Chen PD, Qi LL, Zhou B, Zhang SZ, Liu DJ (1995) Development and molecular cytogenetic analysis of wheat–*Haynaldia villosa* 6VS/6AL translocation lines specifying resistance to powdery mildew. *Theor Appl Genet* 91:1125–1128
- Chen P, Liu W, Yuan J, Wang X, Zhou B, Wang S, Zhang S, Feng Y, Yang B, Liu G, Liu D, Qi L, Zhang P, Friebe B, Gill BS (2005) Development and characterization of wheat–*Leymus racemosus* translocation lines with resistance to *Fusarium* Head Blight. *Theor Appl Genet* 111:941–948
- Crasta OR, Francki MG, Bucholtz DB, Sharma HC, Zhang J, Wang RC, Ohm HW, Anderson JM (2000) Identification and characterization of wheat–wheatgrass translocation lines and localization of barley yellow dwarf virus resistance. *Genome* 43:698–706
- Dai K, Zhao R, Shi M, Xiao J, Yu Z, Jia Q, Wang Z, Yuan C, Sun H, Cao A, Zhang R, Chen P, Li Y, Wang H, Wang X (2019) Dissection and cytological mapping of chromosome arm 4VS by the development of wheat–*Haynaldia villosa* structural aberration library. *Theor Appl Genet* <https://doi.org/10.1007/s00122-019-03452-8>
- Danilova TV, Friebe B, Gill BS (2014) Development of a wheat single gene FISH map for analyzing homoeologous relationship and chromosomal rearrangements within the Triticeae. *Theor Appl Genet* 127:715–730
- Danilova TV, Zhang G, Liu W, Friebe B, Gill BS (2017) Homoeologous recombination-based transfer and molecular cytogenetic mapping of a wheat streak mosaic virus and *Triticum* mosaic

- virus resistance gene *Wsm3* from *Thinopyrum intermedium* to wheat. *Theor Appl Genet* 130:549–556
- Danilova TV, Friebe B, Gill BS (2019) Production of a complete set of wheat–barley group-7 chromosome recombinants with increased grain β -glucan content. *Theor Appl Genet* 132:3129–3141
- Devos KM, Dubcovsky J, Dvorak J, Chinoy CN, Gale MD (1995) Structural evolution of wheat chromosomes 4A, 5A, and 7B and its impact on recombination. *Theor Appl Genet* 91: 282–288.
- Endo TR, Gill BS (1996) The deletion stocks of common wheat. *J Hered* 87:295–307
- Faris JD (2014) Wheat Domestication: Key to Agricultural Revolutions Past and Future. In: Tuberosa R, Graner A, Frison E (eds) *Genomics of plant genetic resources. Vol 1. Managing, sequencing and mining genetic resources*. Springer, Metherlands, pp439–464
- Feldman M, Levy AA (2012) Genome evolution due to allopolyploidization in wheat. *Genetics* 192:763–774
- Friebe B, Jiang J, Raupp WJ, McIntosh RA, Gill BS (1996) Characterization of wheat-alien translocations conferring resistance to diseases and pests: current status. *Euphytica* 91:59–87
- Friebe B, Qi L, Liu C, Gill B (2011) Genetic compensation abilities of *Aegilops speltoides* chromosomes for homoeologous B-genome chromosomes of polyploid wheat in disomic S(B) chromosome substitution lines. *Cytogenet Genome Res* 134:144–150
- Gyawali Y, Zhang W, Chao S, Xu SS, Cai X (2019) Delimitation of wheat *ph1b* deletion and development of the *ph1b*-specific DNA markers. *Theor Appl Genet* 132:195–204
- King J, Grewal S, Yang CY, Hubbart Edwards S, Scholefield D, Ashling S, Harper JA, Allen AM, Edwards KJ, Burrige AJ, King IP (2018) Introgression of *Aegilops speltoides* segments in *Triticum aestivum* and the effect of the gametocidal genes. *Ann Bot* 121:229–240
- Li H, Dong Z, Ma C, Tian X, Qi Z, Wu N, Friebe B, Xiang Z, Xia Q, Liu W, Li T (2019) Physical mapping of stem rust resistance gene *Sr52* from *Dasypyrum villosum* based on *ph1b*-induced homoeologous recombination. *Int J Mol Sci* 20:4887
- Ling H, Ma B, Shi X, Liu H, Dong L, Sun H, Cao Y, Gao Q, Zheng S, Li Y, Yu Y, Du H, Qi M, Li Y, Lu H, Yu H, Cui Y, Wang N, Chen C, Wu H, Zhao Y, Zhang J, Li Y, Zhou W, Zhang B, Hu W, van Eijk MJT, Tang J, Witsenboer HMA, Zhao S, Li Z, Zhang A, Wang D, Liang C (2018) Genome sequence of the progenitor of wheat A subgenome *Triticum urartu*. *Nature* 557:424–428
- Liu W, Danilova TV, Rouse MN, Bowden RL, Friebe B, Gill BG (2013) Development and characterization of a compensating wheat-*Thinopyrum intermedium* Robertsonian translocation with *Sr44* resistance to stem rust (Ug99) *Theor Appl Genet* 126:1167–1177

Long Y, Chao WS, Ma G, Xu SS, Qi L (2017) An innovative SNP genotyping method adapting to multiple platforms and throughputs. *Theor Appl Genet* 130:597–607

Luo M, Gu YQ, Puiu D, Wang H, Twardziok SO, Deal KR, Huo X, Zhu T, Wang L, Wang Y, McGuire PE, Liu S, Long H, Ramasamy RK, Rodriguez JC, Van SL, Yuan L, Wang Z, Xia Z, Xiao L, Anderson OD, Ouyang S, Liang Y, Zimin AV, Perteua G, Qi P, Bennetzen JL, Dai X, Dawson MW, Müller H, Kugler K, Rivarola-Duarte L, Spannagl M, Mayer KFX, Lu F, Becan MW, Lerou P, Li P, You FM, Sun Q, Liu Z, Lyons E, Wicher T, Zalzburg SL, Devos KM, Dvořák J (2017) Genome sequence of the progenitor of the wheat D genome *Aegilops tauschii*. *Nature* 551: 498–502

Lukaszewski A, Rybka K, Korzun V, Malyshev S, Lapinski B, Whitkus R (2004) Genetic and physical mapping of homoeologous recombination points involving wheat chromosome 2B and rye chromosome 2R. *Genome* 47:36–45

Mago R, Spielmeyer W, Lawrence G, Lagudah E, Ellis J, Pryor A (2002) Identification and mapping of molecular markers linked to rust resistance genes located on chromosome 1RS of rye using wheat-rye translocation lines. *Theor Appl Genet* 104:1317–1324

Miftahudin RK, Miftahudin RK, Ma XF, Mahmoud AA, Layton J, Milla MA, Chikmawati T, Ramalingam J, Feril O, Pathan MS, Momirovic GS, Kim S, Chema K, Fang P, Haule L, Struxness H, Birkes J, Yaghoubian C, Skinner R, McAllister J, Nguyen V, Qi LL, Echaliier B, Gill BS, Linkiewicz AM, Dubcovsky J, Akhunov ED, Dvořák J, Dilbirligi M, Gill KS, Peng JH, Lapitan NL, Bermudez-Kandianis CE, Sorrells ME, Hossain KG, Kalavacharla V, Kianian SF, Lazo GR, Chao S, Anderson OD, Gonzalez-Hernandez J, Conley EJ, Anderson JA, Choi DW, Fenton RD, Close TJ, McGuire PE, Qualset CO, Nguyen HT, Gustafson JP (2004) Analysis of expressed sequence tag loci on wheat chromosome group 4. *Genetics* 168: 651–663

Naranjo T, Fernández-Rueda P (1996) Pairing and recombination between individual chromosomes of wheat and rye in hybrids carrying the *ph1b* mutation. *Theor Appl Genet* 93: 242–248

Neelam K, Brown-Guedira G, Huang L. (2013) Development and validation of a breeder-friendly KASPar marker for wheat leaf rust resistance locus *Lr21*. *Mol Breed* 31:233–237

Niu Z, Klindworth DL, Friesen TL, Chao S, Jin Y, Cai X, Xu SS (2011) Targeted introgression of a wheat stem rust resistance gene by DNA marker-assisted chromosome engineering. *Genetics* 187:1011–1021

Niu Z, Klindworth DL, Yu G, Friesen TL, Chao S, Jin Y, Cai X, Ohm J-B, Rasmussen JB, Xu SS (2014) Development and characterization of wheat lines carrying stem rust resistance gene *Sr43* derived from *Thinopyrum ponticum*. *Theor Appl Genet* 129:969–980

Patokar C, Sepsi A, Schwarzacher T, Kishii M, Heslop-Harrison JS (2016) Molecular cytogenetic characterization of novel wheat-*Thinopyrum bessarabicum* recombinant lines carrying intercalary translocations. *Chromosoma* 125:163–172

- Pont C, Leroy T, Seidel M, Tondelli A, Duchemin W, Armisen D, Lang D, Bustos-Korts D, Goué N, Balfourier F, Molnar-Lang M, Lage J, Kilian B, Ozkan H, Waite D, Dyer S, Alaux M, Letellier T, Russell J, Keller B, Eeuwijk F, Spannagl M, Mayer K, Waugh R, Stein N, Cattivelli L, Haberer G, Charmet G, Salse J (2019) Tracing the Ancestry of Modern Bread Wheats. *Nature Genetics* accepted. *Nature Genetics* 51:905–911
- Qi L, Echalié B, Friebe B, Gill B (2003) Molecular characterization of a set of wheat deletion stocks for use in chromosome bin mapping of ESTs. *Funct Integr Genomics* 3:39–55
- Qi LL, Friebe B, Zhang P, Gill BS (2007) Homoeologous recombination, chromosome engineering and crop improvement. *Chromosome Res* 15:3–19
- Rabinovich S (1998) Importance of wheat-rye translocations for breeding modern cultivar of *Triticum aestivum* L. *Euphytica* 100:323–340
- Rey M, Calderón M, Prieto P (2015) The use of the *ph1b* mutant to induce recombination between the chromosomes of wheat and barley. *Front Plant Sci* 5:509
- Riley R, Chapman V (1958) Genetic control of the cytologically diploid behaviour of hexaploid wheat. *Nature* 182:713–715
- Riley R, Chapman V, Kimber G (1959) Genetic control of chromosome pairing in intergeneric hybrids with wheat. *Nature* 185:1244–1246
- Riley R, Chapman V, Johnson R (1968) Introduction of yellow rust resistance of *Aegilops comosa* into wheat by genetically induced homoeologous recombination. *Nature* 217:383–384
- Roberts MA, Reader SM, Dalgliesh C, Miller TE, Foote TN, Fish LJ, Snape JW, Moore G (1999) Induction and characterization of *Ph1* wheat mutants. *Genetics* 153:1909–1918
- Šafař J, Šimková H, Kubaláková M, Číhalíková J, Suchánková P, Bartoš J, Doležel J (2010) Development of chromosome-specific BAC resources for genomics of bread wheat. *Cytogenet Genome Res* 129:211–223
- Schwarzacher T, Ananthawat-Jónsson K, Harrison GE, Islam AKMR, Jia JZ, King IP, Leitch AR, Miller TE, Reader SM, Rogers WJ, Shi M, Heslop-Harrison JS (1992) Genomic in situ hybridization to identify alien chromosomes and chromosome segments in wheat. *Theor Appl Genet* 84:365–375
- Sears ER (1954) The aneuploids of common wheat. *Mo Agric Exp Stn Res Bull* 572:1–59
- Sears ER (1966) Nullisomic-tetrasomic combinations in hexaploid wheat. In: Riley R, Lewis KR (eds) *Chromosome manipulation and plant genetics*. Oliver and Boyd, Edinburgh, pp 29–45
- Sears ER (1977) An induced mutant with homoeologous pairing in common wheat. *Can J Genet Cytol* 19:778–786

- Segal G, Liu B, Vega JM, Abbo S, Rodova M, Feldman M (1997) Identification of a chromosome-specific probe that maps within the *Ph1* deletions in common and durum wheat. *Theor Appl Genet* 94:968–970
- Sourdille P, Singh S, Cadalen T, Brown-Guedira GL, Gay G, Qi L, Gill BS, Dufour P, Murigneux A, Bernard M (2004) Microsatellite-based deletion bin system for the establishment of genetic–physical map relationships in wheat (*Triticum aestivum* L.). *Funct Integr Genomics* 4:12–25
- International Wheat Genome Sequencing Consortium (IWGSC) (2018) Shifting the limits in wheat research and breeding using a fully annotated reference genome. *Science* 361:6403
- Venske E, Santos RS, Busanello C, Gustafson P, Oliveira AC (2019) Bread wheat: a role model for plant domestication and breeding. *Hereditas* 156:16
- Wang S, Wong D, Forrest K, Allen A, Huang BE, Maccaferri M, Salvi S, Milner SG, Cattivelli L, Mastrangelo AM, Whan A, Stephen S, Barker G, Wieseke R, Plieske J, International Wheat Genome Sequencing Consortium, Lillemo M, Mather D, Appels R, Dolferus R, Brown–Guedira G, Korol A, Akhunova AR, Feuillet C, Salse J, Morgante M, Pozniak C, Luo MC, Dvorak J, Morell M, Dubcovsky J, Ganal M, Tuberosa R, Lawley C, Mikoulitch I, Cavanagh C, Edwards KJ, Hayden M, Akhunov E (2014) Characterization of polyploid wheat genomic diversity using a high-density 90,000 single nucleotide polymorphism array. *Plant Biotechnol J* 12:787–796
- Zhang M, Zhang W, Zhu X, Sun Q, Chao S, Yan C, Xu S, Fiedler J, Cai X. (2020) Partitioning and physical mapping of wheat chromosome 3B and its homoeologue 3E in *Thinopyrum elongatum* by inducing homoeologous recombination. *Theor Appl Genet* <https://doi.org/10.1007/s00122-020-03547-7>
- Zhang R, Hou F, Feng Y, Zhang W, Zhang M, Chen P. (2015) Characterization of a *Triticum aestivum*–*Dasypyrum villosum* T2VS·2DL translocation line expressing a longer spike and more kernels traits. *Theor Appl Genet* 128:2415–2425
- Zhang W, Cao Y, Zhang M, Zhu X, Ren S, Long Y, Gyawali Y, Chao S, Xu S, Cai X (2017) Meiotic homoeologous recombination-based alien gene introgression in the genomics era of wheat. *Crop Sci* 57:1189–1198
- Zhang W, Zhang M, Zhu X, Cao Y, Sun Q, Ma G, Chao S, Yan C, Xu S, Cai X (2018a) Molecular cytogenetic and genomic analyses reveal new insights into the origin of the wheat B genome. *Theor Appl Genet* 131:365–375
- Zhang W, Zhu X, Zhang M, Chao S, Xu S, Cai X (2018b) Meiotic homoeologous recombination–based mapping of wheat chromosome 2B and its homoeologues in *Aegilops speltoides* and *Thinopyrum elongatum*. *Theor Appl Genet* 131:2381–2395
- Zhang W, Zhu X, Zhang M, Shi G, Liu Z, Cai X (2019) Chromosome engineering–mediated introgression and molecular mapping of novel *Aegilops speltoides*–derived resistance genes for tan spot and Septoria nodorum blotch diseases in wheat. *Theor Appl Genet* 132:2605–2614

Zhao R, Wang H, Xiao J, Bie T, Cheng S, Jia Q, Yuan C, Zhang R, Cao A, Chen P, Wang X (2013) Induction of 4VS chromosome recombinants using the CS *ph1b* mutant and mapping of the wheat yellow mosaic virus resistance gene from *Haynaldia villosa*. Theor Appl Genet 126:2921–2930

**APPENDIX A. THE 3B-3E RECOMBINANTS/ABERRATIONS AND THEIR
CHROMOSOME CONSTITUTIONS**

Recombinant ID	Original recombinant code	3B-3E recombinant chromosomes and aberrations	Pedigree	Recombination source
I-1	XWC14-186-17	3BS-3ES-3EL	CS DS 3E(3B)/2*CS <i>ph1b</i> mutant//CS DS 3E(3B)	Primary
I-2	XWC14-186-2	3BS-3ES-3EL	CS DS 3E(3B)/2*CS <i>ph1b</i> mutant//CS DS 3E(3B)	Primary
I-3	XWC14-186-124	3BS-3ES-3EL	CS DS 3E(3B)/2*CS <i>ph1b</i> mutant//CS DS 3E(3B)	Primary
I-4	XWC14-186-1	3BS-3ES-3EL	CS DS 3E(3B)/2*CS <i>ph1b</i> mutant//CS DS 3E(3B)	Primary
I-5	XWC14-186-49	3BS-3ES-3EL	CS DS 3E(3B)/2*CS <i>ph1b</i> mutant//CS DS 3E(3B)	Primary
I-6	XWC14-186-67	3BS-3ES-3EL	CS DS 3E(3B)/2*CS <i>ph1b</i> mutant//CS DS 3E(3B)	Primary
I-7	XWC14-722-35	3BS-3ES-3EL	CS DS 3E(3B)/2*CS <i>ph1b</i> mutant//CS DS 3E(3B)	Primary
I-8	XWC14-186-35	3BS-3ES-3EL	CS DS 3E(3B)/2*CS <i>ph1b</i> mutant//CS DS 3E(3B)	Primary
I-9	XWC14-722-36	3BS-3ES-3EL	CS DS 3E(3B)/2*CS <i>ph1b</i> mutant//CS DS 3E(3B)	Primary
I-10	XWC14-186-134	3BS-3ES-3EL	CS DS 3E(3B)/2*CS <i>ph1b</i> mutant//CS DS 3E(3B)	Primary
I-11	XWC14-722-70	3BS-3ES-3EL	CS DS 3E(3B)/2*CS <i>ph1b</i> mutant//CS DS 3E(3B)	Primary
I-12	XWC14-186-13	3ES-3EL-3BL	CS DS 3E(3B)/2*CS <i>ph1b</i> mutant//CS DS 3E(3B)	Primary
I-13	XWC14-186-33	3ES-3EL-3BL	CS DS 3E(3B)/2*CS <i>ph1b</i> mutant//CS DS 3E(3B)	Primary
I-14	XWC14-186-4	3ES-3EL-3BL	CS DS 3E(3B)/2*CS <i>ph1b</i> mutant//CS DS 3E(3B)	Primary
I-15	XWC14-723-9	3ES-3EL-3BL	CS DS 3E(3B)/2*CS <i>ph1b</i> mutant//CS DS 3E(3B)	Primary
I-16	XWC14-186-88	3ES-3EL-3BL	CS DS 3E(3B)/2*CS <i>ph1b</i> mutant//CS DS 3E(3B)	Primary
I-17	XWC14-186-44	3ES-3EL-3BL	CS DS 3E(3B)/2*CS <i>ph1b</i> mutant//CS DS 3E(3B)	Primary
I-18	XWC14-723-21	3ES-3EL-3BL	CS DS 3E(3B)/2*CS <i>ph1b</i> mutant//CS DS 3E(3B)	Primary
I-19	XWC14-722-65	3ES-3EL-3BL	CS DS 3E(3B)/2*CS <i>ph1b</i> mutant//CS DS 3E(3B)	Primary
I-20	XWC14-723-30	3ES-3EL-3BL	CS DS 3E(3B)/2*CS <i>ph1b</i> mutant//CS DS 3E(3B)	Primary
I-22	XWC14-186-47	3ES-3EL-3BL	CS DS 3E(3B)/2*CS <i>ph1b</i> mutant//CS DS 3E(3B)	Primary
I-23	XWC14-722-21	3ES-3EL-3BL	CS DS 3E(3B)/2*CS <i>ph1b</i> mutant//CS DS 3E(3B)	Primary
II-2	XWC14-186-14	3ES-3BS-3BL	CS DS 3E(3B)/2*CS <i>ph1b</i> mutant//CS DS 3E(3B)	Primary
II-4	XWC14-723-29	3ES-3BS-3BL	CS DS 3E(3B)/2*CS <i>ph1b</i> mutant//CS DS 3E(3B)	Primary
II-5	XWC14-722-67	3ES-3BS-3BL	CS DS 3E(3B)/2*CS <i>ph1b</i> mutant//CS DS 3E(3B)	Primary
II-6	XWC14-186-63	3ES-3BS-3BL	CS DS 3E(3B)/2*CS <i>ph1b</i> mutant//CS DS 3E(3B)	Primary
II-7	XWC14-186-37	3ES-3BS-3BL	CS DS 3E(3B)/2*CS <i>ph1b</i> mutant//CS DS 3E(3B)	Primary
II-8	XWC14-722-2	3ES-3BS-3BL	CS DS 3E(3B)/2*CS <i>ph1b</i> mutant//CS DS 3E(3B)	Primary
II-9	XWC14-186-80	3ES-3BS-3BL	CS DS 3E(3B)/2*CS <i>ph1b</i> mutant//CS DS 3E(3B)	Primary

Recombinant ID	Original recombinant code	3B-3E recombinant chromosomes and aberrations	Pedigree	Recombination source
II-10	XWC14-186-120	3ES·3BS·3BL	CS DS 3E(3B)/2*CS <i>ph1b</i> mutant//CS DS 3E(3B)	Primary
II-11	XWC14-466-16	3BS·3BL·3EL	CS DS 3E(3B)/2*CS <i>ph1b</i> mutant (BC ₁ F ₂)	Primary
II-12	XWC14-722-34	3BS·3BL·3EL	CS DS 3E(3B)/2*CS <i>ph1b</i> mutant//CS DS 3E(3B)	Primary
II-14	XWC14-723-17	3BS·3BL·3EL	CS DS 3E(3B)/2*CS <i>ph1b</i> mutant//CS DS 3E(3B)	Primary
II-15	XWC14-466-29	3ES·3BS·3BL	CS DS 3E(3B)/2*CS <i>ph1b</i> mutant (BC ₁ F ₂)	Primary
II-16	XWC14-186-62	3BS·3BL·3EL	CS DS 3E(3B)/2*CS <i>ph1b</i> mutant//CS DS 3E(3B)	Primary
II-18	XWC14-722-3	3BS·3BL·3EL	CS DS 3E(3B)/2*CS <i>ph1b</i> mutant//CS DS 3E(3B)	Primary
II-20	XWC14-186-143	3BS·3BL·3EL	CS DS 3E(3B)/2*CS <i>ph1b</i> mutant//CS DS 3E(3B)	Primary
II-21	XWC14-722-57	3BS·3BL·3EL	CS DS 3E(3B)/2*CS <i>ph1b</i> mutant//CS DS 3E(3B)	Primary
II-24	XWC14-186-138	3BS·3BL·3EL	CS DS 3E(3B)/2*CS <i>ph1b</i> mutant//CS DS 3E(3B)	Primary
II-25	XWC14-722-68	3BS·3BL·3EL	CS DS 3E(3B)/2*CS <i>ph1b</i> mutant//CS DS 3E(3B)	Primary
II-26	XWC14-186-59	3BS·3BL·3EL	CS DS 3E(3B)/2*CS <i>ph1b</i> mutant//CS DS 3E(3B)	Primary
II-29	XWC14-186-115	3BS·3BL·3EL	CS DS 3E(3B)/2*CS <i>ph1b</i> mutant//CS DS 3E(3B)	Primary
III-1	XWC14-186-133	3BS·3ES·3EL·3BL	CS DS 3E(3B)/2*CS <i>ph1b</i> mutant//CS DS 3E(3B)	Primary
IV-1	XWC14-722-79	3ES·3BS·3BL·3EL	CS DS 3E(3B)/2*CS <i>ph1b</i> mutant//CS DS 3E(3B)	Primary
V-1&V-2	XWC14-186-65	3ES·3EL·3BL+3DS·3DL(?)·3EL	CS DS 3E(3B)/2*CS <i>ph1b</i> mutant//CS DS 3E(3B)	Primary
VI-1	XWC14-723-8	3ES·3BL	CS DS 3E(3B)/2*CS <i>ph1b</i> mutant//CS DS 3E(3B)	Primary
VI-2	XWC14-186-34	3BS·3EL	CS DS 3E(3B)/2*CS <i>ph1b</i> mutant//CS DS 3E(3B)	Primary
VII-1	XWC14-186-27	3ES or 3EL	CS DS 3E(3B)/2*CS <i>ph1b</i> mutant//CS DS 3E(3B)	Primary
VII-2	XWC14-186-30	3ES or 3EL	CS DS 3E(3B)/2*CS <i>ph1b</i> mutant//CS DS 3E(3B)	Primary
I-21	MZ15-9-14	3ES·3EL·3BL	XWC14-186-33/CS <i>ph1b</i> mutant//CS DS 3E(3B)	Secondary
II-1	MZ15-9-1	3ES·3BS·3BL	XWC14-186-33/CS <i>ph1b</i> mutant//CS DS 3E(3B)	Secondary
II-3	MZ15-4-1	3ES·3BS·3BL	XWC14-186-13/CS <i>ph1b</i> mutant//CS DS 3E(3B)	Secondary
II-13	MZ15-11-12	3BS·3BL·3EL	XWC14-186-35/CS <i>ph1b</i> mutant//CS DS 3E(3B)	Secondary
II-17	MZ15-2-79	3BS·3BL·3EL	XWC14-186-2/CS <i>ph1b</i> mutant//CS DS 3E(3B)	Secondary
II-19	MZ15-11-5	3BS·3BL·3EL	XWC14-186-35/CS <i>ph1b</i> mutant//CS DS 3E(3B)	Secondary
II-22	MZ15-2-56	3BS·3BL·3EL	XWC14-186-2/CS <i>ph1b</i> mutant//CS DS 3E(3B)	Secondary
II-23	MZ15-2-47	3BS·3BL·3EL	XWC14-186-2/CS <i>ph1b</i> mutant//CS DS 3E(3B)	Secondary

Recombinant ID	Original recombinant code	3B-3E recombinant chromosomes and aberrations	Pedigree	Recombination source
II-27	MZ15-1-5	3BS·3BL-3EL	XWC14-186-1/CS <i>ph1b</i> mutant//CS DS 3E(3B)	Secondary
II-28	MZ15-2-2	3BS·3BL-3EL	XWC14-186-2/CS <i>ph1b</i> mutant//CS DS 3E(3B)	Secondary
III-2	MZ15-2-7	3BS-3ES·3EL-3BL	XWC14-186-2/CS <i>ph1b</i> mutant//CS DS 3E(3B)	Secondary
III-3	MZ15-11-13	3BS-3ES·3EL-3BL	XWC14-186-35/CS <i>ph1b</i> mutant//CS DS 3E(3B)	Secondary
III-4	MZ15-2-58	3BS-3ES·3EL-3BL	XWC14-186-2/CS <i>ph1b</i> mutant//CS DS 3E(3B)	Secondary
III-5	MZ15-4-3	3BS-3ES·3EL-3BL	XWC14-186-13/CS <i>ph1b</i> mutant//CS DS 3E(3B)	Secondary
III-6	MZ15-2-43	3BS-3ES·3EL-3BL	XWC14-186-2/CS <i>ph1b</i> mutant//CS DS 3E(3B)	Secondary
III-7	MZ15-2-72	3BS-3ES·3EL-3BL	XWC14-186-2/CS <i>ph1b</i> mutant//CS DS 3E(3B)	Secondary
III-8	MZ15-11-35	3BS-3ES·3EL-3BL	XWC14-186-35/CS <i>ph1b</i> mutant//CS DS 3E(3B)	Secondary
III-9	MZ15-2-68	3BS-3ES·3EL-3BL	XWC14-186-2/CS <i>ph1b</i> mutant//CS DS 3E(3B)	Secondary
III-10	MZ15-11-36	3BS-3ES·3EL-3BL	XWC14-186-35/CS <i>ph1b</i> mutant//CS DS 3E(3B)	Secondary
III-11	MZ15-11-21	3BS-3ES·3EL-3BL	XWC14-186-35/CS <i>ph1b</i> mutant//CS DS 3E(3B)	Secondary
III-12	MZ15-2-37	3BS-3ES·3EL-3BL	XWC14-186-2/CS <i>ph1b</i> mutant//CS DS 3E(3B)	Secondary
III-13	MZ15-14-6	3BS-3ES·3EL-3BL	XWC14-186-47/CS <i>ph1b</i> mutant//CS DS 3E(3B)	Secondary
III-16	MZ15-14-58	3BS-3ES·3EL-3BL	XWC14-186-47/CS <i>ph1b</i> mutant//CS DS 3E(3B)	Secondary
III-17	MZ15-14-76	3BS-3ES·3EL-3BL	XWC14-186-47/CS <i>ph1b</i> mutant//CS DS 3E(3B)	Secondary
III-18	MZ15-14-44	3BS-3ES·3EL-3BL	XWC14-186-47/CS <i>ph1b</i> mutant//CS DS 3E(3B)	Secondary
III-19	MZ15-14-29	3BS-3ES·3EL-3BL	XWC14-186-47/CS <i>ph1b</i> mutant//CS DS 3E(3B)	Secondary
IV-2	MZ15-2-11	3BS-3ES-3BS·3BL	XWC14-186-2/CS <i>ph1b</i> mutant//CS DS 3E(3B)	Secondary
IV-6	MZ15-2-34	3BS·3BL-3EL-3BL	XWC14-186-2/CS <i>ph1b</i> mutant//CS DS 3E(3B)	Secondary
IV-8	MZ15-4-2	3BS·3BL-3EL-3BL	XWC14-186-13/CS <i>ph1b</i> mutant//CS DS 3E(3B)	Secondary
III-14	MZ16-3rd-3-39	3BS-3ES·3EL-3BL	MZ15-11-21/CS <i>ph1b</i> mutant//CS DS 3E(3B)	Tertiary
III-15	MZ16-3rd-4-12	3BS-3ES·3EL-3BL	MZ15-11-21/CS <i>ph1b</i> mutant//CS DS 3E(3B)	Tertiary
III-20	MZ16-3rd-3-28	3BS-3ES·3EL-3BL	MZ15-11-21/CS <i>ph1b</i> mutant//CS DS 3E(3B)	Tertiary
IV-3	MZ16-3rd-1-5	3BS-3ES-3BS·3BL	MZ15-11-21/CS <i>ph1b</i> mutant//CS DS 3E(3B)	Tertiary
IV-4	MZ16-3rd-3-35	3BS·3BL-3EL-3BL	MZ15-11-21/CS <i>ph1b</i> mutant//CS DS 3E(3B)	Tertiary
IV-5	MZ16-3rd-3-17	3BS·3BL-3EL-3BL	MZ15-11-21/CS <i>ph1b</i> mutant//CS DS 3E(3B)	Tertiary
IV-7	MZ16-3rd-1-13	3BS·3BL-3EL-3BL	MZ15-11-21/CS <i>ph1b</i> mutant//CS DS 3E(3B)	Tertiary

^a Homozygous means disomic for the recombinant, while heterozygous means double monosomic for the recombinant and 3E.

**APPENDIX B. MEASUREMENT AND SIZE CALCULATION OF THE 3B-3E
RECOMBINANT CHROMOSOMES**

Recombination source	Recombinant ID	Original recombinant code	Recombinant chromosome composition	Cells	Absolute physical length (μm)				Relative length of 3E segment ^a	Mean relative length of the proximal segment in the recombinant short arm ^b	Mean relative length of the proximal segment in the recombinant long arm ^c	Note
					3E segments on the short arm	3B segments on the short arm	3E segments on the long arm	3B segments on the long arm				
Primary	III-1	XWC14-186-133	3BS-3ES-3EL-3BL	1	2.56	0.34	2.67	0.76	0.83	0.86	0.83	Double crossover
				2	2.60	0.38	3.35	0.70	0.85			
				3	2.65	0.54	4.20	0.68	0.85			
				Mean	2.60	0.42	3.41	0.71	0.84			
Primary	IV-1	XWC14-722-79	3ES-3BS-3BL-3EL	1	0.59	3.35	0.97	5.23	0.15	0.85	0.80	Double crossover
				2	0.69	4.41	1.62	7.01	0.17			
				3	0.67	3.05	1.29	4.98	0.20			
				4	0.69	3.39	1.14	4.39	0.19			
				5	0.59	3.20	1.46	4.03	0.22			
				6	0.60	3.99	0.92	4.79	0.15			
				Mean	0.64	3.57	1.23	5.07	0.18			
Primary	I-2	XWC14-186-2	3BS-3ES-3EL	1	3.18	0.64	5.47	0.00	0.93	0.84	-	Single crossover on short arm
				2	3.40	0.64	7.06	0.00	0.94			
				3	2.57	0.69	4.91	0.00	0.92			
				4	2.47	0.46	4.66	0.00	0.94			
				5	2.75	0.40	5.22	0.00	0.95			
				Mean	2.87	0.57	5.46	0.00	0.94			
Primary	II-10	XWC14-186-120	3ES-3BS-3BL	1	0.74	4.73	0.00	7.07	0.06	0.84	-	Single crossover on short arm
				2	0.85	4.79	0.00	6.38	0.07			
				3	0.92	4.62	0.00	6.36	0.08			
				4	0.91	3.41	0.00	6.51	0.08			
				Mean	0.86	4.39	0.00	6.58	0.07			
Primary	I-1	XWC14-186-17	3BS-3ES-3EL	1	2.70	0.66	6.05	0.00	0.93	0.83	-	Single crossover on short arm
				2	5.64	0.92	14.99	0.00	0.96			
				3	3.49	0.82	6.46	0.00	0.92			
				4	4.43	0.74	9.17	0.00	0.95			
				Mean	4.07	0.79	9.17	0.00	0.94			
Primary	II-9	XWC14-186-80	3ES-3BS-3BL	1	0.74	4.72	0.00	6.65	0.06	0.82	-	Single crossover on short arm
				2	1.09	5.20	0.00	9.49	0.07			
				3	2.05	9.10	0.00	14.97	0.08			
				4	1.49	4.68	0.00	10.40	0.09			
				Mean	1.34	5.93	0.00	10.38	0.08			

Recombination source	Recombinant ID	Original recombinant code	Recombinant chromosome composition	Cells	Absolute physical length (μm)				Relative length of 3E segment ^a	Mean relative length of the proximal segment in the recombinant short arm ^b	Mean relative length of the proximal segment in the recombinant long arm ^c	Note
					3E segments on the short arm	3B segments on the short arm	3E segments on the long arm	3B segments on the long arm				
Primary	I-3	XWC14-186-124	3BS-3ES-3EL	1	3.36	0.89	6.66	0.00	0.92	0.80	-	Single crossover on short arm
				2	2.73	0.71	7.01	0.00	0.93			
				3	3.88	0.81	6.80	0.00	0.93			
				4	2.75	0.68	5.79	0.00	0.93			
				5	3.69	0.81	6.83	0.00	0.93			
				6	2.97	0.73	6.72	0.00	0.93			
				7	2.84	0.72	6.27	0.00	0.93			
				Mean	3.17	0.76	6.58	0.00	0.93			
Primary	I-4	XWC14-186-1	3BS-3ES-3EL	1	3.76	0.87	5.84	0.00	0.92	0.78	-	Single crossover on short arm
				2	3.30	0.93	5.88	0.00	0.91			
				3	3.00	0.77	5.66	0.00	0.92			
				4	2.29	0.76	5.02	0.00	0.91			
				5	3.29	1.10	6.39	0.00	0.90			
				Mean	3.13	0.89	5.76	0.00	0.91			
Primary	II-8	XWC14-722-2	3ES-3BS-3BL	1	1.14	4.38	0.00	7.66	0.09	0.77	-	Single crossover on short arm
				2	1.03	4.23	0.00	6.11	0.09			
				3	1.26	3.37	0.00	5.91	0.12			
				4	1.14	3.41	0.00	6.28	0.11			
				Mean	1.14	3.85	0.00	6.49	0.10			
Primary	II-7	XWC14-186-37	3ES-3BS-3BL	1	1.63	4.03	0.00	7.55	0.12	0.76	-	Single crossover on short arm
				2	1.63	4.54	0.00	7.02	0.12			
				3	0.92	3.63	0.00	5.41	0.09			
				4	1.02	3.70	0.00	5.35	0.10			
				5	0.97	3.31	0.00	5.35	0.10			
				Mean	1.23	3.84	0.00	6.14	0.11			
Primary	II-5	XWC14-722-67	3ES-3BS-3BL	1	1.62	5.04	0.00	8.70	0.11	0.74	-	Single crossover on short arm
				2	1.57	4.81	0.00	7.69	0.11			
				3	1.54	3.83	0.00	7.29	0.12			
				Mean	1.58	4.56	0.00	7.89	0.11			
Primary	II-6	XWC14-186-63	3ES-3BS-3BL	1	0.87	2.45	0.00	4.20	0.12	0.74	-	Single crossover on short arm
				2	1.21	3.61	0.00	6.15	0.11			
				Mean	1.04	3.03	0.00	5.18	0.11			

Recombination source	Recombinant ID	Original recombinant code	Recombinant chromosome composition	Cells	Absolute physical length (μm)				Relative length of 3E segment ^a	Mean relative length of the proximal segment in the recombinant short arm ^b	Mean relative length of the proximal segment in the recombinant long arm ^c	Note
					3E segments on the short arm	3B segments on the short arm	3E segments on the long arm	3B segments on the long arm				
Primary	I-5	XWC14-186-49	3BS-3ES-3EL	1	2.05	0.70	4.61	0.00	0.90	0.73	-	Single crossover on short arm
				2	2.76	0.99	6.89	0.00	0.91			
				3	2.58	1.09	6.33	0.00	0.89			
				Mean	2.46	0.93	5.94	0.00	0.90			
Primary	I-6	XWC14-186-67	3BS-3ES-3EL	1	2.65	1.09	5.55	0.00	0.88	0.73	-	Single crossover on short arm
				2	3.05	1.09	5.72	0.00	0.89			
				3	2.60	0.99	5.56	0.00	0.89			
				4	2.78	1.04	4.73	0.00	0.88			
				5	2.92	0.99	5.02	0.00	0.89			
				Mean	2.80	1.04	5.32	0.00	0.89			
Primary	I-7	XWC14-722-35	3BS-3ES-3EL	1	2.08	1.21	5.99	0.00	0.87	0.73	-	Single crossover on short arm
				2	2.54	0.85	4.99	0.00	0.90			
				3	2.05	0.72	4.44	0.00	0.90			
				4	1.99	0.71	4.30	0.00	0.90			
				5	2.86	0.87	4.51	0.00	0.89			
				Mean	2.30	0.87	4.85	0.00	0.89			
Primary	I-8	XWC14-186-35	3BS-3ES-3EL	1	3.47	1.45	5.48	0.00	0.86	0.73	-	Single crossover on short arm
				2	4.06	1.30	7.35	0.00	0.90			
				3	3.87	1.65	8.48	0.00	0.88			
				4	3.18	1.12	6.34	0.00	0.89			
				Mean	3.65	1.38	6.91	0.00	0.88			
Primary	I-9	XWC14-722-36	3BS-3ES-3EL	1	2.63	1.06	5.54	0.00	0.89	0.70	-	Single crossover on short arm
				2	2.31	0.90	4.62	0.00	0.89			
				3	2.12	0.90	4.38	0.00	0.88			
				4	1.60	0.85	5.16	0.00	0.89			
				Mean	2.17	0.93	4.93	0.00	0.88			
Primary	II-4	XWC14-723-29	3ES-3BS-3BL	1	0.94	1.77	0.00	4.22	0.14	0.69	-	Single crossover on short arm
				2	1.17	2.91	0.00	5.12	0.13			
				Mean	1.06	2.34	0.00	4.67	0.13			
				1	3.09	1.95	8.53	0.00	0.86			
Primary	I-10	XWC14-186-134	3BS-3ES-3EL	2	3.81	2.17	9.19	0.00	0.86	0.62	-	Single crossover on short arm
				3	5.40	3.21	12.45	0.00	0.85			
				4	3.33	2.00	7.45	0.00	0.84			
				5	2.94	1.98	7.77	0.00	0.84			
				6	2.85	1.73	7.48	0.00	0.86			
				Mean	3.57	2.17	8.81	0.00	0.85			

Recombination source	Recombinant ID	Original recombinant code	Recombinant chromosome composition	Cells	Absolute physical length (μm)				Relative length of 3E segment ^a	Mean relative length of the proximal segment in the recombinant short arm ^b	Mean relative length of the proximal segment in the recombinant long arm ^c	Note
					3E segments on the short arm	3B segments on the short arm	3E segments on the long arm	3B segments on the long arm				
Primary	II-2	XWC14-186-14	3ES-3BS-3BL	1	1.79	2.39	0.00	5.72	0.18	0.62	-	Single crossover on short arm
				2	1.64	3.41	0.00	8.28	0.12			
				3	1.99	3.06	0.00	7.08	0.16			
				4	1.17	2.47	0.00	5.88	0.12			
				5	1.46	1.99	0.00	6.23	0.15			
				6	1.38	2.24	0.00	5.70	0.15			
				Mean	1.54	2.46	0.00	6.40	0.15			
Primary	I-11	XWC14-722-70	3BS-3ES-3EL	1	1.85	2.80	5.84	0.00	0.73	0.42	-	Single crossover on short arm
				2	2.39	3.15	6.48	0.00	0.74			
				Mean	2.12	2.98	6.16	0.00	0.74			
Secondary	III-16	MZ15-14-58	3BS-3ES-3EL-3BL	1	3.73	1.02	2.43	4.11	0.55	0.79	-	Single crossover on short arm
				2	3.08	0.72	2.32	2.84	0.60			
				3	3.52	1.04	1.85	3.15	0.56			
				Mean	3.44	0.93	2.20	3.37	0.57			
Secondary	III-18	MZ15-14-44	3BS-3ES-3EL-3BL	1	2.60	0.92	2.19	3.40	0.53	0.77	-	Single crossover on short arm
				2	2.98	0.76	1.84	2.67	0.58			
				Mean	2.79	0.84	2.02	3.04	0.55			
Secondary	III-17	MZ15-14-76	3BS-3ES-3EL-3BL	1	2.67	0.72	1.57	2.08	0.60	0.76	-	Single crossover on short arm
				2	2.39	0.85	1.53	2.41	0.55			
				Mean	2.53	0.79	1.55	2.25	0.57			
Secondary	III-13	MZ15-14-6	3BS-3ES-3EL-3BL	1	4.41	1.21	4.25	3.95	0.63	0.75	-	Single crossover on short arm
				2	4.01	1.29	3.16	3.44	0.60			
				3	3.36	1.30	3.36	3.02	0.61			
				Mean	3.93	1.27	3.59	3.47	0.61			
Secondary	IV-2	MZ15-2-11	3BS-3ES-3BS-3BL	1	0.62	0.54+3.60	0.00	5.80	0.06	0.72	-	Single crossover on short arm
				2	0.68	0.51+2.58	0.00	5.04	0.08			
				Mean	0.65	0.53+3.09	0.00	5.42	0.07			
Secondary	III-5	MZ15-4-3	3BS-3ES-3EL-3BL	1	4.06	1.38	6.25	1.25	0.80	0.72	-	Single crossover on short arm
				2	4.02	1.61	6.11	0.84	0.81			
				3	3.65	1.45	6.18	1.02	0.80			
				4	4.99	1.78	8.43	1.40	0.81			
				5	3.33	1.56	5.85	0.83	0.79			
				Mean	4.01	1.56	6.56	1.07	0.80			

Recombination source	Recombinant ID	Original recombinant code	Recombinant chromosome composition	Cells	Absolute physical length (µm)				Relative length of 3E segment ^a	Mean relative length of the proximal segment in the recombinant short arm ^b	Mean relative length of the proximal segment in the recombinant long arm ^c	Note
					3E segments on the short arm	3B segments on the short arm	3E segments on the long arm	3B segments on the long arm				
Secondary	III-19	MZ15-14-29	3BS-3ES-3EL-3BL	1	2.76	1.14	1.62	3.24	0.50	0.70	-	Single crossover on short arm
				2	2.39	1.02	1.54	3.42	0.47			
				3	2.54	1.04	1.88	2.91	0.53			
				4	2.08	1.04	1.74	2.06	0.55			
				Mean	2.44	1.06	1.70	2.91	0.51			
Secondary	II-3	MZ15-4-1	3ES-3BS-3BL	1	1.53	2.76	0.00	5.96	0.15	0.68	-	Single crossover on short arm
				2	1.24	2.75	0.00	4.85	0.14			
				3	1.48	3.44	0.00	5.52	0.14			
				Mean	1.42	2.98	0.00	5.44	0.14			
Secondary	II-1	MZ15-9-1	3ES-3BS-3BL	1	2.34	1.73	0.00	5.60	0.24	0.37	-	Single crossover on short arm
				2	2.52	1.45	0.00	4.76	0.29			
				3	2.39	1.14	0.00	5.11	0.28			
				Mean	2.42	1.44	0.00	5.16	0.27			
97 Tertiary	IV-3	MZ16-3rd-1-5	3BS-3ES-3BS-3BL	1	0.85	1.54+3.77	0.00	8.82	0.06	0.55	-	Single crossover on short arm
				2	0.85	1.38+2.48	0.00	7.41	0.07			
				3	0.54	1.08+1.74	0.00	5.14	0.06			
				Mean	0.75	1.33+2.66	0.00	7.12	0.06			
Primary	I-12	XWC14-186-13	3ES-3EL-3BL	1	4.95	0.00	6.78	1.32	0.90	-	0.85	Single crossover on long arm
				2	2.45	0.00	3.75	0.77	0.89			
				3	3.19	0.00	5.19	0.81	0.91			
				4	3.72	0.00	5.77	0.77	0.92			
				5	3.93	0.00	4.36	0.91	0.90			
				Mean	3.65	0.00	5.17	0.92	0.91			
Primary	I-13	XWC14-186-33	3ES-3EL-3BL	1	4.46	0.00	6.54	1.33	0.89	-	0.85	Single crossover on long arm
				2	5.11	0.00	6.52	1.12	0.91			
				3	4.02	0.00	4.54	0.64	0.93			
				4	6.15	0.00	7.03	1.19	0.92			
				Mean	4.94	0.00	6.16	1.07	0.91			
Primary	II-29	XWC14-186-115	3BS-3BL-3EL	1	0.00	3.95	0.72	4.96	0.07	-	0.85	Single crossover on long arm
				2	0.00	3.62	0.72	4.01	0.09			
				3	0.00	2.98	0.62	3.04	0.09			
				Mean	0.00	3.52	0.69	4.00	0.08			
Primary	II-26	XWC14-186-59	3BS-3BL-3EL	1	0.00	4.49	0.99	4.99	0.09	-	0.84	Single crossover on long arm
				2	0.00	4.59	1.09	5.60	0.10			
				Mean	0.00	4.54	1.04	5.30	0.10			

Recombination source	Recombinant ID	Original recombinant code	Recombinant chromosome composition	Cells	Absolute physical length (μm)				Relative length of 3E segment ^a	Mean relative length of the proximal segment in the recombinant short arm ^b	Mean relative length of the proximal segment in the recombinant long arm ^c	Note
					3E segments on the short arm	3B segments on the short arm	3E segments on the long arm	3B segments on the long arm				
Primary	II-25	XWC14-722-68	3BS-3BL-3EL	1	0.00	3.98	1.03	4.20	0.11	-	0.82	Single crossover on long arm
				2	0.00	7.62	1.63	7.86	0.10			
				3	0.00	4.68	1.14	4.21	0.11			
				4	0.00	5.24	1.43	6.07	0.11			
				5	0.00	4.53	1.02	5.85	0.09			
				6	0.00	4.66	1.06	4.75	0.10			
				Mean	0.00	5.17	1.22	5.46	0.10			
Primary	I-14	XWC14-186-4	3ES-3EL-3BL	1	3.17	0.00	4.24	0.77	0.91	-	0.81	Single crossover on long arm
				2	3.53	0.00	4.73	0.87	0.90			
				3	3.40	0.00	4.94	0.93	0.90			
				4	3.24	0.00	3.59	1.13	0.86			
				5	3.35	0.00	4.41	1.28	0.86			
				Mean	3.34	0.00	4.38	1.00	0.89			
Primary	I-15	XWC14-723-9	3ES-3EL-3BL	1	5.50	0.00	6.52	1.54	0.89	-	0.81	Single crossover on long arm
				2	5.34	0.00	6.25	1.38	0.89			
				3	5.12	0.00	5.63	1.27	0.89			
				4	5.95	0.00	7.29	1.87	0.88			
				Mean	5.48	0.00	6.42	1.52	0.89			
Primary	II-24	XWC14-186-138	3BS-3BL-3EL	1	0.00	4.00	1.09	4.90	0.11	-	0.81	Single crossover on long arm
				2	0.00	3.87	1.43	5.55	0.13			
				3	0.00	4.51	1.10	4.77	0.11			
				4	0.00	4.75	1.43	5.77	0.12			
Primary	I-16	XWC14-186-88	3ES-3EL-3BL	5	0.00	6.62	1.51	7.35	0.10	-	0.76	Single crossover on long arm
				Mean	0.00	4.75	1.31	5.67	0.11			
				1	2.79	0.00	2.91	0.99	0.85			
Primary	I-17	XWC14-186-44	3ES-3EL-3BL	2	3.01	0.00	3.23	0.93	0.87	-	0.74	Single crossover on long arm
				Mean	2.90	0.00	3.07	0.96	0.86			
Primary	II-21	XWC14-722-57	3BS-3BL-3EL	1	3.17	0.00	3.41	1.23	0.84	-	0.72	Single crossover on long arm
				2	2.52	0.00	2.65	0.87	0.86			
				Mean	2.85	0.00	3.03	1.05	0.85			
				1	0.00	4.87	2.02	5.06	0.17			
				2	0.00	4.61	1.88	4.46	0.17			
Primary	II-21	XWC14-722-57	3BS-3BL-3EL	3	0.00	4.65	1.38	4.11	0.14	-	0.72	Single crossover on long arm
				4	0.00	3.85	1.91	4.73	0.18			
				5	0.00	3.87	1.53	4.12	0.16			
				Mean	0.00	4.37	1.74	4.50	0.16			

Recombination source	Recombinant ID	Original recombinant code	Recombinant chromosome composition	Cells	Absolute physical length (μm)				Relative length of 3E segment ^a	Mean relative length of the proximal segment in the recombinant short arm ^b	Mean relative length of the proximal segment in the recombinant long arm ^c	Note
					3E segments on the short arm	3B segments on the short arm	3E segments on the long arm	3B segments on the long arm				
Primary	II-20	XWC14-186-143	3BS-3BL-3EL	1	0.00	5.05	2.29	5.65	0.18	-	0.71	Single crossover on long arm
				2	0.00	4.57	1.68	4.53	0.16			
				3	0.00	3.71	1.37	3.39	0.16			
				4	0.00	4.52	1.73	3.77	0.17			
				5	0.00	3.41	1.54	3.46	0.18			
				6	0.00	3.58	1.42	3.27	0.17			
				Mean	0.00	4.14	1.67	4.01	0.17			
Primary	II-18	XWC14-722-3	3BS-3BL-3EL	1	0.00	5.49	2.58	4.38	0.21	-	0.68	Single crossover on long arm
				2	0.00	5.40	2.63	5.49	0.19			
				3	0.00	6.43	2.74	5.94	0.18			
				4	0.00	5.95	2.36	5.32	0.17			
				5	0.00	4.96	2.13	5.27	0.17			
				Mean	0.00	5.65	2.49	5.28	0.19			
Primary	I-18	XWC14-723-21	3ES-3EL-3BL	1	2.85	0.00	2.67	1.25	0.82	-	0.67	Single crossover on long arm
				2	2.86	0.00	3.14	1.69	0.78			
				3	5.80	0.00	5.22	2.38	0.82			
				Mean	3.84	0.00	3.68	1.77	0.81			
Primary	II-16	XWC14-186-62	3BS-3BL-3EL	1	0.00	2.96	1.28	3.13	0.17	-	0.63	Single crossover on long arm
				2	0.00	2.73	1.41	3.23	0.19			
				3	0.00	2.68	1.81	2.70	0.25			
				4	0.00	5.26	3.25	4.20	0.26			
Mean	0.00	3.41	1.94	3.32	0.22							
Primary	II-15	XWC14-466-29	3BS-3BL-3EL	1	0.00	3.16	1.83	2.96	0.23	-	0.62	Single crossover on long arm
				2	0.00	3.74	2.48	4.06	0.24			
				3	0.00	3.50	2.42	3.95	0.25			
				Mean	0.00	3.47	2.24	3.66	0.24			
Primary	II-14	XWC14-723-17	3BS-3BL-3EL	1	0.00	3.65	2.00	3.01	0.23	-	0.58	Single crossover on long arm
				2	0.00	3.25	2.09	2.84	0.26			
				3	0.00	6.04	3.36	4.07	0.25			
				4	0.00	4.32	1.86	3.06	0.20			
				5	0.00	4.90	2.16	3.47	0.21			
				6	0.00	3.86	2.82	3.62	0.27			
Mean	0.00	4.34	2.38	3.35	0.24							

Recombination source	Recombinant ID	Original recombinant code	Recombinant chromosome composition	Cells	Absolute physical length (μm)				Relative length of 3E segment ^a	Mean relative length of the proximal segment in the recombinant short arm ^b	Mean relative length of the proximal segment in the recombinant long arm ^c	Note
					3E segments on the short arm	3B segments on the short arm	3E segments on the long arm	3B segments on the long arm				
Primary	I-19	XWC14-722-65	3ES-3EL-3BL	1	3.25	0.00	2.35	2.34	0.71	-	0.56	Single crossover on long arm
				2	5.60	0.00	4.83	3.69	0.74			
				3	4.68	0.00	3.99	3.39	0.72			
				4	3.41	0.00	2.79	2.21	0.74			
				5	3.28	0.00	3.00	2.32	0.73			
				6	5.29	0.00	4.83	3.38	0.75			
				Mean	4.25	0.00	3.63	2.89	0.73			
Primary	II-12	XWC14-722-34	3BS-3BL-3EL	1	0.00	3.41	2.44	3.21	0.27	-	0.55	Single crossover on long arm
				2	0.00	3.66	3.02	3.46	0.30			
				Mean	0.00	3.54	2.73	3.34	0.28			
Primary	I-20	XWC14-723-30	3ES-3EL-3BL	1	4.17	0.00	2.25	2.43	0.73	-	0.49	Single crossover on long arm
				2	3.16	0.00	1.67	1.77	0.73			
				3	3.12	0.00	2.21	2.09	0.72			
				4	2.70	0.00	2.02	2.14	0.69			
				Mean	2.63	0.00	1.63	1.69	0.72			
Primary	I-22	XWC14-186-47	3ES-3EL-3BL	1	2.78	0.00	1.47	3.04	0.58	-	0.32	Single crossover on long arm
				1	3.59	0.00	1.38	3.08	0.62			
				Mean	3.04	0.00	1.46	3.08	0.59			
Primary	II-11	XWC14-466-16	3BS-3BL-3EL	1	0.00	4.70	6.53	2.26	0.48	-	0.29	Single crossover on long arm
				2	0.00	4.28	4.96	1.99	0.44			
				3	0.00	4.15	4.51	1.91	0.43			
				4	0.00	4.78	3.67	1.78	0.36			
				Mean	0.00	4.48	4.92	1.99	0.43			
Primary	I-23	XWC14-722-21	3ES-3EL-3BL	1	3.88	0.00	1.53	3.66	0.60	-	0.27	Single crossover on long arm
				2	3.37	0.00	1.46	3.71	0.57			
				3	3.21	0.00	1.04	3.64	0.54			
				4	3.03	0.00	1.23	3.42	0.55			
				Mean	3.87	0.00	1.90	4.55	0.56			
Secondary	II-28	MZ15-2-2	3BS-3BL-3EL	1	3.47	0.00	1.43	3.80	0.56	-	0.85	Single crossover on long arm
				1	0.00	4.74	0.99	5.50	0.09			
				2	0.00	4.62	0.76	5.20	0.07			
				3	0.00	4.12	0.92	4.28	0.10			
				4	0.00	4.22	0.85	5.20	0.08			
				5	0.00	4.21	0.92	4.81	0.09			
Mean	0.00	4.38	0.89	5.00	0.09							

Recombination source	Recombinant ID	Original recombinant code	Recombinant chromosome composition	Cells	Absolute physical length (μm)				Relative length of 3E segment ^a	Mean relative length of the proximal segment in the recombinant short arm ^b	Mean relative length of the proximal segment in the recombinant long arm ^c	Note
					3E segments on the short arm	3B segments on the short arm	3E segments on the long arm	3B segments on the long arm				
Secondary	III-3	MZ15-11-13	3BS-3ES-3EL-3BL	1	3.05	0.99	4.96	0.92	0.81	-	0.85	Single crossover on long arm
				2	2.81	0.92	4.28	0.85	0.80			
				3	2.90	1.04	4.03	0.72	0.80			
				4	3.31	0.99	5.07	0.85	0.82			
				5	2.61	1.04	5.17	0.76	0.81			
Mean	2.94	1.00	4.70	0.82	0.81							
Secondary	II-27	MZ15-1-5	3BS-3BL-3EL	1	0.00	3.98	0.81	4.53	0.09	-	0.84	Single crossover on long arm
				2	0.00	4.38	0.87	4.81	0.09			
				3	0.00	4.73	1.07	5.55	0.09			
Mean	0.00	4.36	0.92	4.96	0.09							
Secondary	III-2	MZ15-2-7	3BS-3ES-3EL-3BL	1	2.78	0.70	4.89	0.99	0.82	-	0.84	Single crossover on long arm
				2	4.11	0.68	5.04	0.85	0.86			
				3	2.70	0.72	4.72	0.87	0.82			
Mean	3.20	0.70	4.88	0.90	0.83							
Secondary	III-10	MZ15-11-36	3BS-3ES-3EL-3BL	1	2.12	1.33	3.41	0.86	0.72	-	0.82	Single crossover on long arm
				2	1.95	1.23	2.88	0.54	0.73			
				3	2.05	1.02	3.19	0.69	0.75			
Mean	2.04	1.19	3.16	0.70	0.73							
Secondary	III-4	MZ15-2-58	3BS-3ES-3EL-3BL	1	4.50	1.28	6.27	1.42	0.80	-	0.81	Single crossover on long arm
				2	4.34	1.05	5.07	1.28	0.80			
				Mean	4.42	1.17	5.67	1.35	0.80			
Secondary	II-23	MZ15-2-47	3BS-3BL-3EL	1	0.00	4.42	1.31	5.26	0.12	-	0.79	Single crossover on long arm
				2	0.00	3.56	1.17	4.68	0.12			
				3	0.00	4.20	1.13	5.00	0.11			
				4	0.00	4.45	1.49	4.64	0.14			
Mean	0.00	4.16	1.28	4.90	0.12							
Secondary	II-22	MZ15-2-56	3BS-3BL-3EL	1	0.00	4.10	1.02	4.38	0.11	-	0.77	Single crossover on long arm
				2	0.00	5.19	2.28	6.71	0.16			
				3	0.00	4.59	1.43	4.41	0.14			
Mean	0.00	4.63	1.58	5.17	0.14							
Secondary	III-11	MZ15-11-21	3BS-3ES-3EL-3BL	1	2.08	0.87	3.30	0.85	0.76	-	0.76	Single crossover on long arm
				2	2.33	1.25	3.09	1.03	0.70			
				3	2.13	1.09	3.21	0.99	0.72			
				4	2.54	1.09	3.74	1.14	0.74			
				5	1.88	0.97	2.68	1.07	0.69			
Mean	2.19	1.05	3.20	1.02	0.72							

Recombination source	Recombinant ID	Original recombinant code	Recombinant chromosome composition	Cells	Absolute physical length (μm)				Relative length of 3E segment ^a	Mean relative length of the proximal segment in the recombinant short arm ^b	Mean relative length of the proximal segment in the recombinant long arm ^c	Note
					3E segments on the short arm	3B segments on the short arm	3E segments on the long arm	3B segments on the long arm				
Secondary	III-8	MZ15-11-35	3BS-3ES-3EL-3BL	1	2.35	0.62	3.57	0.80	0.81	-	0.76	Single crossover on long arm
				2	2.45	0.89	3.47	1.21	0.74			
				3	2.74	0.92	3.15	1.12	0.74			
				4	2.32	0.90	3.50	1.33	0.72			
				5	2.21	0.85	3.49	0.99	0.76			
Mean	2.41	0.84	3.44	1.09	0.75							
Secondary	III-9	MZ15-2-68	3BS-3ES-3EL-3BL	1	2.81	1.03	3.42	1.53	0.71	-	0.74	Single crossover on long arm
				2	2.32	0.85	3.37	1.34	0.72			
				3	3.52	0.92	5.59	1.54	0.79			
Mean	2.88	0.93	4.13	1.47	0.74							
Secondary	IV-8	MZ15-4-2	3BS-3BL-3EL-3BL	1	0.00	5.24	1.09	5.31+0.85	0.09	-	0.73	Single crossover on long arm
				2	0.00	3.85	0.62	3.85+0.76	0.07			
				3	0.00	4.13	0.87	4.16+0.70	0.09			
Mean	0.00	4.41	0.86	4.44+0.77	0.08							
Secondary	III-6	MZ15-2-43	3BS-3ES-3EL-3BL	1	3.54	0.56	3.70	1.56	0.77	-	0.71	Single crossover on long arm
				2	5.01	1.20	5.39	1.93	0.77			
				3	2.52	0.38	2.95	1.41	0.75			
Mean	3.69	0.71	4.01	1.63	0.77							
Secondary	III-7	MZ15-2-72	3BS-3ES-3EL-3BL	1	3.64	0.74	4.79	2.41	0.73	-	0.71	Single crossover on long arm
				2	3.26	0.54	4.41	1.53	0.79			
				3	2.11	0.79	3.72	1.45	0.72			
Mean	3.00	0.69	4.31	1.80	0.75							
Secondary	II-17	MZ15-2-79	3BS-3BL-3EL	1	0.00	5.06	2.47	5.83	0.18	-	0.68	Single crossover on long arm
				2	0.00	4.68	2.24	4.27	0.20			
				Mean	0.00	4.87	2.36	5.05	0.19			
Secondary	II-19	MZ15-11-5	3BS-3BL-3EL	1	0.00	5.07	3.07	4.80	0.24	-	0.67	Single crossover on long arm
				2	0.00	4.70	1.90	4.75	0.17			
				3	0.00	5.23	2.25	5.02	0.18			
				4	0.00	4.82	2.12	4.23	0.19			
				Mean	0.00	4.96	2.34	4.70	0.19			
Secondary	IV-6	MZ15-2-34	3BS-3BL-3EL-3BL	1	0.00	3.59	0.76	0.71+2.78	0.10	-	0.63	Single crossover on long arm
				2	0.00	3.68	0.99	0.92+3.09	0.11			
				3	0.00	3.68	1.26	0.64+3.05	0.15			
				4	0.00	2.94	0.94	0.81+2.94	0.12			
				Mean	0.00	3.47	0.99	0.77+2.97	0.12			

Recombination source	Recombinant ID	Original recombinant code	Recombinant chromosome composition	Cells	Absolute physical length (μm)				Relative length of 3E segment ^a	Mean relative length of the proximal segment in the recombinant short arm ^b	Mean relative length of the proximal segment in the recombinant long arm ^c	Note
					3E segments on the short arm	3B segments on the short arm	3E segments on the long arm	3B segments on the long arm				
Secondary	III-12	MZ15-2-37	3BS-3ES-3EL-3BL	1	1.60	0.74	2.27	1.25	0.66	-	0.57	Single crossover on long arm
				2	1.74	0.71	1.71	1.71	0.59			
				3	2.12	0.68	2.09	1.77	0.63			
				4	2.57	0.57	3.06	2.19	0.67			
				Mean	2.01	0.68	2.28	1.73	0.64			
Secondary	II-13	MZ15-11-12	3BS-3BL-3EL	1	0.00	4.66	2.54	2.81	0.25	-	0.51	Single crossover on long arm
				2	0.00	5.17	3.30	3.41	0.28			
				3	0.00	3.97	2.56	2.60	0.28			
				Mean	0.00	4.60	2.80	2.94	0.27			
Secondary	I-21	MZ15-9-14	3ES-3EL-3BL	1	4.21	0.00	3.82	3.46	0.70	-	0.50	Single crossover on long arm
				2	4.11	0.00	2.16	2.60	0.71			
				Mean	4.16	0.00	2.99	3.03	0.70			
Tertiary	IV-7	MZ16-3rd-1-13	3BS-3BL-3EL-3BL	1	0.00	6.66	1.09	5.82+1.47	0.07	-	0.67	Single crossover on long arm
				2	0.00	5.64	1.08	3.89+1.14	0.09			
				Mean	0.00	6.15	1.09	4.86+1.31	0.08			
Tertiary	IV-5	MZ16-3rd-3-17	3BS-3BL-3EL-3BL	1	0.00	4.50	1.48	3.18+1.37	0.14	-	0.55	Single crossover on long arm
				2	0.00	4.44	1.02	2.60+0.76	0.12			
				Mean	0.00	4.47	1.25	2.89+1.07	0.13			
Tertiary	III-14	MZ16-3rd-3-39	3BS-3ES-3EL-3BL	1	2.08	0.89	2.43	1.89	0.62	-	0.55	Single crossover on long arm
				2	1.93	0.76	1.94	1.58	0.62			
				3	2.41	1.53	3.21	2.62	0.58			
				Mean	2.14	1.06	2.53	2.03	0.60			
Tertiary	III-15	MZ16-3rd-4-12	3BS-3ES-3EL-3BL	1	2.51	0.91	2.96	2.29	0.63	-	0.54	Single crossover on long arm
				2	2.65	1.43	3.19	2.90	0.57			
				3	1.41	1.14	3.02	2.77	0.53			
				Mean	2.19	1.16	3.06	2.65	0.58			
Tertiary	IV-4	MZ16-3rd-3-35	3BS-3BL-3EL-3BL	1	0.00	3.88	1.73	2.62+1.02	0.19	-	0.46	Single crossover on long arm
				2	0.00	4.54	1.83	2.25+0.82	0.19			
				3	0.00	3.89	1.96	2.37+1.05	0.21			
				Mean	0.00	4.10	1.84	2.41+0.96	0.20			
Tertiary	III-20	MZ16-3rd-3-28	3BS-3ES-3EL-3BL	1	2.10	1.03	1.96	3.71	0.46	-	0.32	Single crossover on long arm
				2	1.80	0.97	1.33	2.85	0.45			
				3	1.94	1.44	1.48	3.71	0.40			
				Mean	1.95	1.15	1.59	3.42	0.44			

^aAbsolute physical length of the 3E segments/total length of the recombinant chromosome

^bAbsolute physical length of the proximal segment on short arm/total length of the recombinant short arm

^cAbsolute physical length of the proximal segment on long arm/total length of the recombinant long arm

**APPENDIX C. THE GENETIC AND PHYSICAL POSITION OF SNPS ASSIGNED TO
THE COMPOSITE BIN MAP**

Index	SNP Name	Genetic position (cM)^a	Physical position (bp)	E-value
70524	Tdurum_contig3507_103	5.858341	1754906	4.00E-46
56145	RAC875_c27986_1460	4.540652	1757412	2.00E-26
53709	RAC875_c13385_1268	5.858341	2620500	4.00E-46
41710	Kukri_c17082_519	5.858341	2621494	4.00E-46
11873	BS00094406_51	5.858341	2641215	4.00E-46
73423	Tdurum_contig77551_586	51.07983	3145069	1.00E-43
72138	Tdurum_contig50954_880	51.07233	3491459	4.00E-34
72137	Tdurum_contig50954_475	51.07233	3492201	4.00E-40
71813	Tdurum_contig47506_251	8.49872	3981913	4.00E-46
64989	RFL_Contig5360_1282	9.698893	5709055	6.00E-36
56857	RAC875_c33648_760	12.64682	5710182	5.00E-27
23457	Excalibur_c20277_483	9.698893	5711960	4.00E-46
35226	IAAV6644	12.64682	5712240	1.00E-97
10800	BS00075373_51	14.10453	5799593	4.00E-46
10801	BS00075374_51	14.10453	5799671	4.00E-46
8755	BS00058860_51	11.8367	5800826	4.00E-46
66968	Tdurum_contig11192_130	14.10453	5801745	4.00E-46
20762	Ex_c4578_544	13.79198	5801746	4.00E-46
14318	CAP7_c9234_109	11.8367	6085500	4.00E-46
78856	wsnp_Ex_c8360_14085858	11.25912	6086489	2.00E-50
3843	BobWhite_c54480_387	11.8367	6353721	1.00E-43
11523	BS00087757_51	11.8742	6383649	4.00E-46
73929	Tdurum_contig9514_807	5.858341	6383751	4.00E-46
70488	Tdurum_contig34149_219	11.46415	6526064	4.00E-46
12194	BS00102648_51	11.55916	6692679	4.00E-43
12193	BS00102646_51	11.55916	6694030	4.00E-46
51224	Ra_c16527_465	11.55916	6805622	4.00E-46
43766	Kukri_c2972_110	9.723896	6816413	4.00E-46
21900	Excalibur_c11505_806	20.13539	12196052	1.00E-43
75222	tplb0059m03_622	20.13539	12196192	4.00E-46
6402	BS00011438_51	19.31527	12196340	4.00E-46
75221	tplb0059m03_1516	20.13539	12197086	4.00E-46
29081	Excalibur_c8386_1009	14.10453	12376892	4.00E-46
78861	wsnp_Ex_c8386_14128029	20.13539	12377476	1.00E-100
80635	wsnp_Ku_c6602_11531957	21.33306	12377634	1.00E-105
13878	CAP7_c1997_79	14.10453	12378819	6.00E-39
8467	BS00047528_51	14.10453	12807215	4.00E-46

Index	SNP Name	Genetic position (cM) ^a	Physical position (bp)	E-value
4343	BobWhite_c7454_363	14.10453	12807375	4.00E-46
34624	IAAV2853	14.10453	13605940	1.00E-100
41244	Kukri_c14642_917	14.10453	13606214	4.00E-46
6931	BS00022154_51	14.10453	13649775	4.00E-46
7919	BS00033209_51	23.35335	14178180	4.00E-46
12253	BS00105741_51	14.10453	14208290	4.00E-46
6054	BS00009393_51	14.10453	14208365	4.00E-46
77234	w SNP_ Ex_c22154_31342077	23.35335	14209627	1.00E-105
27758	Excalibur_c5779_263	14.10453	14284327	6.00E-36
37219	JD_c23336_253	23.35335	14285635	2.00E-45
65094	RFL_Contig5709_3446	25.0936	14911089	4.00E-46
64001	RFL_Contig2585_1280	14.10453	15046659	4.00E-46
71417	Tdurum_contig43378_256	14.10453	15060886	4.00E-46
19838	Ex_c14144_581	14.10453	17642925	7.00E-43
74456	tp1b0032a08_1721	14.10453	17643312	4.00E-46
64711	RFL_Contig4531_1195	12.64682	19097498	4.00E-46
29792	Excalibur_rep_c102055_320	12.64682	19097795	9.00E-32
68698	Tdurum_contig17943_547	14.10453	19294922	4.00E-46
22990	Excalibur_c17599_988	13.79198	19296876	4.00E-46
26277	Excalibur_c41820_354	30.33436	19491265	4.00E-46
9415	BS00064956_51	29.9618	21041047	4.00E-46
30032	Excalibur_rep_c104498_168	32.98724	21987684	1.00E-43
48628	Kukri_rep_c101341_425	14.10453	21994485	6.00E-45
30862	Excalibur_rep_c67448_528	32.98724	21996727	4.00E-43
77087	w SNP_ Ex_c19993_29024127	32.20963	22615887	1.00E-105
8163	BS00039218_51	33.72734	23544061	4.00E-46
52160	Ra_c488_923	33.72734	23761782	5.00E-24
52159	Ra_c488_1335	33.72734	23764095	4.00E-46
8751	BS00058753_51	32.98724	23764557	4.00E-46
21073	Ex_c66395_270	33.72734	23765939	4.00E-46
36123	IACX6214	33.72734	24071874	9.00E-41
73013	Tdurum_contig6501_449	34.19991	24512053	2.00E-41
7629	BS00026471_51	5.78583	24512231	4.00E-46
50786	Ra_c10565_1109	34.19991	25121884	4.00E-46
68098	Tdurum_contig13898_648	34.19991	25640151	4.00E-46
60454	RAC875_c7724_1312	34.19991	25816388	4.00E-46
34803	IAAV3924	34.60747	26209910	1.00E-101
67002	Tdurum_contig11297_571	34.61997	26578018	4.00E-46
8377	BS00044752_51	37.28785	29667800	4.00E-46
10462	BS00070455_51	34.19991	30651555	3.00E-44
34181	GENE-4824_212	37.6404	30983234	3.00E-37

Index	SNP Name	Genetic position (cM)^a	Physical position (bp)	E-value
2169	BobWhite_c28090_175	37.6404	30983825	4.00E-46
64363	RFL_Contig3455_700	41.32594	33769249	4.00E-46
64362	RFL_Contig3455_629	14.10453	33769320	4.00E-46
8453	BS00047114_51	48.12691	41179912	1.00E-43
1583	BobWhite_c22370_352	50.03968	49022733	1.00E-30
63642	RFL_Contig1456_842	50.03968	49467165	4.00E-46
38620	Ku_c17747_568	56.75565	52298429	1.00E-43
6987	BS00022242_51	54.2953	52298792	4.00E-46
26832	Excalibur_c47078_1918	56.75565	52517932	1.00E-43
26831	Excalibur_c47078_1842	56.75565	52518149	2.00E-35
46435	Kukri_c54561_272	56.75565	52535450	4.00E-46
25620	Excalibur_c35645_587	56.57312	53226507	4.00E-46
42033	Kukri_c18797_409	54.68535	53827178	4.00E-46
43841	Kukri_c30370_109	54.68535	53883422	2.00E-41
4121	BobWhite_c62702_587	54.68535	60252917	4.00E-46
74747	tplb0042o10_1533	54.68535	60254567	4.00E-46
11759	BS00092488_51	57.97083	60364949	4.00E-46
30709	Excalibur_rep_c116253_175	57.23822	61258830	3.00E-45
35437	IAAV8162	57.23822	61260960	7.00E-31
6294	BS00010818_51	57.97083	63548013	4.00E-46
41163	Kukri_c14140_347	57.97083	64158793	4.00E-46
10863	BS00076248_51	57.97083	64252923	4.00E-46
75862	w SNP_CAP11_c323_263800	61.63885	66367511	8.00E-70
14564	CAP8_c1799_237	61.63885	66367682	4.00E-46
75861	w SNP_CAP11_c323_263628	61.63885	66367683	6.00E-81
38850	Ku_c23207_988	61.63885	66643938	2.00E-29
21926	Excalibur_c11594_246	59.77858	71253803	3.00E-28
4450	BobWhite_c828_329	57.23822	71254647	2.00E-39
77560	w SNP_Ex_c2820_5215394	57.23822	71254648	6.00E-93
33758	GENE-4064_715	59.77858	71255516	3.00E-44
24683	Excalibur_c2820_889	59.77858	71257204	4.00E-46
80400	w SNP_Ku_c33335_42844680	56.80816	71880294	1.00E-104
54939	RAC875_c20041_976	56.80816	71880295	4.00E-46
80399	w SNP_Ku_c33335_42844594	57.23822	71880380	1.00E-104
54938	RAC875_c20041_1062	59.77858	71880381	4.00E-46
42446	Kukri_c2118_264	60.25115	74534815	3.00E-44
34153	GENE-4761_106	61.40631	74537512	1.00E-43
6079	BS00009566_51	61.63885	74541088	1.00E-43
35623	IACX1024	59.77858	74541171	6.00E-58
7439	BS00023137_51	60.25115	74700125	6.00E-45
79920	w SNP_JD_c9805_10591233	60.25115	74714672	1.00E-105

Index	SNP Name	Genetic position (cM) ^a	Physical position (bp)	E-value
50435	Kukri_rep_c85024_274	59.77858	75468927	4.00E-46
45902	Kukri_c48750_1372	61.89389	77500513	4.00E-46
45903	Kukri_c48750_1416	61.89389	77500557	4.00E-46
5332	BobWhite_rep_c63085_120	60.72122	77891942	6.00E-45
10937	BS00077528_51	61.63885	78174094	4.00E-46
57062	RAC875_c35310_987	61.63885	79232964	2.00E-38
57061	RAC875_c35310_770	61.63885	79234644	2.00E-41
7390	BS00023037_51	61.40631	79761587	4.00E-46
6436	BS00011570_51	61.89389	79887518	4.00E-46
26800	Excalibur_c4661_915	61.63885	80897492	1.00E-43
76769	wsnp_Ex_c15944_24350833	62.56898	91728193	2.00E-50
76244	wsnp_Ex_c1097_2105311	62.56898	94211536	1.00E-105
76243	wsnp_Ex_c1097_2105209	62.56898	94211638	1.00E-105
77214	wsnp_Ex_c21930_31102213	62.56898	106939346	2.00E-62
78274	wsnp_Ex_c4927_8772847	62.56898	108623982	1.00E-100
57	BobWhite_c10402_170	62.56898	112728314	4.00E-46
30974	Excalibur_rep_c68583_1067	62.56898	120570635	4.00E-46
48816	Kukri_rep_c102888_154	62.56898	122207495	4.00E-46
26240	Excalibur_c41477_1387	62.6665	125845884	3.00E-45
79735	wsnp_JD_c2623_3541255	62.56898	126473824	8.00E-77
25874	Excalibur_c37787_925	62.31145	126474138	6.00E-42
42275	Kukri_c20199_83	62.56898	127886330	3.00E-44
48693	Kukri_rep_c101837_143	62.56898	127887669	4.00E-46
79895	wsnp_JD_c8629_9593995	62.56898	132314569	1.00E-68
55784	RAC875_c25375_236	62.31145	144711632	1.00E-43
29321	Excalibur_c90987_248	62.6665	145008358	4.00E-46
35616	IAAV993	62.31145	146072501	1.00E-105
78263	wsnp_Ex_c4888_8714379	62.31145	146073959	1.00E-105
65260	RFL_Contig738_557	62.6665	152485728	1.00E-27
71405	Tdurum_contig43263_243	62.31145	152783852	1.00E-43
44174	Kukri_c3305_2048	62.31145	157667398	4.00E-46
79923	wsnp_JD_c9902_10674626	62.31145	157667399	1.00E-102
44006	Kukri_c3168_521	62.6665	159438856	6.00E-45
66519	Tdurum_contig10437_346	73.35303	160644788	4.00E-46
25607	Excalibur_c35491_788	62.6665	162444675	2.00E-41
56329	RAC875_c29373_483	67.45468	173382234	1.00E-43
23258	Excalibur_c19108_321	67.45468	173387540	4.00E-46
79682	wsnp_JD_c17082_16025440	64.59177	202125322	1.00E-105
44271	Kukri_c34038_562	65.55441	223836608	4.00E-46
35317	IAAV7265	65.72194	226078785	3.00E-88
55272	RAC875_c21955_719	65.72194	233490754	1.00E-43

Index	SNP Name	Genetic position (cM) ^a	Physical position (bp)	E-value
8317	BS00042337_51	65.72194	233706272	4.00E-46
13382	CAP12_c3646_76	64.7868	239305455	1.00E-43
45768	Kukri_c4747_330	63.83667	241793829	4.00E-46
10755	BS00074688_51	65.55441	244026021	8.00E-26
77086	w SNP_Ex_c19982_29009504	64.0467	244066659	1.00E-105
12299	BS00106922_51	63.96169	244067794	4.00E-46
12003	BS00097481_51	65.72194	247280726	4.00E-46
75535	w SNP_BE497469B_Ta_2_1	63.83667	248518437	6.00E-58
14775	CAP8_c490_173	63.83667	251345407	4.00E-46
73984	Tdurum_contig97351_247	63.83667	251345408	4.00E-46
40524	Kukri_c11120_462	63.83667	251715641	4.00E-46
36433	Jagger_c1219_603	64.7493	252827154	4.00E-46
79546	w SNP_Ex_rep_c70174_69125822	64.7493	252827155	1.00E-105
10391	BS00069274_51	65.55441	289973271	4.00E-46
22499	Excalibur_c14803_1088	65.55441	384915500	2.00E-45
10723	BS00074287_51	65.55441	421607136	4.00E-46
968	BobWhite_c16847_99	65.70693	427407918	4.00E-46
72453	Tdurum_contig55486_176	66.40704	430577514	4.00E-46
26717	Excalibur_c45968_83	67.13714	460113378	4.00E-46
64191	RFL_Contig304_729	67.13714	461645490	1.00E-33
236	BobWhite_c11540_60	67.19715	465177699	6.00E-39
74433	tplb0031e09_1230	67.45468	465622636	6.00E-45
74434	tplb0031e09_1763	67.45468	465623894	8.00E-29
76215	w SNP_Ex_c10717_17456391	67.45468	468118938	4.00E-98
11913	BS00095061_51	67.45468	468118939	4.00E-46
31431	Excalibur_rep_c94717_2115	67.45468	468727131	4.00E-46
30256	Excalibur_rep_c107277_109	67.45468	468727464	4.00E-46
31434	Excalibur_rep_c94717_959	67.45468	468728286	4.00E-46
62316	RAC875_rep_c115365_100	67.45468	468729178	4.00E-46
77452	w SNP_Ex_c2580_4800027	67.45468	470066584	1.00E-69
70852	Tdurum_contig42100_381	67.45468	470077350	4.00E-46
41868	Kukri_c18009_398	67.66972	475234856	4.00E-46
76269	w SNP_Ex_c1116_2138756	67.66972	475234857	1.00E-105
11270	BS00082644_51	67.66972	476385948	4.00E-46
76960	w SNP_Ex_c18624_27492167	67.45468	479057001	2.00E-54
35272	IAAV6934	67.45468	479228666	1.00E-100
7782	BS00030534_51	67.45468	479737194	4.00E-46
62162	RAC875_rep_c112642_422	67.45468	479737227	1.00E-43
80213	w SNP_Ku_c19631_29148397	67.45468	482887306	1.00E-103
80299	w SNP_Ku_c26257_36216869	67.45468	483146213	1.00E-105
10666	BS00073407_51	67.78473	487793847	2.00E-41

Index	SNP Name	Genetic position (cM) ^a	Physical position (bp)	E-value
8629	BS00053566_51	67.66972	492010775	4.00E-46
8630	BS00053568_51	67.66972	492011217	4.00E-46
77752	wsnp_Ex_c3227_5948436	67.66972	493343811	4.00E-57
35700	IACX11401	67.66972	493861281	1.00E-105
63776	RFL_Contig1945_110	68.10228	493864297	4.00E-46
22863	Excalibur_c16842_743	67.66972	494005069	4.00E-46
28828	Excalibur_c77101_90	68.10228	494005846	4.00E-46
77307	wsnp_Ex_c2330_4366134	68.86989	496421548	8.00E-74
57657	RAC875_c40919_1075	68.86989	496421549	3.00E-44
12267	BS00105995_51	69.09992	498277551	4.00E-46
35991	IACX5407	68.86989	498792382	2.00E-57
76394	wsnp_Ex_c123_244117	68.86989	498792443	1.00E-104
8186	BS00039734_51	68.86989	499095754	4.00E-46
80712	wsnp_Ku_c8722_14766699	68.86989	499095884	3.00E-58
21579	Excalibur_c10219_352	68.86989	500893218	4.00E-46
78385	wsnp_Ex_c5378_9505533	68.70986	501582669	1.00E-105
78384	wsnp_Ex_c5378_9505087	68.86989	501583115	1.00E-105
77221	wsnp_Ex_c22016_31191407	68.86989	502269585	1.00E-105
1851	BobWhite_c24774_186	68.86989	502269586	4.00E-46
10777	BS00074997_51	68.70986	504273506	4.00E-46
8047	BS00036352_51	68.70986	506488138	4.00E-34
8716	BS00057451_51	66.78209	507019361	4.00E-46
75705	wsnp_BG263758B_Ta_2_1	68.70986	511406619	6.00E-58
65080	RFL_Contig5682_86	69.61749	523285786	4.00E-46
8616	BS00052423_51	69.61749	523285876	4.00E-46
52028	Ra_c4096_921	69.52748	524749814	4.00E-46
27586	Excalibur_c55621_291	69.52748	524750655	2.00E-39
5282	BobWhite_rep_c61884_158	69.52748	527228249	2.00E-41
6527	BS00012080_51	69.52748	527788376	4.00E-46
32565	GENE-1624_193	69.52748	527789741	3.00E-39
28145	Excalibur_c62737_51	69.52748	534297241	6.00E-39
32657	GENE-1787_339	69.52748	534297405	2.00E-35
37751	JD_c6678_319	69.52748	535609869	1.00E-43
7785	BS00030581_51	69.52748	538792003	4.00E-46
7784	BS00030580_51	69.52748	538792235	4.00E-46
59720	RAC875_c62872_293	69.52748	538803062	4.00E-46
28034	Excalibur_c61285_135	69.52748	538803392	6.00E-45
11393	BS00084911_51	69.52748	539720046	4.00E-46
23340	Excalibur_c19552_319	69.72001	540900124	6.00E-39
67009	Tdurum_contig11307_628	69.59999	552628694	2.00E-41
72928	Tdurum_contig63030_778	69.59999	553057949	4.00E-46

Index	SNP Name	Genetic position (cM) ^a	Physical position (bp)	E-value
73182	Tdurum_contig70783_1548	69.59999	554313345	4.00E-46
8522	BS00049008_51	69.72001	557743002	4.00E-46
3723	BobWhite_c5095_634	69.72001	558877350	6.00E-36
35908	IACX3190	69.72001	559029461	6.00E-55
26579	Excalibur_c44713_137	69.72001	559064217	8.00E-23
47760	Kukri_c783_1833	69.72001	559969109	1.00E-43
8908	BS00062734_51	70.02505	560252994	1.00E-24
48764	Kukri_rep_c102334_1871	71.34024	567478506	4.00E-46
3229	BobWhite_c4233_180	71.34024	570413066	6.00E-42
80726	wsnp_Ku_c93664_84327484	71.34024	571339948	3.00E-30
8320	BS00042456_51	71.34024	572332650	4.00E-46
9708	BS00066060_51	73.35303	573318031	1.00E-24
12538	BS00110445_51	71.34024	575122225	4.00E-46
27257	Excalibur_c5182_93	71.34024	575342950	4.00E-34
35937	IACX3871	71.0752	576451719	2.00E-57
11599	BS00089166_51	71.0652	576749712	4.00E-46
28943	Excalibur_c80041_400	71.34024	576753519	3.00E-28
38055	Ku_c101932_436	71.00019	577643179	4.00E-46
40700	Kukri_c11910_445	70.08756	580455873	4.00E-46
40352	Kukri_c10464_653	71.0752	580818000	4.00E-46
1301	BobWhite_c19725_1329	70.08756	581453903	4.00E-46
453	BobWhite_c13099_755	70.11757	582018863	6.00E-39
25478	Excalibur_c34581_339	70.11757	582019259	2.00E-40
29033	Excalibur_c82403_135	71.12271	588621281	4.00E-46
27903	Excalibur_c5977_383	70.69765	589862522	4.00E-46
27904	Excalibur_c5977_440	70.69765	589862579	2.00E-38
7903	BS00032695_51	70.69765	589866278	4.00E-40
7901	BS00032692_51	70.69765	589869211	4.00E-46
28150	Excalibur_c62826_254	70.69765	593422816	3.00E-45
3120	BobWhite_c40455_116	72.23787	594588908	4.00E-46
80849	wsnp_Ku_rep_c72821_72480395	72.23787	595024099	1.00E-105
78441	wsnp_Ex_c5547_9774195	71.34024	595024670	1.00E-105
64673	RFL_Contig4421_1490	72.23787	596782508	4.00E-46
64674	RFL_Contig4421_1724	72.23787	596782742	4.00E-46
38943	Ku_c25346_508	71.65028	597080925	4.00E-46
38942	Ku_c25346_503	71.65028	597080931	4.00E-46
71969	Tdurum_contig49477_548	71.94533	597523159	4.00E-46
71967	Tdurum_contig49477_187	71.94533	597523631	4.00E-46
238	BobWhite_c11562_133	71.34024	597523758	4.00E-46
31045	Excalibur_rep_c69241_274	72.4329	603587946	4.00E-46
35408	IAAV792	73.133	610352333	1.00E-105

Index	SNP Name	Genetic position (cM) ^a	Physical position (bp)	E-value
53138	RAC875_c106500_413	73.133	610749791	4.00E-46
40726	Kukri_c12041_94	73.25302	615935934	4.00E-46
11721	BS00091643_51	73.03799	618466236	5.00E-27
49250	Kukri_rep_c107323_210	74.26316	620058346	3.00E-25
75575	wsnp_BE517914B_Ta_2_5	74.26316	627097536	2.00E-38
68457	Tdurum_contig15724_118	74.22565	631232266	4.00E-46
74291	tplb0026h15_986	74.22565	637704623	4.00E-46
71336	Tdurum_contig42711_1483	74.26316	640262248	4.00E-46
73162	Tdurum_contig70056_255	74.26316	642828763	1.00E-43
80632	wsnp_Ku_c6430_11257008	74.26316	643397496	3.00E-69
78565	wsnp_Ex_c6129_10723211	74.26316	645076488	1.00E-56
27565	Excalibur_c55414_254	74.26316	645077292	3.00E-30
39502	Ku_c47648_1403	74.26316	645220934	3.00E-45
11998	BS00097383_51	74.43319	648287365	4.00E-46
58033	RAC875_c44290_511	74.70823	651510403	2.00E-39
11501	BS00087427_51	76.91104	674746268	4.00E-46
77099	wsnp_Ex_c20168_29214721	76.91104	675961954	8.00E-71
77014	wsnp_Ex_c1934_3648048	76.91104	676286799	1.00E-75
3100	BobWhite_c40087_93	75.1908	678073174	2.00E-42
24338	Excalibur_c25567_225	77.24609	682301381	4.00E-46
25163	Excalibur_c31960_1492	77.22859	682987099	1.00E-43
81104	wsnp_Ra_c3289_6166914	77.22859	682988584	2.00E-56
76178	wsnp_Ex_c10499_17161734	77.24609	684193957	6.00E-93
58890	RAC875_c530_354	77.22859	684335469	4.00E-46
59075	RAC875_c54868_77	76.91104	684339639	4.00E-46
12466	BS00110072_51	77.22859	684350435	1.00E-43
77213	wsnp_Ex_c21924_31095740	76.91104	686989104	1.00E-105
55756	RAC875_c25203_969	76.91104	686993691	4.00E-46
51803	Ra_c3129_2015	75.1908	687269990	4.00E-46
7617	BS00026264_51	78.16122	690465578	4.00E-46
38582	Ku_c172_840	78.16122	692198681	4.00E-46
11298	BS00083391_51	80.12901	702605774	4.00E-46
7127	BS00022512_51	80.12901	702605797	4.00E-46
54326	RAC875_c16625_182	80.12901	704348033	2.00E-42
75386	wsnp_BE424246B_Ta_2_2	80.12901	704518133	4.00E-57
52107	Ra_c44591_213	80.12901	719624572	1.00E-43
49175	Kukri_rep_c106420_312	80.99163	722331418	4.00E-46
68915	Tdurum_contig21043_186	80.99163	723086777	4.00E-46
33456	GENE-3543_165	80.99163	723397337	4.00E-46
13058	CAP11_c797_273	80.99163	725280621	4.00E-46
1640	BobWhite_c22794_470	80.99163	725839453	4.00E-46

Index	SNP Name	Genetic position (cM) ^a	Physical position (bp)	E-value
77660	wsnp_Ex_c3040_5615597	80.99163	725839454	1.00E-105
1639	BobWhite_c22794_111	80.99163	725839812	4.00E-46
38430	Ku_c14074_2900	80.99163	730660089	5.00E-18
76452	wsnp_Ex_c12781_20280445	80.99163	730662189	1.00E-104
25978	Excalibur_c38785_222	80.99163	730665289	2.00E-41
76343	wsnp_Ex_c11837_18996495	80.99163	733011780	3.00E-98
36207	IACX7527	80.12901	735758644	1.00E-103
56230	RAC875_c2879_2784	80.99163	735777871	4.00E-46
77976	wsnp_Ex_c39124_46489956	80.99163	737741124	4.00E-97
79678	wsnp_JD_c16245_15468917	80.7616	737741403	2.00E-86
50871	Ra_c109604_751	80.75659	737741623	8.00E-23
23301	Excalibur_c19367_76	80.99163	738210983	4.00E-46
12008	BS00097541_51	80.99163	738213312	4.00E-46
6203	BS00010316_51	80.99163	738214070	1.00E-43
35905	IACX3169	81.20166	738352639	2.00E-57
32512	GENE-1511_622	81.20166	739436283	4.00E-46
59283	RAC875_c5739_1262	81.79675	739630605	4.00E-46
13886	CAP7_c2116_545	81.79675	740422471	4.00E-40
38503	Ku_c1575_485	81.79675	741192233	4.00E-46
80965	wsnp_Ra_c18164_27178459	81.79675	741193855	1.00E-104
27458	Excalibur_c54205_696	84.48963	743617148	4.00E-46
27457	Excalibur_c54205_381	84.48963	743617699	3.00E-28
27456	Excalibur_c54205_336	84.48963	743617995	1.00E-33
76498	wsnp_Ex_c13154_20785032	82.1868	743623404	1.00E-103
76497	wsnp_Ex_c13154_20784674	82.1868	743623761	1.00E-105
78610	wsnp_Ex_c64005_62986957	82.1868	743632523	1.00E-104
13267	CAP12_c1991_127	80.99163	747114954	4.00E-46
75541	wsnp_BE497740B_Ta_2_1	82.1568	748524407	6.00E-58
75542	wsnp_BE497740B_Ta_2_2	82.1568	748524495	1.00E-52
70415	Tdurum_contig33192_76	82.1568	748528801	9.00E-32
12079	BS00099633_51	82.1568	748848946	4.00E-46
11034	BS00078844_51	85.02721	751673953	4.00E-46
35001	IAAV5302	86.97499	752505891	1.00E-105
51093	Ra_c14132_2575	86.97499	752505892	4.00E-46
51903	Ra_c35_3184	88.31268	754784229	4.00E-46
8244	BS00040742_51	88.31268	756408562	1.00E-43
73140	Tdurum_contig69073_365	88.31268	756569334	4.00E-46
13376	CAP12_c3551_85	88.07515	757225145	2.00E-41
78844	wsnp_Ex_c8208_13870372	88.07515	757301451	1.00E-105
24050	Excalibur_c2381_214	89.1278	757302739	3.00E-45
8775	BS00059416_51	88.07515	760432653	4.00E-46

Index	SNP Name	Genetic position (cM) ^a	Physical position (bp)	E-value
7061	BS00022403_51	90.87305	760873210	4.00E-46
47344	Kukri_c66862_96	90.62551	761501128	4.00E-46
12530	BS00110416_51	93.56844	764355065	9.00E-32
70345	Tdurum_contig32277_121	93.90598	765989799	4.00E-46
23681	Excalibur_c21708_555	97.61652	772153046	2.00E-38
10322	BS00068473_51	105.3551	785126983	4.00E-46
72700	Tdurum_contig59953_282	107.1529	788062748	4.00E-46
64607	RFL_Contig4186_852	107.1529	788062749	4.00E-46
20327	Ex_c26158_622	106.3353	788705049	1.00E-33
12975	CAP11_c59_418	115.3591	795898611	4.00E-46
75890	w SNP_CAP11_c59_99702	115.7991	795898803	1.00E-104
75891	w SNP_CAP11_c59_99769	115.3591	795898871	1.00E-104
42624	Kukri_c2227_583	115.6316	797470134	4.00E-46
9228	BS00064227_51	115.3591	799289775	1.00E-43
75968	w SNP_CAP12_c2297_1121142	119.3771	799913092	1.00E-100
25460	Excalibur_c34433_220	123.4002	808042644	2.00E-39
10560	BS00071598_51	125.3655	812997019	4.00E-46
10559	BS00071597_51	125.3655	812997024	4.00E-46
10751	BS00074629_51	125.3655	813002432	4.00E-46
8118	BS00037871_51	125.3655	813013483	4.00E-46
14514	CAP8_c1329_129	125.3655	813448216	2.00E-41
33031	GENE-2712_367	125.3655	813458293	8.00E-33
74074	Tdurum_contig99764_139	125.3655	813645557	1.00E-43
32925	GENE-2405_488	125.3655	813648022	4.00E-46
73670	Tdurum_contig84676_145	123.6002	814989227	4.00E-46
42697	Kukri_c22748_211	134.8344	816073106	4.00E-46
42890	Kukri_c23955_144	134.8344	816073154	4.00E-46
55459	RAC875_c23148_680	134.8344	816073931	4.00E-46
10017	BS00067324_51	134.8344	816804473	1.00E-43
20793	Ex_c47471_416	136.3596	818905413	4.00E-46
54249	RAC875_c16251_618	136.3121	822437989	4.00E-46
1595	BobWhite_c22447_112	136.3121	825208797	2.00E-41
13855	CAP7_c1794_121	136.3596	826785749	4.00E-46
77565	w SNP_Ex_c284_548711	134.8344	828934019	2.00E-90
28159	Excalibur_c63009_102	136.3121	828934020	1.00E-43
42423	Kukri_c21041_263	137.1997	829425746	1.00E-38
53715	RAC875_c13406_65	137.1997	829426578	1.00E-43
57141	RAC875_c35955_210	137.1997	829426579	2.00E-32
8385	BS00044955_51	139.6176	830695941	4.00E-46
8384	BS00044949_51	139.6176	830698249	4.00E-46
48859	Kukri_rep_c103205_101	139.6176	830699246	4.00E-46

Index	SNP Name	Genetic position (cM)^a	Physical position (bp)	E-value
8383	BS00044944_51	139.6176	830699486	4.00E-46
8382	BS00044942_51	139.6176	830699536	4.00E-46
27534	Excalibur_c55096_613	139.6176	830839763	2.00E-41
28241	Excalibur_c63859_401	139.6176	831764723	4.00E-46
45539	Kukri_c45513_83	139.6176	833470282	1.00E-43
9387	BS00064876_51	139.6176	833664271	4.00E-46
33964	GENE-4458_691	139.6176	834438115	1.00E-41
81501	wsnp_RFL_Contig3524_3689801	139.6176	834884886	4.00E-34
11049	BS00079029_51	140.5077	840540799	4.00E-46
10667	BS00073411_51	144.7433	844712069	4.00E-46
8058	BS00036547_51	144.7433	844873878	4.00E-46
28522	Excalibur_c6906_2385	144.7433	847805046	4.00E-46
81341	wsnp_Ra_rep_c75740_73183118	144.7433	847816539	8.00E-71
35514	IAAV8659	144.7433	847816540	8.00E-71
10531	BS00071183_51	144.7433	850793240	4.00E-46
20447	Ex_c303_3825	154.4772	851109994	4.00E-46
51602	Ra_c2553_1880	154.4772	851126805	4.00E-46
72656	Tdurum_contig59566_1534	143.2931	851577261	4.00E-46
46567	Kukri_c55981_194	143.2931	851577680	4.00E-46
79690	wsnp_JD_c18509_16968425	143.2931	851579501	1.00E-104
72658	Tdurum_contig59566_4435	143.2931	851580138	4.00E-46
66935	Tdurum_contig11114_335	144.3832	851720657	4.00E-46
72194	Tdurum_contig51605_542	144.3832	851866866	4.00E-46

^aFrom Wang et al. (2014)

**APPENDIX D. PHYSICAL POSITION OF THE RECOMBINATION BREAKPOINTS IN
THE CRITICAL 3B-3E RECOMBINANTS USED FOR THE CONSTRUCTION OF THE
COMPOSITE BIN MAP**

Recombinant ID	Original recombinant code	Recombinant chromosome composition	Physical positions of recombinant breakpoints (bp)^a	
I-12	XWC14-186-13	3ES·3EL·3BL	803977868	
I-15	XWC14-723-9	3ES·3EL·3BL	786594866	
I-14	XWC14-186-4	3ES·3EL·3BL	778640015	
I-18	XWC14-723-21	3ES·3EL·3BL	691332130	
VI-1	XWC14-723-8	3ES·3BL	337444386	
II-2	XWC14-186-14	3ES·3BS·3BL	160041822	
II-4	XWC14-723-29	3ES·3BS·3BL	158553128	
II-8	XWC14-722-2	3ES·3BS·3BL	68948871	
II-7	XWC14-186-37	3ES·3BS·3BL	45101323	
II-10	XWC14-186-120	3ES·3BS·3BL	28122909	
IV-1	XWC14-722-79	3ES·3BS·3BL·3EL	23079974	788383899
II-18	XWC14-722-3	3BS·3BL·3EL	3318264	740026538
IV-2	MZ15-2-11	3BS·3ES·3BS·3BL	28122909	65310217
IV-3	MZ16-3rd-1-5	3BS·3ES·3BS·3BL	73208098	149279844
I-23	XWC14-722-21	3ES·3EL·3BL	3737057	537200936
III-20	MZ16-3rd-3-28	3BS·3ES·3EL·3BL	73208098	540310085
III-14	MZ16-3rd-3-39	3BS·3ES·3EL·3BL	73208098	663128336
I-19	XWC14-722-65	3ES·3EL·3BL	4845484	663128336
III-15	MZ16-3rd-4-12	3BS·3ES·3EL·3BL	73208098	745373739
III-8	MZ15-11-35	3BS·3ES·3EL·3BL	73208098	760652932
III-11	MZ15-11-21	3BS·3ES·3EL·3BL	73208098	778640015
III-2	MZ15-2-7	3BS·3ES·3EL·3BL	28122909	803977868
III-5	MZ15-4-3	3BS·3ES·3EL·3BL	68948871	803977868
III-3	MZ15-11-13	3BS·3ES·3EL·3BL	73208098	792301830
III-10	MZ15-11-36	3BS·3ES·3EL·3BL	73208098	786594866
IV-4	MZ16-3rd-3-35	3BS·3BL·3EL·3BL	546764409	778640015
IV-5	MZ16-3rd-3-17	3BS·3BL·3EL·3BL	623577941	778640015
IV-7	MZ16-3rd-1-13	3BS·3BL·3EL·3BL	704433083	778640015
IV-8	MZ15-4-2	3BS·3BL·3EL·3BL	745373739	803977868
II-28	MZ15-2-2	3BS·3BL·3EL	827859884	
II-29	XWC14-186-115	3BS·3BL·3EL	823823393	
II-26	XWC14-186-59	3BS·3BL·3EL	803977868	
II-21	XWC14-722-57	3BS·3BL·3EL	762928097	
II-20	XWC14-186-143	3BS·3BL·3EL	745373739	

Recombinant ID	Original recombinant code	Recombinant chromosome composition	Physical positions of recombinant breakpoints (bp)^a
II-19	MZ15-11-5	3BS·3BL·3EL	742405502
II-14	XWC14-723-17	3BS·3BL·3EL	663128336
II-13	MZ15-11-12	3BS·3BL·3EL	600555852
VI-2	XWC14-186-34	3BS·3EL	337444386
I-11	XWC14-722-70	3BS·3ES·3EL	167913455
I-10	XWC14-186-134	3BS·3ES·3EL	86312843
I-8	XWC14-186-35	3BS·3ES·3EL	73208098
I-9	XWC14-722-36	3BS·3ES·3EL	68948871
I-7	XWC14-722-35	3BS·3ES·3EL	37474616
I-2	XWC14-186-2	3BS·3ES·3EL	28122909
III-1	XWC14-186-133	3BS·3ES·3EL·3BL	23079974
I-4	XWC14-186-1	3BS·3ES·3EL	19394071

^aThe physical position of a recombination breakpoint was estimated according to the physical location of the middle point between the SNPs immediately flanking the recombination breakpoint in the IWGSC RefSeq v2.0 (<https://wheat-urgi.versailles.inra.fr/>).

Note: The recombinants highlighted in yellow showed discrepancy in their FGISH and SNP delineation results, which was discussed in the text of this paper.

**APPENDIX E. PRIMER SEQUENCES AND PHYSICAL LOCATIONS OF THE
CHROMOSOME-SPECIFIC STARP MARKERS**

Markers	Forward and reverse primers ^a	SNP physical position (bp) ^b on wheat chromosomes		
		3B	3A	3D
<i>Xwgc2200</i>	F1: 5' [Tail1]-GAGGACAATTTTGTGCCCTTC 3'			
	F2: 5' [Tail2]-GAGGACAATTTTGTGCCCTCTT 3'	3,490,856	1,484,258	1,284,228
	R: 5' GTAGAACCTTCCTTTGTTTTAGATGC 3'			
<i>Xwgc2201</i>	F1: 5' [Tail2]-ACATATGTTACTTGTCTTTCCACA 3'			
	F2: 5' [Tail1]-ACATATGTTACTTGTCTTTACCG 3'	66,645,755	45,851,272	33,191,888
	R: 5' GCTACATCACAGAAAGAAGAAAGAC 3'			
<i>Xwgc2202</i>	F1: 5' [Tail2]-TGCGATGCATGCTATAAT 3'			
	F2: 5' [Tail1]-TGCGATGCATGCTACGAC 3'	83,591,270	58,260,819	46,341,034
	R: 5' GTAAGTTCTGCAATGGATCAAGCC 3'			
<i>Xwgc2203</i>	F1: 5' [Tail1]-CAGAGTACCAGAACCTACG 3'			
	F2: 5' [Tail2]-CAGAGTACCAGAACCCGCA 3'	132,321,773	88,926,026	75,209,804
	R: 5' CTCTTTCGTTTGATGAGAGAAACGG 3'			
<i>Xwgc2204</i>	F1: 5' [Tail1]-TTGTACTCGGCTACCGCC 3'			
	F2: 5' [Tail2]-TTGTACTCGGCTACTACT 3'	175,409,378	-	-
	R: 5' CTCTTCTGAACCCAAGGCTGG 3'			
<i>Xwgc2205</i>	F1: 5' [Tail1]-GCACTCACAAACATTACG 3'			
	F2: 5' [Tail2]-GCACTCACAAACATCGCA 3'	248,518,905	198,380,623	161,156,616
	R: 5' GCCCCATGATCAATGACAACC 3'			
<i>Xwgc2206</i>	F1: 5' [Tail1]-CACTATTTGGACTCAGTTCC 3'			
	F2: 5' [Tail2]-CACTATTTGGACTCAGCCCT 3'	264,857,141	225,629,349	175,311,145
	R: 5' CTTGTGGTTAATGCCATCCAATAAC 3'			
<i>Xwgc2207</i>	F1: 5' [Tail2]-GCTGCGGAAAAAATACTCG 3'			
	F2: 5' [Tail1]-GCTGCGGAAAAAATATCCC 3'	325,970,528	345,408,468	251,521,190
	R: 5' TGTAACATTATTTTGCTGTTGAGCAA 3'			
<i>Xwgc2208</i>	F1: 5' [Tail1]-GTTCCAGCGGCATTCGTC 3'			
	F2: 5' [Tail2]-GTTCCAGCGGCATTATT 3'	361,280,132	-	239,062,521
	R: 5' CTGCACCCACCGTGTC 3'			
<i>Xwgc2209</i>	F1: 5' [Tail1]-CTGATGCACATGTATTCCC 3'			
	F2: 5' [Tail2]-CTGATGCACATGTATCTCG 3'	392,994,065	391,171,375	290,574,818
	R: 5' CATGGGATGCTGATGTACCC 3'			

Markers	Forward and reverse primers ^a	SNP physical position (bp) ^b on wheat chromosomes		
		3B	3A	3D
<i>Xwgc2210</i>	F1: 5' [Tail1]-ATATCATGACTCTGGGTGTACTG 3'			
	F2: 5' [Tail2]-ATATCATGACTCTGGGTGTCTTA 3'	407,893,843	411,821,827	302,073,102
	R: 5' TTCCAAGACCAAGACCACGG 3'			
<i>Xwgc2211</i>	F1: 5' [Tail1]-TCGGTGAATCAACAATACG 3'			
	F2: 5' [Tail2]-TCGGTGAATCAACAACGCA 3'	415,066,634	425,014,630	308,649,157
	R: 5' GAGAGTCCATCGCAGGTGT 3'			
<i>Xwgc2212</i>	F1: 5' [Tail1]-TGTTGGCTCCCTGGAAG 3'			
	F2: 5' [Tail2]-TGTTGGCTCCCTGAGAA 3'	419,059,351	427,625,849	311,018,846
	R: 5' TCTTTCACGCTGGTAAGAAAATGA 3'			
<i>Xwgc2213</i>	F1: 5' [Tail1]-GTTGACCTTGAGGTTTTTAATTTC 3'			
	F2: 5' [Tail2]-GTTGACCTTGAGGTTTTTAACCTT 3'	438,878,743	454,610,006	329,960,224
	R: 5' TGGCGACTCCTCCAGCA 3'			
<i>Xwgc2214</i>	F1: 5' [Tail2]-CCATCATATGGAGGAATAAAAAAT 3'			
	F2: 5' [Tail1]-CCATCATATGGAGGAATAAACGAC 3'	464,504,726	482,293,437	353,770,380
	R: 5' CTCCACCTTCTGAATAAACACCTC 3'			
<i>Xwgc2215</i>	F1: 5' [Tail2]-CCAGGAAAACCATCTGCAGA 3'			
	F2: 5' [Tail1]-CCAGGAAAACCATCTGACGT 3'	482,869,018	492,472,561	362,195,290
	R: 5' TCTGCTTAATGTATGCCGCAA 3'			
<i>Xwgc2216</i>	F1: 5' [Tail1]-GCAGGTAATTGTCATTTAGC 3'			
	F2: 5' [Tail2]-GCAGGTAATTGTCATTTCCGT 3'	527,230,784	524,897,193	394,868,465
	R: 5' GCTTCAGTTCGCCCCGAAC 3'			
<i>Xwgc2217</i>	F1: 5' [Tail1]-AGAACTTCCTCATTCGTTATAC 3'			
	F2: 5' [Tail2]-AGAACTTCCTCATTCGTTGCAT 3'	599106833	587,247,454	446,173,688
	R: 5' CCAAGGGCCTCAGCAAATTG 3'			
<i>Xwgc2218</i>	F1: 5' [Tail1]-AAATCGTCTTAGTTCATTCAAAAAC 3'			
	F2: 5' [Tail2]-AAATCGTCTTAGTTCATTCAAGCAG 3'	747,302,246	688,781,535	552,745,796
	R: 5' CGAGCATAACTGTGGTCCTGA 3'			
<i>Xwgc2219</i>	F1: 5' [Tail2]-GAAAACTGGCGCATGCAT 3'			
	F2: 5' [Tail1]-GAAAACTGGCGCATATAC 3'	780,701,151	711,392,600	577,144,717
	R: 5' TGTAAAGCTGTTCAAAGTTGTCAC 3'			
<i>Xwgc2220</i>	F1: 5' [Tail2]-GTTGATGTTGTTGCTGGA 3'			
	F2: 5' [Tail1]-GTTGATGTTGTTGCCAGG 3'	799,649,332	-	589,420,344
	R: 5' TCATACTGCTGACCAGGAGAAT 3'			

Markers	Forward and reverse primers ^a	SNP physical position (bp) ^b on wheat chromosomes		
		3B	3A	3D
<i>Xwgc2221</i>	F1: 5' [Tail2]-CAAGGATGGACTTCATTCT 3'			
	F2: 5' [Tail1]-CAAGGATGGACTTCATCCCC 3'	834,700,453	739,183,826	610,690,595
	R: 5' GAACACCCTCGCTAGGACCA 3'			

**APPENDIX F. THE 7B-7E AND 7B-7S RECOMBINANTS/ABERRATIONS AND THEIR
COMPOSITIONS AND PEDIGREE**

Recombinant ID	Original recombinant code	Recombinant chromosomes and aberrations	Pedigree
I-1	XWC14-260-120	7ES·7EL-7BL	CS DS 7E(7B)/2*CS <i>ph1b</i> mutant//CS DS 7E(7B)
I-2	XWC14-757-21	7ES·7EL-7BL	CS DS 7E(7B)/2*CS <i>ph1b</i> mutant//CS DS 7E(7B)
I-3	XWC14-760-14	7ES·7EL-7BL	CS DS 7E(7B)/2*CS <i>ph1b</i> mutant//CS DS 7E(7B)
I-4	XWC14-257-94	7ES·7EL-7BL	CS DS 7E(7B)/2*CS <i>ph1b</i> mutant//CS DS 7E(7B)
I-5	XWC14-762-3	7ES·7EL-7BL	CS DS 7E(7B)/2*CS <i>ph1b</i> mutant//CS DS 7E(7B)
I-6	XWC14-759-26	7ES·7EL-7BL	CS DS 7E(7B)/2*CS <i>ph1b</i> mutant//CS DS 7E(7B)
I-7	XWC14-257-38	7ES·7EL-7BL	CS DS 7E(7B)/2*CS <i>ph1b</i> mutant//CS DS 7E(7B)
I-8	XWC14-257-50	7ES·7EL-7BL	CS DS 7E(7B)/2*CS <i>ph1b</i> mutant//CS DS 7E(7B)
II-1	XWC14-260-121	7ES·7EL-7BL	CS DS 7E(7B)/2*CS <i>ph1b</i> mutant//CS DS 7E(7B)
II-2	XWC14-760-7	7ES·7EL-7BL	CS DS 7E(7B)/2*CS <i>ph1b</i> mutant//CS DS 7E(7B)
II-3	XWC14-258-86	7ES·7EL-7BL	CS DS 7E(7B)/2*CS <i>ph1b</i> mutant//CS DS 7E(7B)
II-4	XWC14-255-11	7ES·7EL-7BL	CS DS 7E(7B)/2*CS <i>ph1b</i> mutant//CS DS 7E(7B)
II-5	XWC14-260-47	7ES·7EL-7BL	CS DS 7E(7B)/2*CS <i>ph1b</i> mutant//CS DS 7E(7B)
II-6	XWC14-260-26	7ES·7EL-7BL	CS DS 7E(7B)/2*CS <i>ph1b</i> mutant//CS DS 7E(7B)
II-7	XWC14-259-36	7ES·7EL-7BL	CS DS 7E(7B)/2*CS <i>ph1b</i> mutant//CS DS 7E(7B)
II-8	XWC14-260-17	7BS·7ES·7EL	CS DS 7E(7B)/2*CS <i>ph1b</i> mutant//CS DS 7E(7B)
III-1	XWC14-255-24	7BS·7BL-7EL	CS DS 7E(7B)/2*CS <i>ph1b</i> mutant//CS DS 7E(7B)
III-2	XWC14-255-25	7BS·7BL-7EL	CS DS 7E(7B)/2*CS <i>ph1b</i> mutant//CS DS 7E(7B)
III-3	XWC14-760-25	7BS·7BL-7EL	CS DS 7E(7B)/2*CS <i>ph1b</i> mutant//CS DS 7E(7B)
III-4	XWC14-258-72	7BS·7BL-7EL	CS DS 7E(7B)/2*CS <i>ph1b</i> mutant//CS DS 7E(7B)
III-5	XWC14-759-37	7BS·7BL-7EL	CS DS 7E(7B)/2*CS <i>ph1b</i> mutant//CS DS 7E(7B)
III-6	XWC14-258-33	7BS·7BL-7EL	CS DS 7E(7B)/2*CS <i>ph1b</i> mutant//CS DS 7E(7B)
III-7	XWC14-255-23	7BS·7BL-7EL	CS DS 7E(7B)/2*CS <i>ph1b</i> mutant//CS DS 7E(7B)
III-8	XWC14-759-52	7BS·7BL-7EL	CS DS 7E(7B)/2*CS <i>ph1b</i> mutant//CS DS 7E(7B)
IV-1	XWC14-255-3	7BS·7BL-7EL	CS DS 7E(7B)/2*CS <i>ph1b</i> mutant//CS DS 7E(7B)
IV-2	XWC14-762-36	7BS·7BL-7EL	CS DS 7E(7B)/2*CS <i>ph1b</i> mutant//CS DS 7E(7B)
IV-3	XWC14-255-34	7BS·7BL-7EL	CS DS 7E(7B)/2*CS <i>ph1b</i> mutant//CS DS 7E(7B)

Recombinant ID	Original recombinant code	Recombinant chromosomes and aberrations	Pedigree
IV-4	XWC14-258-83	7BS·7BL-7EL	CS DS 7E(7B)/2*CS <i>ph1b</i> mutant//CS DS 7E(7B)
IV-5	XWC14-759-17	7BS·7BL-7EL	CS DS 7E(7B)/2*CS <i>ph1b</i> mutant//CS DS 7E(7B)
VI-1	XWC14-260-107	7ES·7BL	CS DS 7E(7B)/2*CS <i>ph1b</i> mutant//CS DS 7E(7B)
VI-2	XWC14-260-30	7ES·7BL	CS DS 7E(7B)/2*CS <i>ph1b</i> mutant//CS DS 7E(7B)
VI-3	XWC14-260-49	7ES·7BL	CS DS 7E(7B)/2*CS <i>ph1b</i> mutant//CS DS 7E(7B)
VI-4	XWC14-760-5	7ES·7BL	CS DS 7E(7B)/2*CS <i>ph1b</i> mutant//CS DS 7E(7B)
VI-5	XWC14-257-82	7ES·7BL	CS DS 7E(7B)/2*CS <i>ph1b</i> mutant//CS DS 7E(7B)
VI-6	XWC14-258-29	7ES·7BL	CS DS 7E(7B)/2*CS <i>ph1b</i> mutant//CS DS 7E(7B)
VI-7	XWC14-260-62	7BS·7EL	CS DS 7E(7B)/2*CS <i>ph1b</i> mutant//CS DS 7E(7B)
VII-1	XWC14-258-76	7ES or 7EL	CS DS 7E(7B)/2*CS <i>ph1b</i> mutant//CS DS 7E(7B)
I-9	XWC14-704-4	7SS·7SL-7BL	CS DS 7S(7B)/2*CS <i>ph1b</i> mutant//CS DS 7S(7B)
I-10	XWC14-90-4	7SS·7SL-7BL	CS DS 7S(7B)/2*CS <i>ph1b</i> mutant//CS DS 7S(7B)
I-11	XWC14-705-21	7SS·7SL-7BL	CS DS 7S(7B)/2*CS <i>ph1b</i> mutant//CS DS 7S(7B)
I-12	XWC14-705-8	7SS·7SL-7BL	CS DS 7S(7B)/2*CS <i>ph1b</i> mutant//CS DS 7S(7B)
I-13	XWC14-707-8	7SS·7SL-7BL	CS DS 7S(7B)/2*CS <i>ph1b</i> mutant//CS DS 7S(7B)
I-14	XWC14-87-12	7SS·7SL-7BL	CS DS 7S(7B)/2*CS <i>ph1b</i> mutant//CS DS 7S(7B)
I-15	XWC14-87-1	7SS·7SL-7BL	CS DS 7S(7B)/2*CS <i>ph1b</i> mutant//CS DS 7S(7B)
I-16	XWC14-709-3	7SS·7SL-7BL	CS DS 7S(7B)/2*CS <i>ph1b</i> mutant//CS DS 7S(7B)
I-17	XWC14-705-1	7SS·7SL-7BL	CS DS 7S(7B)/2*CS <i>ph1b</i> mutant//CS DS 7S(7B)
I-18	XWC14-707-25	7SS·7SL-7BL	CS DS 7S(7B)/2*CS <i>ph1b</i> mutant//CS DS 7S(7B)
I-19	XWC14-705-18	7SS·7SL-7BL	CS DS 7S(7B)/2*CS <i>ph1b</i> mutant//CS DS 7S(7B)
I-20	XWC14-708-29	7SS·7SL-7BL	CS DS 7S(7B)/2*CS <i>ph1b</i> mutant//CS DS 7S(7B)
I-21	XWC14-703-22	7SS·7SL-7BL	CS DS 7S(7B)/2*CS <i>ph1b</i> mutant//CS DS 7S(7B)
I-22	XWC14-709-42	7SS·7SL-7BL	CS DS 7S(7B)/2*CS <i>ph1b</i> mutant//CS DS 7S(7B)
I-23	XWC14-93-11	7SS·7SL-7BL	CS DS 7S(7B)/2*CS <i>ph1b</i> mutant//CS DS 7S(7B)
II-9	XWC14-709-1	7SS·7SL-7BL	CS DS 7S(7B)/2*CS <i>ph1b</i> mutant//CS DS 7S(7B)
II-10	XWC14-709-32	7SS·7SL-7BL	CS DS 7S(7B)/2*CS <i>ph1b</i> mutant//CS DS 7S(7B)
II-11	XWC14-706-19	7SS·7SL-7BL	CS DS 7S(7B)/2*CS <i>ph1b</i> mutant//CS DS 7S(7B)

Recombinant ID	Original recombinant code	Recombinant chromosomes and aberrations	Pedigree
II-12	XWC14-709-46	7SS·7SL-7BL	CS DS 7S(7B)/2*CS <i>ph1b</i> mutant//CS DS 7S(7B)
II-13	XWC14-709-50	7SS·7SL-7BL	CS DS 7S(7B)/2*CS <i>ph1b</i> mutant//CS DS 7S(7B)
II-14	XWC14-704-22	7SS·7SL-7BL	CS DS 7S(7B)/2*CS <i>ph1b</i> mutant//CS DS 7S(7B)
II-15	XWC14-708-9	7SS·7SL-7BL	CS DS 7S(7B)/2*CS <i>ph1b</i> mutant//CS DS 7S(7B)
II-16	XWC14-708-8	7SS·7SL-7BL	CS DS 7S(7B)/2*CS <i>ph1b</i> mutant//CS DS 7S(7B)
II-17	XWC14-704-43	7SS·7SL-7BL	CS DS 7S(7B)/2*CS <i>ph1b</i> mutant//CS DS 7S(7B)
II-18	XWC14-708-19	7SS·7SL-7BL	CS DS 7S(7B)/2*CS <i>ph1b</i> mutant//CS DS 7S(7B)
II-19	XWC14-709-4	7SS·7SL-7BL	CS DS 7S(7B)/2*CS <i>ph1b</i> mutant//CS DS 7S(7B)
II-20	XWC14-707-11	7SS·7SL-7BL	CS DS 7S(7B)/2*CS <i>ph1b</i> mutant//CS DS 7S(7B)
II-21	XWC14-91-13	7BS·7SS·7SL	CS DS 7S(7B)/2*CS <i>ph1b</i> mutant//CS DS 7S(7B)
II-22	XWC14-87-14	7BS·7SS·7SL	CS DS 7S(7B)/2*CS <i>ph1b</i> mutant//CS DS 7S(7B)
II-23	XWC14-94-13	7BS·7SS·7SL	CS DS 7S(7B)/2*CS <i>ph1b</i> mutant//CS DS 7S(7B)
III-9	XWC14-708-34	7SS·7BS·7BL	CS DS 7S(7B)/2*CS <i>ph1b</i> mutant//CS DS 7S(7B)
III-10	XWC14-708-3	7SS·7BS·7BL	CS DS 7S(7B)/2*CS <i>ph1b</i> mutant//CS DS 7S(7B)
III-11	XWC14-91-7	7SS·7BS·7BL	CS DS 7S(7B)/2*CS <i>ph1b</i> mutant//CS DS 7S(7B)
III-12	XWC14-89-1	7SS·7BS·7BL	CS DS 7S(7B)/2*CS <i>ph1b</i> mutant//CS DS 7S(7B)
III-13	XWC14-707-21	7BS·7BL-7SL	CS DS 7S(7B)/2*CS <i>ph1b</i> mutant//CS DS 7S(7B)
III-14	XWC14-705-10	7BS·7BL-7SL	CS DS 7S(7B)/2*CS <i>ph1b</i> mutant//CS DS 7S(7B)
III-15	XWC14-704-54	7BS·7BL-7SL	CS DS 7S(7B)/2*CS <i>ph1b</i> mutant//CS DS 7S(7B)
III-16	XWC14-95-15	7BS·7BL-7SL	CS DS 7S(7B)/2*CS <i>ph1b</i> mutant//CS DS 7S(7B)
III-17	XWC14-706-40	7BS·7BL-7SL	CS DS 7S(7B)/2*CS <i>ph1b</i> mutant//CS DS 7S(7B)
III-18	XWC14-703-12	7BS·7BL-7SL	CS DS 7S(7B)/2*CS <i>ph1b</i> mutant//CS DS 7S(7B)
III-19	XWC14-91-3	7BS·7BL-7SL	CS DS 7S(7B)/2*CS <i>ph1b</i> mutant//CS DS 7S(7B)
III-20	XWC14-708-15	7BS·7BL-7SL	CS DS 7S(7B)/2*CS <i>ph1b</i> mutant//CS DS 7S(7B)
III-21	XWC14-709-21	7BS·7BL-7SL	CS DS 7S(7B)/2*CS <i>ph1b</i> mutant//CS DS 7S(7B)
III-22	XWC14-709-18	7BS·7BL-7SL	CS DS 7S(7B)/2*CS <i>ph1b</i> mutant//CS DS 7S(7B)
III-23	XWC14-95-2	7BS·7BL-7SL	CS DS 7S(7B)/2*CS <i>ph1b</i> mutant//CS DS 7S(7B)
IV-9	XWC14-89-13	7BS·7BL-7SL	CS DS 7S(7B)/2*CS <i>ph1b</i> mutant//CS DS 7S(7B)

Recombinant ID	Original recombinant code	Recombinant chromosomes and aberrations	Pedigree
IV-10	XWC16-93-12	7BS·7BL-7SL	CS DS 7S(7B)/2*CS ph1b mutant//CS DS 7S(7B)
IV-11	XWC14-87-4	7BS·7BL-7SL	CS DS 7S(7B)/2*CS ph1b mutant//CS DS 7S(7B)
IV-12	XWC14-707-1	7BS·7BL-7SL	CS DS 7S(7B)/2*CS ph1b mutant//CS DS 7S(7B)
IV-13	XWC14-709-36	7BS·7BL-7SL	CS DS 7S(7B)/2*CS ph1b mutant//CS DS 7S(7B)
IV-14	XWC14-709-49	7BS·7BL-7SL	CS DS 7S(7B)/2*CS ph1b mutant//CS DS 7S(7B)
IV-15	XWC14-95-19	7BS·7BL-7SL	CS DS 7S(7B)/2*CS ph1b mutant//CS DS 7S(7B)
IV-16	XWC14-707-3	7BS·7BL-7SL	CS DS 7S(7B)/2*CS ph1b mutant//CS DS 7S(7B)
IV-17	XWC14-708-1	7BS·7BL-7SL	CS DS 7S(7B)/2*CS ph1b mutant//CS DS 7S(7B)
IV-18	XWC14-704-31	7BS·7BL-7SL	CS DS 7S(7B)/2*CS ph1b mutant//CS DS 7S(7B)
IV-19	XWC14-704-21	7BS·7BL-7SL	CS DS 7S(7B)/2*CS ph1b mutant//CS DS 7S(7B)
IV-20	XWC14-704-24	7BS·7BL-7SL	CS DS 7S(7B)/2*CS ph1b mutant//CS DS 7S(7B)
V-9	XWC14-95-8	7SS·7SL-7BL-7SL	CS DS 7S(7B)/2*CS ph1b mutant//CS DS 7S(7B)
V-10	XWC14-705-30	7SS·7SL-7BL-7SL-7BL	CS DS 7S(7B)/2*CS ph1b mutant//CS DS 7S(7B)
V-11	XWC14-709-44	7BS-7SS·7SL-7BL-7SL	CS DS 7S(7B)/2*CS ph1b mutant//CS DS 7S(7B)
V-12	XWC14-95-10	7BS·7BL-7SL-7BL	CS DS 7S(7B)/2*CS ph1b mutant//CS DS 7S(7B)
VI-9	XWC14-707-7	7SS·7BL	CS DS 7S(7B)/2*CS ph1b mutant//CS DS 7S(7B)
VI-10	XWC14-707-16	7SS·7BL	CS DS 7S(7B)/2*CS ph1b mutant//CS DS 7S(7B)
VI-11	XWC14-705-2	7SS·7BL	CS DS 7S(7B)/2*CS ph1b mutant//CS DS 7S(7B)
VI-12	XWC14-705-4	7SS·7BL	CS DS 7S(7B)/2*CS ph1b mutant//CS DS 7S(7B)
VII-9	XWC14-90-19	7SS or 7SL	CS DS 7S(7B)/2*CS ph1b mutant//CS DS 7S(7B)
VII-10	XWC16-96-6	7SS or 7SL	CS DS 7S(7B)/2*CS ph1b mutant//CS DS 7S(7B)
VII-11	XWC16-96-8	7SS or 7SL	CS DS 7S(7B)/2*CS ph1b mutant//CS DS 7S(7B)
VII-12	XWC16-96-10	7SS or 7SL	CS DS 7S(7B)/2*CS ph1b mutant//CS DS 7S(7B)
VII-13	XWC14-89-2	7SS or 7SL	CS DS 7S(7B)/2*CS ph1b mutant//CS DS 7S(7B)
VIII-9	XWC14-703-11	7SS·7SL	CS DS 7S(7B)/2*CS ph1b mutant//CS DS 7S(7B)
VIII-10	XWC14-703-17	7SS·7SL	CS DS 7S(7B)/2*CS ph1b mutant//CS DS 7S(7B)
VIII-11	XWC14-703-14	7SS·7SL	CS DS 7S(7B)/2*CS ph1b mutant//CS DS 7S(7B)

APPENDIX G. POLYMORPHIC SNPS ASSIGNED TO THE CHROMOSOME 7B

Wheat 90K SNP Index	SNP designation	Genetic position (cM) (Wang et al. 2014)	Physical position (bp)	E value
46416	Kukri_c542_1538	0	427328	2.00E-29
39295	Ku_c3662_836	3.267154	1053113	4.00E-46
52844	Ra_c9687_1038	3.267154	1085911	4.00E-46
44681	Kukri_c3734_892	3.267154	1265892	4.00E-46
27367	Excalibur_c53111_215	3.267154	1267671	4.00E-46
22624	Excalibur_c15405_808	3.267154	1267828	4.00E-46
36522	Jagger_c3075_99	7.312053	3667928	4.00E-46
53101	RAC875_c10555_178	8.783209	3870999	4.00E-46
6919	BS00022127_51	8.783209	3871311	4.00E-46
66787	Tdurum_contig10861_942	10.06071	4175506	4.00E-46
74022	Tdurum_contig98005_272	10.06071	5241413	4.00E-46
76332	w SNP_Ex_c11658_18773086	13.7058	6249500	3.00E-53
73685	Tdurum_contig85266_280	21.86432	6492905	4.00E-46
25433	Excalibur_c3423_1170	24.05075	6711293	4.00E-46
70085	Tdurum_contig30677_55	27.26793	6732753	9.00E-44
70086	Tdurum_contig30677_66	27.26793	6732765	9.00E-44
3164	BobWhite_c41356_62	36.073	10546597	4.00E-46
24875	Excalibur_c29698_76	42.44489	16806255	9.00E-44
26212	Excalibur_c41298_459	49.38212	30795162	4.00E-46
13841	CAP7_c1655_441	51.9996	36639266	9.00E-44
40127	Ku_c8929_274	53.04284	40098746	8.00E-32
6883	BS00022056_51	53.04284	40370588	4.00E-46
78206	w SNP_Ex_c46274_51831129	56.04762	44502349	2.00E-73
33940	GENE-4376_439	55.64469	44503017	4.00E-46
7854	BS00031746_51	56.04762	46348374	4.00E-46
8652	BS00054881_51	56.04762	47083691	9.00E-44
9255	BS00064344_51	55.64469	47338105	4.00E-46
78200	w SNP_Ex_c46061_51675763	53.75499	48799953	1.00E-49
50233	Kukri_rep_c72909_657	53.75499	48802090	4.00E-46
72576	Tdurum_contig57370_82	53.75499	49334846	4.00E-46
71732	Tdurum_contig46877_84	56.87846	49447270	9.00E-44
8019	BS00035630_51	53.75499	49448072	4.00E-46
36633	Jagger_c5321_98	58.17158	50190568	6.00E-46
39492	Ku_c46689_1653	58.17158	50910703	4.00E-46
78654	w SNP_Ex_c6590_11419735	58.17158	53491529	1.00E-105
73519	Tdurum_contig81683_217	58.17158	53491530	4.00E-46
66897	Tdurum_contig11028_398	58.17158	54972415	4.00E-46
64830	RFL_Contig492_751	58.17158	56034847	4.00E-46
77898	w SNP_Ex_c36325_44308589	58.59637	56050524	9.00E-89
71980	Tdurum_contig49572_643	58.59637	56051210	4.00E-46
49859	Kukri_rep_c69164_94	58.59637	56052208	4.00E-46

Wheat 90K SNP Index	SNP designation	Genetic position (cM) (Wang et al. 2014)	Physical position (bp)	E value
70551	Tdurum_contig35652_348	58.59637	56614981	4.00E-46
3402	BobWhite_c4481_96	58.17158	60627784	4.00E-46
77847	wsnp_Ex_c3501_6408181	58.17158	60627785	1.00E-105
80638	wsnp_Ku_c665_1371448	58.17158	61105169	1.00E-104
39783	Ku_c665_985	58.17158	61105278	4.00E-46
6712	BS00021683_51	58.17158	61592166	4.00E-46
75691	wsnp_BF485380B_Ta_2_1	58.17158	62016353	5.00E-58
36476	Jagger_c2161_211	57.44069	62018229	9.00E-44
23883	Excalibur_c22903_710	58.4402	62018489	4.00E-46
34207	GENE-4862_901	58.4402	62058336	3.00E-35
34204	GENE-4862_1014	58.4402	62058425	6.00E-43
34186	GENE-4826_641	57.05338	64491390	4.00E-46
35528	IAAV872	57.05338	65595930	1.00E-105
10705	BS00074083_51	58.17158	65625467	4.00E-46
6364	BS00011186_51	58.17158	66517494	2.00E-38
78625	wsnp_Ex_c64709_63402325	58.63073	67683122	1.00E-100
76919	wsnp_Ex_c17882_26646153	60.01443	71507654	6.00E-62
75526	wsnp_be496863B_Ta_2_2	60.01443	71509569	5.00E-58
68850	Tdurum_contig20094_458	61.13888	74920119	4.00E-46
70399	Tdurum_contig32954_195	61.13888	75761835	4.00E-46
11385	BS00084788_51	61.25757	84112561	4.00E-46
7150	BS00022550_51	61.25757	84112587	4.00E-46
33883	GENE-4273_67	56.87846	84374944	4.00E-46
13708	CAP7_c10566_170	62.51009	86607633	4.00E-46
11047	BS00079017_51	62.51009	86878737	4.00E-46
11048	BS00079019_51	62.51009	86878839	4.00E-46
7285	BS00022841_51	62.51009	86881047	4.00E-46
35361	IAAV7544	62.51009	86910083	9.00E-67
34706	IAAV3391	62.51009	86910556	9.00E-70
7118	BS00022498_51	62.51009	87822859	4.00E-46
57670	RAC875_c4108_2179	62.51009	90689480	9.00E-44
58046	RAC875_c4454_1270	63.63454	91201001	2.00E-44
14578	CAP8_c195_441	63.08793	97242884	3.00E-31
75622	wsnp_BF200891B_Ta_2_1	63.08793	99925284	5.00E-58
32502	GENE-1477_748	65.4399	107067715	4.00E-46
79142	wsnp_Ex_rep_c107796_91279476	71.66187	108318363	1.00E-105
30294	Excalibur_rep_c107796_229	71.66187	108318548	5.00E-39
59024	RAC875_c54366_845	64.44351	108593888	1.00E-45
43688	Kukri_c29304_447	64.44351	108593946	4.00E-46
47911	Kukri_c82121_100	64.44351	110683612	5.00E-39
12657	CAP11_c106_97	64.44351	111814111	4.00E-46
20628	Ex_c39052_1533	64.44351	111954251	4.00E-46
46912	Kukri_c61145_539	67.47328	118710442	8.00E-35

Wheat 90K SNP Index	SNP designation	Genetic position (cM) (Wang et al. 2014)	Physical position (bp)	E value
72335	Tdurum_contig53986_316	67.47328	121527364	4.00E-46
63589	RFL_Contig124_558	67.47328	123912495	3.00E-34
46521	Kukri_c5556_1830	71.66187	129382253	4.00E-46
21814	Excalibur_c11146_1322	67.47328	129383752	4.00E-46
62362	RAC875_rep_c116436_106	67.47328	129384910	1.00E-36
79186	wsnp_Ex_rep_c66351_64532511	66.61745	132364202	1.00E-105
79535	wsnp_Ex_rep_c69954_68913307	67.47328	132593722	1.00E-104
69576	Tdurum_contig28644_281	68.32912	139236558	4.00E-46
23720	Excalibur_c21931_664	71.66187	140702772	9.00E-44
54853	RAC875_c19552_137	67.47328	140703787	4.00E-46
35596	IAAV9153	68.32912	140716110	1.00E-105
50943	Ra_c11468_305	68.32912	146308889	4.00E-46
31169	Excalibur_rep_c71057_1199	68.32912	146312281	1.00E-36
34748	IAAV3646	67.81374	147703417	1.00E-105
62994	RAC875_rep_c73990_174	68.32912	147703418	4.00E-46
73957	Tdurum_contig9619_68	69.92521	149840012	9.00E-44
69305	Tdurum_contig27385_131	69.92521	151229585	4.00E-46
66769	Tdurum_contig10833_308	69.92521	155028856	8.00E-38
27341	Excalibur_c52820_61	71.32765	157521135	2.00E-35
41453	Kukri_c15760_310	71.32765	158669698	4.00E-46
41452	Kukri_c15760_212	71.32765	158669797	4.00E-24
69619	Tdurum_contig28763_206	71.66187	160012540	3.00E-37
12878	CAP11_c436_168	71.32765	160012574	4.00E-46
75939	wsnp_CAP11_rep_c6622_3044459	71.32765	160012722	1.00E-105
4698	BobWhite_rep_c48793_750	71.32765	160012723	4.00E-46
12923	CAP11_c5041_78	71.66187	160012806	4.00E-46
38901	Ku_c24482_1132	71.32765	160179996	4.00E-46
77536	wsnp_Ex_c27373_36578273	68.83512	164005297	5.00E-50
49816	Kukri_rep_c68742_543	68.83512	164005298	1.00E-24
8672	BS00055761_51	70.14385	165637076	4.00E-46
8226	BS00040415_51	71.32765	165986807	1.00E-33
78526	wsnp_Ex_c5925_10397213	69.92521	168816491	1.00E-104
46683	Kukri_c57677_355	68.83512	169386771	4.00E-46
78799	wsnp_Ex_c7783_13259751	69.08812	169561137	1.00E-105
11564	BS00088495_51	69.92521	170868936	4.00E-46
46585	Kukri_c56220_237	71.32765	172580742	4.00E-46
40173	Ku_c9598_2119	71.32765	172782463	4.00E-46
81528	wsnp_RFL_Contig3854_4205716	69.92521	173153587	2.00E-20
52696	Ra_c7974_559	71.32765	173153748	9.00E-44
34962	IAAV503	69.92521	174118729	1.00E-105
76923	wsnp_Ex_c1790_3378771	69.3911	180376991	6.00E-85
54770	RAC875_c19065_474	69.92521	183060645	4.00E-46
35064	IAAV5646	69.3911	185574757	1.00E-103

Wheat 90K SNP Index	SNP designation	Genetic position (cM) (Wang et al. 2014)	Physical position (bp)	E value
2029	BobWhite_c26689_85	69.92521	187437241	4.00E-46
77423	wsnp_Ex_c2539_4733110	69.92521	187437242	4.00E-63
57902	RAC875_c43108_1021	69.92521	188140131	4.00E-46
10459	BS00070399_51	71.66187	189569726	4.00E-46
57783	RAC875_c4186_1198	69.92521	190259996	4.00E-46
58816	RAC875_c52266_76	69.3911	191963242	4.00E-46
39639	Ku_c5666_203	69.92521	194608634	5.00E-36
10628	BS00072941_51	71.32765	195710359	4.00E-46
4684	BobWhite_c9958_624	69.92521	196504296	4.00E-46
60430	RAC875_c7671_148	71.32765	199169350	4.00E-46
47762	Kukri_c78330_327	71.32765	199169924	4.00E-46
11945	BS00095819_51	71.66187	204371573	4.00E-46
71523	Tdurum_contig44382_932	71.66187	204781376	4.00E-46
24548	Excalibur_c27158_671	71.66187	208674949	4.00E-46
74635	tplb0037k05_1475	71.66187	212281813	5.00E-33
957	BobWhite_c16787_205	71.66187	212343530	5.00E-39
62732	RAC875_rep_c70874_1920	71.66187	212667775	4.00E-46
62731	RAC875_rep_c70874_1309	71.66187	212668387	4.00E-46
36189	IACX727	71.66187	213499362	4.00E-57
5343	BobWhite_rep_c63166_725	71.66187	226959962	3.00E-40
75908	wsnp_CAP11_c847_522893	71.66187	231479942	5.00E-85
56099	RAC875_c27722_73	71.66187	231479943	4.00E-46
30711	Excalibur_rep_c116278_53	71.66187	234927187	4.00E-46
54688	RAC875_c18513_376	71.66187	236409032	4.00E-46
3379	BobWhite_c44558_325	71.66187	236887748	4.00E-46
80200	wsnp_Ku_c18780_28136150	71.66187	237311846	1.00E-105
26016	Excalibur_c39238_158	71.66187	239090309	4.00E-46
62820	RAC875_rep_c71932_86	71.66187	244367319	2.00E-23
75782	wsnp_BQ169669B-Ta_2_2	71.66187	250770297	5.00E-58
58073	RAC875_c4471_2378	71.66187	250771974	4.00E-46
48336	Kukri_c9353_642	71.78368	258756388	4.00E-46
21851	Excalibur_c11337_1183	71.66187	259221504	3.00E-31
30097	Excalibur_rep_c105109_1223	71.66187	284589075	4.00E-46
59164	RAC875_c56066_200	71.66187	284592443	4.00E-46
22463	Excalibur_c14572_2086	71.66187	286794526	4.00E-46
2352	BobWhite_c30285_272	71.66187	290180882	4.00E-46
359	BobWhite_c1240_1470	71.66187	299139275	6.00E-43
62205	RAC875_rep_c113331_55	71.66187	299514113	4.00E-46
65538	TA002339-0978	71.66187	313338527	6.00E-99
81504	wsnp_RFL_Contig3544_3722687	71.66187	321403586	5.00E-39
50445	Kukri_rep_c86135_111	71.66187	327141489	4.00E-46
64447	RFL_Contig3671_404	71.66187	329017483	4.00E-46
35692	IACX1134	71.66187	337099041	2.00E-56

Wheat 90K SNP Index	SNP designation	Genetic position (cM) (Wang et al. 2014)	Physical position (bp)	E value
43434	Kukri_c27438_164	71.66187	339866095	5.00E-33
39613	Ku_c5529_824	72.26781	342093869	3.00E-45
62174	RAC875_rep_c112798_813	71.66187	375915844	9.00E-44
25426	Excalibur_c34151_535	72.74258	386081132	4.00E-46
56254	RAC875_c28962_1393	73.38602	395872900	9.00E-44
23740	Excalibur_c22044_119	73.38602	405831971	6.00E-45
40563	Kukri_c11274_862	72.74258	407835778	4.00E-46
40564	Kukri_c11274_886	72.74258	407835803	4.00E-46
40565	Kukri_c11274_973	72.74258	407835890	4.00E-46
46738	Kukri_c58460_303	62.51009	407999993	4.00E-46
45752	Kukri_c47328_133	72.74258	410227948	4.00E-46
34033	GENE-4597_197	73.38602	412184355	6.00E-43
42040	Kukri_c18871_1338	73.38602	414063957	4.00E-46
61189	RAC875_c9715_679	72.74258	415441769	4.00E-46
69425	Tdurum_contig28085_87	74.02321	426054176	4.00E-46
72141	Tdurum_contig50984_599	72.74258	431196989	9.00E-44
61735	RAC875_rep_c107823_121	73.38602	437684561	4.00E-46
34098	GENE-4676_1364	73.38602	440112762	4.00E-46
61666	RAC875_rep_c107141_117	73.38602	440137251	9.00E-44
75486	wsnp_be490149B_Ta_1_1	72.74258	440535600	5.00E-58
72360	Tdurum_contig54532_206	72.74258	442325445	4.00E-46
1060	BobWhite_c17544_776	72.74258	443101626	7.00E-26
74449	tplb0031m07_1342	72.74258	444471179	4.00E-46
3457	BobWhite_c45353_232	72.74258	445973293	4.00E-46
71499	Tdurum_contig44171_1744	72.74258	445974417	4.00E-46
49544	Kukri_rep_c112161_392	72.74258	445974419	2.00E-41
34492	IAAV2037	72.74258	455024434	1.00E-105
37585	JD_c5200_835	72.74258	456375279	2.00E-41
78642	wsnp_Ex_c65605_63952614	72.74258	456375280	1.00E-105
36277	IACX82	73.38602	461796940	5.00E-58
60403	RAC875_c7610_81	73.38602	462199078	4.00E-46
22908	Excalibur_c17078_400	73.38602	472357723	1.00E-24
71838	Tdurum_contig47735_380	73.38602	474897570	4.00E-46
24436	Excalibur_c26387_87	73.38602	474897571	4.00E-46
40982	Kukri_c13142_974	73.38602	474897782	4.00E-46
26171	Excalibur_c40829_188	73.38602	478753272	5.00E-39
61728	RAC875_rep_c107704_155	73.38602	484679899	3.00E-22
22838	Excalibur_c16687_476	73.79208	492774186	4.00E-46
34102	GENE-4678_150	76.30959	492780427	1.00E-39
3274	BobWhite_c42974_184	73.79208	493066606	8.00E-32
451	BobWhite_c13098_526	73.79208	494179910	4.00E-46
47779	Kukri_c78788_84	73.79208	495761072	4.00E-46
56488	RAC875_c30547_72	76.30647	516168614	4.00E-46

Wheat 90K SNP Index	SNP designation	Genetic position (cM) (Wang et al. 2014)	Physical position (bp)	E value
15008	CAP8_rep_c3680_203	76.30647	516591128	4.00E-46
57075	RAC875_c35489_303	76.30647	516987620	4.00E-46
26679	Excalibur_c4556_776	76.30647	517875277	4.00E-46
26677	Excalibur_c4556_113	76.30647	517876479	1.00E-33
71496	Tdurum_contig44138_1546	76.30647	517876480	1.00E-33
73339	Tdurum_contig76013_352	76.30959	518732001	4.00E-46
2834	BobWhite_c36268_275	73.79208	518732002	4.00E-46
73340	Tdurum_contig76013_605	76.30647	518732975	4.00E-46
73341	Tdurum_contig76013_766	76.30647	518734540	4.00E-46
34097	GENE-4676_1080	73.79208	520696441	6.00E-43
59470	RAC875_c59860_167	73.79208	520703989	9.00E-44
31012	Excalibur_rep_c68963_163	73.79208	520710344	4.00E-46
2384	BobWhite_c30662_274	76.30647	521526978	4.00E-46
48409	Kukri_c95270_1069	76.30959	521532645	4.00E-46
49909	Kukri_rep_c69562_747	76.30959	521544191	1.00E-30
75409	wsnp_BE443010B_Ta_2_2	76.30647	523129609	5.00E-58
73892	Tdurum_contig93706_517	75.36943	532908276	9.00E-44
59338	RAC875_c58060_75	75.36943	532908277	4.00E-46
73891	Tdurum_contig93706_390	75.36943	532908403	4.00E-46
73890	Tdurum_contig93706_108	75.36943	532908685	4.00E-46
61623	RAC875_rep_c106651_490	75.36943	532922753	4.00E-46
30564	Excalibur_rep_c111831_114	75.36943	532922809	4.00E-46
40796	Kukri_c12317_1332	75.36943	534519530	4.00E-46
40800	Kukri_c12317_367	75.36943	534521656	4.00E-46
40799	Kukri_c12317_336	75.36943	534521687	4.00E-46
68768	Tdurum_contig19022_1555	75.36943	534521688	4.00E-46
26274	Excalibur_c41771_990	75.36943	535774000	4.00E-46
69212	Tdurum_contig25895_484	75.36943	535784105	4.00E-46
60181	RAC875_c68398_75	75.36943	535784106	6.00E-45
64761	RFL_Contig467_431	76.30959	535792775	9.00E-44
46001	Kukri_c49530_762	74.05444	539528597	2.00E-41
75647	wsnp_BF293181B_Ta_2_1	75.36943	539772634	3.00E-56
76200	wsnp_Ex_c106_217340	76.01286	543118992	1.00E-105
72254	Tdurum_contig52239_120	76.01286	543118993	4.00E-46
78221	wsnp_Ex_c47153_52447514	76.30959	543126769	2.00E-79
80349	wsnp_Ku_c29256_39161320	76.30959	543480500	9.00E-95
40901	Kukri_c12822_132	76.30959	543480790	4.00E-46
72504	Tdurum_contig56342_134	76.16904	551660999	4.00E-46
72505	Tdurum_contig56342_259	76.16904	551661123	4.00E-46
29286	Excalibur_c8994_1297	76.30647	555357501	2.00E-41
56477	RAC875_c30453_292	76.30959	556420247	4.00E-46
30544	Excalibur_rep_c111629_239	76.98426	557727250	4.00E-46
11601	BS00089181_51	77.12794	557905497	4.00E-46

Wheat 90K SNP Index	SNP designation	Genetic position (cM) (Wang et al. 2014)	Physical position (bp)	E value
41673	Kukri_c16907_390	77.12794	558448148	5.00E-39
26634	Excalibur_c451_1290	77.12794	558463371	4.00E-46
6831	BS00021972_51	77.12794	560700607	4.00E-46
10769	BS00074919_51	77.12794	563367595	4.00E-46
26230	Excalibur_c41452_997	77.12794	563384506	9.00E-44
79153	w SNP_ Ex_ rep_ c109138_ 92064554	77.12794	564748828	3.00E-85
20908	Ex_c54863_29	77.12794	565961512	1.00E-26
19721	Ex_c12057_797	77.12794	569231023	9.00E-44
76246	w SNP_ Ex_ c11003_ 17857272	77.12794	569916216	1.00E-105
66386	Tdurum_contig102328_129	77.12794	569916475	4.00E-46
76247	w SNP_ Ex_ c11003_ 17857759	77.12794	569916816	1.00E-105
46152	Kukri_c51296_438	77.12794	570077904	2.00E-44
48538	Kukri_c99107_143	77.59334	570637274	4.00E-46
2567	BobWhite_c3269_141	77.12794	570640388	1.00E-45
37345	JD_c3269_342	77.12794	570640590	4.00E-46
12371	BS00108573_51	77.12794	572706678	4.00E-46
73840	Tdurum_contig93081_162	76.30959	573624498	4.00E-46
8805	BS00060341_51	76.30959	573624499	4.00E-46
77993	w SNP_ Ex_ c3974_ 7194320	77.13107	579744472	3.00E-76
59499	RAC875_c60161_448	76.98426	587720050	4.00E-46
81212	w SNP_ Ra_ c60161_ 61164325	77.13107	587720266	1.00E-104
49430	Kukri_rep_c110003_99	77.13107	587720460	4.00E-46
59495	RAC875_c60161_1223	77.16543	587720825	1.00E-39
59552	RAC875_c60770_82	77.13107	588273560	3.00E-34
36465	Jagger_c1882_85	77.13107	588545895	4.00E-46
68451	Tdurum_contig15690_195	78.33048	588553950	2.00E-26
41271	Kukri_c14804_352	78.43668	589043266	4.00E-46
41272	Kukri_c14804_757	78.43668	589049505	4.00E-46
41273	Kukri_c14804_876	78.43668	589049624	4.00E-46
57668	RAC875_c41055_395	78.43668	590876647	9.00E-44
47700	Kukri_c76860_181	78.43668	590903333	1.00E-36
40249	Kukri_c10108_115	78.43668	592263104	4.00E-46
70499	Tdurum_contig34357_160	81.08539	596033819	4.00E-46
68522	Tdurum_contig16275_277	80.78553	596837477	4.00E-46
30972	Excalibur_rep_c68565_1411	82.1255	597956913	9.00E-44
63629	RFL_Contig1404_351	81.5664	602470152	4.00E-46
34202	GENE-4861_106	82.88763	602764782	1.00E-39
35732	IACX1302	83.06879	607319819	4.00E-57
24749	Excalibur_c28715_447	83.06879	607653593	2.00E-35
56260	RAC875_c29004_652	82.77518	608196146	4.00E-46
60324	RAC875_c7251_656	83.98084	608406525	4.00E-46
60292	RAC875_c7123_1703	82.77518	610806257	4.00E-46
42528	Kukri_c21628_1215	85.28333	613149662	5.00E-39

Wheat 90K SNP Index	SNP designation	Genetic position (cM) (Wang et al. 2014)	Physical position (bp)	E value
27692	Excalibur_c5700_244	86.68265	613336626	4.00E-46
27833	Excalibur_c58742_144	86.38592	613343349	2.00E-44
10797	BS00075332_51	87.42916	616330697	4.00E-46
73755	Tdurum_contig90495_232	87.42916	616430910	3.00E-25
58429	RAC875_c4834_694	89.12833	617894859	4.00E-46
24847	Excalibur_c29455_476	88.4724	618320482	4.00E-46
75636	wsnp_BF291608B_Ta_2_1	89.12833	619304202	4.00E-57
14408	CAP7_rep_c5216_143	89.82487	627967058	4.00E-46
330	BobWhite_c12256_96	89.12833	630993883	4.00E-46
11629	BS00089938_51	90.4152	631346293	2.00E-29
11631	BS00089942_51	90.4152	631346309	4.00E-46
56080	RAC875_c27548_234	92.52042	631346377	4.00E-46
34065	GENE-4624_79	91.2398	632401381	4.00E-46
69178	Tdurum_contig25773_174	91.40222	634509053	4.00E-46
69177	Tdurum_contig25773_144	91.40222	634509083	4.00E-46
75195	tplb0059a12_588	91.03053	635173302	4.00E-46
57705	RAC875_c4128_926	92.52042	638072459	4.00E-46
81554	wsnp_RFL_Contig4236_4881643	90.36211	638072756	4.00E-46
78779	wsnp_Ex_c758_1488368	91.02116	638072757	1.00E-105
42955	Kukri_c24366_104	92.35175	638758394	4.00E-46
21986	Excalibur_c11857_1196	92.35175	639359644	4.00E-46
7572	BS00025278_51	92.00817	641941282	4.00E-46
7573	BS00025286_51	92.00817	641941516	4.00E-46
9018	BS00063208_51	91.9582	643040348	4.00E-46
40237	Kukri_c10078_1683	92.52042	643673466	1.00E-33
9820	BS00066484_51	92.52042	644554070	4.00E-46
55199	RAC875_c21537_368	93.16386	645009177	4.00E-46
8017	BS00035559_51	93.16386	645418686	2.00E-44
7710	BS00029286_51	94.83492	645471464	4.00E-46
7711	BS00029287_51	94.83492	645471491	4.00E-46
6881	BS00022053_51	95.70637	646530445	9.00E-44
38938	Ku_c25310_669	98.29885	648122522	4.00E-46
38939	Ku_c25310_780	98.29885	648122634	4.00E-46
38940	Ku_c25310_843	98.29885	648122697	3.00E-45
56856	RAC875_c3361_403	98.96727	648985790	4.00E-46
80709	wsnp_Ku_c854_1768346	98.96727	650059750	1.00E-105
77781	wsnp_Ex_c3309_6096114	98.62994	650059797	1.00E-104
72124	Tdurum_contig5083_1164	98.62994	650059798	4.00E-46
80708	wsnp_Ku_c854_1768062	98.96727	650060034	1.00E-105
9120	BS00063744_51	98.29885	650149409	3.00E-34
80167	wsnp_Ku_c16895_25861847	98.62994	650738709	1.00E-104
38566	Ku_c16895_793	98.62994	650738740	4.00E-46
38567	Ku_c16895_803	98.29885	650738749	4.00E-46

Wheat 90K SNP Index	SNP designation	Genetic position (cM) (Wang et al. 2014)	Physical position (bp)	E value
78178	wsnp_Ex_c45195_51056617	98.62994	650745308	6.00E-70
76194	wsnp_Ex_c10571_17258682	97.16815	650861767	1.00E-105
10070	BS00067530_51	101.1849	654626881	4.00E-46
11138	BS00080621_51	105.3704	654629105	4.00E-46
35241	IAAV6740	101.1849	654629214	1.00E-103
6608	BS00014946_51	101.1849	654629215	4.00E-46
76151	wsnp_Ex_c10193_16730126	101.1849	654629325	1.00E-100
77284	wsnp_Ex_c22955_32173776	101.1849	655975979	1.00E-105
58112	RAC875_c45062_305	101.1849	656368336	9.00E-44
31227	Excalibur_rep_c74234_183	102.7935	660834447	6.00E-42
9204	BS00064146_51	102.7935	661696662	4.00E-46
34302	GENE-4996_592	102.7935	663739274	4.00E-46
75604	wsnp_BE605194B_Ta_2_7	102.7935	663739445	5.00E-58
75603	wsnp_BE605194B_Ta_2_1	102.7935	663740429	5.00E-58
71473	Tdurum_contig43995_370	105.2923	664108812	4.00E-46
75693	wsnp_BG262287B_Td_2_5	106.7666	665469497	4.00E-57
33977	GENE-4478_394	106.7666	665472714	2.00E-35
42503	Kukri_c21416_483	106.7666	665483631	5.00E-33
71832	Tdurum_contig47633_304	106.7666	665876084	1.00E-30
46102	Kukri_c50873_79	106.7666	665876872	2.00E-41
41479	Kukri_c15912_1189	112.4419	680859093	4.00E-46
71789	Tdurum_contig47317_100	113.1697	682085432	5.00E-39
40527	Kukri_c11141_203	113.8662	682249069	4.00E-46
6146	BS00009995_51	113.8662	682249283	5.00E-36
43699	Kukri_c29396_58	113.8662	682254388	4.00E-46
35490	IAAV8521	118.0861	686930160	5.00E-96
72318	Tdurum_contig5360_329	113.7132	686930438	4.00E-43
20616	Ex_c3837_2055	118.6733	686930515	6.00E-42
35230	IAAV6659	118.0861	686930522	6.00E-65
43667	Kukri_c292_2231	118.0861	686930523	4.00E-46
25127	Excalibur_c31707_302	120.1101	687249569	4.00E-46
8451	BS00047083_51	118.2422	687297797	4.00E-46
67638	Tdurum_contig12525_769	119.679	688154454	4.00E-46
12171	BS00101364_51	120.1101	691028158	4.00E-46
78468	wsnp_Ex_c56425_58548596	120.4193	691096041	1.00E-105
72939	Tdurum_contig63207_82	116.44	691100684	4.00E-46
7845	BS00031588_51	120.8129	692136813	2.00E-35
55731	RAC875_c25019_1132	121.6031	694951103	2.00E-41
22199	Excalibur_c13033_261	121.6031	694971844	4.00E-46
10280	BS00068305_51	121.6031	695305983	4.00E-46
29313	Excalibur_c90713_226	129.7741	700876975	4.00E-46
76991	wsnp_Ex_c19_38763	130.6768	701043572	1.00E-105
41065	Kukri_c1362_137	133.591	708680902	4.00E-46

Wheat 90K SNP Index	SNP designation	Genetic position (cM) (Wang et al. 2014)	Physical position (bp)	E value
694	BobWhite_c14736_188	133.591	708681551	4.00E-46
37730	JD_c6531_201	133.591	709139948	9.00E-44
48454	Kukri_c9683_723	133.591	709139969	5.00E-39
71571	Tdurum_contig44948_1132	133.591	709142657	4.00E-46
71573	Tdurum_contig44948_1812	133.591	709143882	4.00E-46
71575	Tdurum_contig44948_2237	133.591	709144307	4.00E-46
43871	Kukri_c30593_75	133.591	709145682	4.00E-46
76864	w SNP_Ex_c17176_25816766	134.3812	709693984	6.00E-99
47991	Kukri_c8405_1394	134.3812	709694716	4.00E-46
75632	w SNP_BF202806B_Ta_2_1	133.591	709694994	4.00E-57
73409	Tdurum_contig77073_193	129.7741	709852194	2.00E-41
27158	Excalibur_c50612_409	129.7741	709852195	2.00E-41
35704	IACX11443	133.591	709871945	3.00E-42
6544	BS00012264_51	133.591	709871966	1.00E-24
21669	Excalibur_c1055_565	133.591	709872980	2.00E-29
76866	w SNP_Ex_c1721_3261986	133.591	710468578	1.00E-105
78819	w SNP_Ex_c7934_13467460	133.591	710482468	1.00E-64
7134	BS00022522_51	133.591	710484424	4.00E-46
7456	BS00023166_51	133.591	710508788	9.00E-44
3718	BobWhite_c5046_372	136.2553	710515501	4.00E-46
34912	IAAV4699	136.2553	710515502	3.00E-94
57797	RAC875_c41938_471	133.591	710636106	4.00E-46
78347	w SNP_Ex_c5268_9320618	133.591	711686697	1.00E-105
7635	BS00026694_51	135.9742	712627084	4.00E-46
69657	Tdurum_contig28884_460	140.144	713392150	4.00E-43
34599	IAAV2686	139.9691	713392151	3.00E-42
69655	Tdurum_contig28884_302	139.9691	713392531	5.00E-39
73869	Tdurum_contig93425_441	139.9691	713598553	9.00E-44
42933	Kukri_c24148_254	136.2553	713620629	4.00E-46
46543	Kukri_c55780_296	142.2368	715811556	4.00E-46
37197	JD_c22211_269	143.23	715811681	4.00E-46
76050	w SNP_CAP7_c4513_2055201	142.6865	716132057	2.00E-77
77852	w SNP_Ex_c351_689415	143.23	716132245	1.00E-105
51787	Ra_c3092_741	142.6865	716132579	4.00E-46
80658	w SNP_Ku_c707_1465395	142.6865	716133326	1.00E-104
34837	IAAV4141	142.6865	716133979	1.00E-104
79683	w SNP_JD_c17128_16056425	142.6865	716135662	1.00E-105
73399	Tdurum_contig76864_755	143.23	716137872	4.00E-46
20596	Ex_c3738_390	142.6865	716138144	4.00E-46
39684	Ku_c5969_1667	142.6865	716138289	4.00E-46
3163	BobWhite_c4134_984	143.23	716141866	5.00E-33
52567	Ra_c72121_602	143.23	716184660	4.00E-41
65152	RFL_Contig5898_1464	143.23	716188359	4.00E-46

Wheat 90K SNP Index	SNP designation	Genetic position (cM) (Wang et al. 2014)	Physical position (bp)	E value
65154	RFL_Contig5898_807	143.23	716189552	4.00E-46
71559	Tdurum_contig44876_1362	143.23	717794499	4.00E-46
10844	BS00075960_51	143.23	717797991	4.00E-46
10476	BS00070583_51	143.23	717798489	4.00E-46
8215	BS00040283_51	144.8043	718646114	4.00E-46
8216	BS00040285_51	144.8043	718646457	9.00E-44
71977	Tdurum_contig49543_568	144.8043	718767474	4.00E-46
12068	BS00099421_51	144.8043	718927448	4.00E-46
6574	BS00012542_51	144.8043	718939298	4.00E-46
27056	Excalibur_c4948_90	144.8043	718939311	1.00E-33
33998	GENE-4528_28	144.8043	719023554	1.00E-32
48256	Kukri_c91360_220	144.9948	720941507	4.00E-46
8577	BS00049961_51	144.9948	721317007	4.00E-46
12557	BS00110528_51	144.9948	721475221	4.00E-46
13219	CAP12_c1587_142	144.9948	721485285	4.00E-46
34117	GENE-4710_573	144.8043	721485715	4.00E-46
12377	BS00108630_51	145.2853	723520857	4.00E-46
21268	Ex_c72265_351	147.1375	724108582	4.00E-46
72833	Tdurum_contig61884_836	147.5717	725513597	4.00E-46
5853	BS00003630_51	150.5983	726488079	7.00E-26
36018	IACX5767	150.5983	726488080	5.00E-31
71290	Tdurum_contig42586_290	150.5983	727294131	2.00E-26
71291	Tdurum_contig42586_720	150.5983	727294832	4.00E-46
71292	Tdurum_contig42586_990	150.5983	727295317	5.00E-27
1883	BobWhite_c2514_109	150.5983	727673756	4.00E-46
11951	BS00096151_51	150.5983	727673875	4.00E-46
47549	Kukri_c7284_674	150.5983	727677757	4.00E-46
45661	Kukri_c46447_1738	150.5983	727785033	4.00E-46
343	BobWhite_c12355_1548	150.3297	727785699	9.00E-44
11145	BS00080759_51	150.5983	727994270	4.00E-46
10819	BS00075616_51	150.5983	728005639	4.00E-46
8092	BS00037198_51	150.5983	728060705	4.00E-46
54207	RAC875_c16049_89	150.5983	728356922	1.00E-39
6321	BS00010953_51	150.5983	728400816	7.00E-23
8868	BS00062611_51	150.5983	728581864	4.00E-46
40603	Kukri_c11467_993	150.5983	729360872	4.00E-46
9496	BS00065265_51	150.5983	729854271	4.00E-46
21716	Excalibur_c1070_1978	150.1173	729897522	4.00E-46
21717	Excalibur_c1070_2327	153.2595	729897871	4.00E-46
69562	Tdurum_contig28598_245	152.413	731036268	2.00E-35
6699	BS00021666_51	155.4147	735586157	4.00E-46
80516	w SNP_Ku_c44600_51841068	157.0233	737803777	2.00E-37
57859	RAC875_c42647_153	157.0233	738209215	4.00E-46

Wheat 90K SNP Index	SNP designation	Genetic position (cM) (Wang et al. 2014)	Physical position (bp)	E value
12163	BS00101258_51	155.4147	738209331	4.00E-46
23473	Excalibur_c20408_81	148.6524	738313552	9.00E-44
26595	Excalibur_c4484_985	157.0233	738314055	4.00E-46
76017	wsnp_CAP7_c172_96407	158.9754	738314056	1.00E-104
52455	Ra_c69234_623	163.1609	739369855	2.00E-26
6295	BS00010819_51	157.0077	739370084	9.00E-41
50620	Kukri_s109646_139	157.0077	739370186	9.00E-44
10520	BS00071025_51	155.4147	740833290	4.00E-46
41906	Kukri_c18148_1234	163.1609	740840751	4.00E-46
75461	wsnp_BE445506B_Ta_2_2	159.6689	740850451	5.00E-58
7586	BS00025724_51	158.1134	741768914	1.00E-45
8586	BS00050320_51	158.1134	741770977	4.00E-46
8587	BS00050328_51	158.1134	741771286	4.00E-46
8762	BS00058970_51	158.1134	741772418	4.00E-46
8761	BS00058969_51	158.1134	741772459	4.00E-46
50136	Kukri_rep_c71636_533	158.1134	741773790	9.00E-44
7512	BS00023884_51	158.3383	743330217	4.00E-46
44297	Kukri_c34272_108	160.431	743871623	5.00E-36
21509	Excalibur_c100544_112	158.9754	743873392	5.00E-36
42622	Kukri_c22243_73	158.9754	743874127	2.00E-44
56659	RAC875_c31851_529	160.5903	743875024	4.00E-46
55488	RAC875_c23333_489	160.431	743877268	3.00E-40
44608	Kukri_c3676_483	162.1114	744132081	9.00E-44
5972	BS00004376_51	171.1102	745003862	2.00E-35
61978	RAC875_rep_c110526_324	163.3015	745005427	4.00E-46
49181	Kukri_rep_c106477_365	171.1102	745005634	9.00E-41
8304	BS00042112_51	162.1114	745071422	4.00E-46
25962	Excalibur_c3870_288	162.2239	745072591	4.00E-46
25963	Excalibur_c3870_89	171.1102	745072789	2.00E-41
22872	Excalibur_c1688_436	171.1102	745084975	4.00E-46
30725	Excalibur_rep_c66257_477	171.1102	745085268	9.00E-44
57955	RAC875_c43579_80	171.1102	745085374	4.00E-24
62682	RAC875_rep_c70367_185	171.1102	745085655	4.00E-46
62681	RAC875_rep_c70367_158	171.1102	745085682	4.00E-46
23318	Excalibur_c19455_3496	163.1609	746047676	2.00E-41
12638	BS00111247_51	163.1609	746082232	4.00E-46
9811	BS00066456_51	163.9105	747428589	9.00E-44
47876	Kukri_c81094_434	164.2416	751554109	4.00E-46
34196	GENE-4848_95	165.0475	752096845	4.00E-46
27877	Excalibur_c5938_1703	171.1102	752204148	4.00E-46
27876	Excalibur_c5938_1669	171.1102	752204183	4.00E-46
27818	Excalibur_c5851_1661	171.1102	752223665	4.00E-46
64015	RFL_Contig2647_624	166.9903	753743389	3.00E-31

Wheat 90K SNP Index	SNP designation	Genetic position (cM) (Wang et al. 2014)	Physical position (bp)	E value
75239	tplb0060b03_921	166.9903	754572519	3.00E-34
13260	CAP12_c194_240	171.1102	754573117	6.00E-45
24202	Excalibur_c2464_202	171.1102	755165529	4.00E-35
10676	BS00073560_51	166.9903	755660726	4.00E-46
58838	RAC875_c525_1885	167.2745	755697674	3.00E-37
58841	RAC875_c525_811	167.2745	755700493	2.00E-26
58835	RAC875_c525_106	166.9903	755702522	4.00E-46
8824	BS00060980_51	171.1102	756213675	4.00E-46
9064	BS00063474_51	166.9903	756245873	4.00E-46
64172	RFL_Contig3005_669	171.1102	756379516	4.00E-46
64173	RFL_Contig3005_899	171.1102	756379747	4.00E-46
64169	RFL_Contig3005_1031	171.1102	756379878	4.00E-46
73641	Tdurum_contig83564_600	171.1102	756380013	4.00E-46
6469	BS00011767_51	167.3995	756384008	4.00E-46
51167	Ra_c15460_1031	171.1102	756384461	4.00E-46
29199	Excalibur_c87219_179	168.7551	758636478	4.00E-46
12247	BS00105550_51	167.6712	761567818	4.00E-46
43892	Kukri_c30714_633	167.7024	761956392	4.00E-46
53695	RAC875_c1329_225	171.1102	762003200	2.00E-29
53698	RAC875_c1329_488	188.6391	762003839	1.00E-39
9405	BS00064933_51	167.5588	762346994	9.00E-44
29106	Excalibur_c8449_280	171.1102	762379141	1.00E-42
27073	Excalibur_c49685_207	171.1102	762493450	2.00E-41
7408	BS00023069_51	171.1102	762991032	4.00E-46
42703	Kukri_c22826_137	168.7551	763200816	9.00E-44
47728	Kukri_c77849_131	168.7551	763307755	1.00E-39
70127	Tdurum_contig30909_76	167.996	763311995	4.00E-43

**APPENDIX H. PHYSICAL POSITIONS OF THE RECOMBINATION BREAKPOINTS
OF THE REPRESENTATIVE 7B-7E AND 7B-7S RECOMBINANTS**

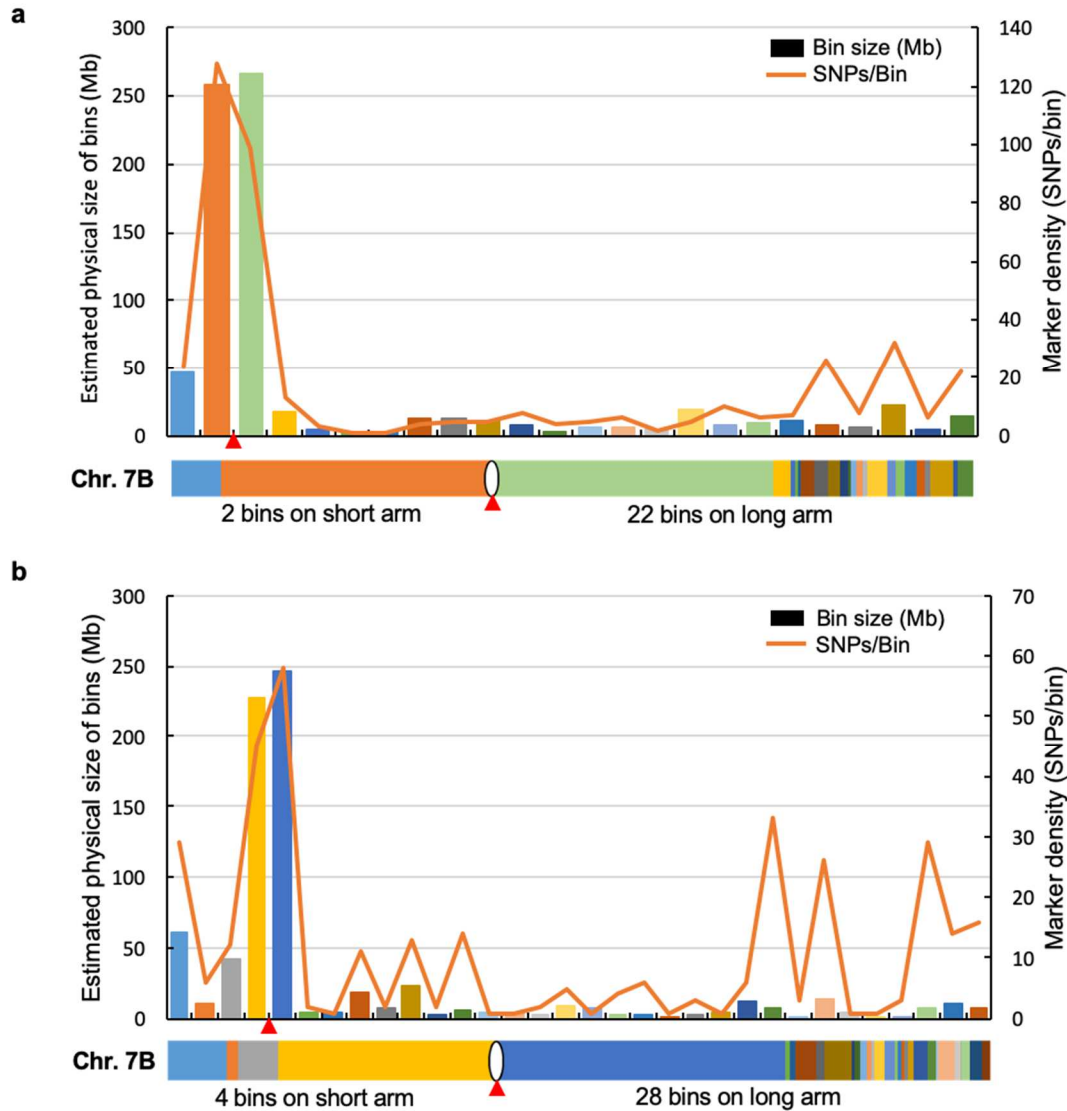
Rec. ID	Original recombinant code	Recombinant chromosome composition	Physical positions of recombination breakpoints (bp)^a	
I-1	XWC14-260-120	7ES·7EL-7BL	748818171	
I-2	XWC14-757-21	7ES·7EL-7BL	722231182	
I-3	XWC14-760-14	7ES·7EL-7BL	716989580	
I-4	XWC14-257-94	7ES·7EL-7BL	709419146	
I-5	XWC14-762-3	7ES·7EL-7BL	689196919	
I-6	XWC14-759-26	7ES·7EL-7BL	681472263	
I-7	XWC14-257-38	7ES·7EL-7BL	652682795	
I-8	XWC14-257-50	7ES·7EL-7BL	646797007	
II-1	XWC14-260-121	7ES·7EL-7BL	644113768	
II-2	XWC14-760-7	7ES·7EL-7BL	625149043	
II-4	XWC14-255-11	7ES·7EL-7BL	599653815	
II-6	XWC14-260-26	7ES·7EL-7BL	596435648	
II-7	XWC14-259-36	7ES·7EL-7BL	594148462	
VI-1	XWC14-260-107	7ES·7BL	306426320	
IV-5	XWC14-759-17	7BS·7BL-7EL	722231182	
IV-4	XWC14-258-83	7BS·7BL-7EL	698091479	
IV-2	XWC14-762-36	7BS·7BL-7EL	689196919	
III-8	XWC14-759-52	7BS·7BL-7EL	662718054	
IV-1	XWC14-255-3	7BS·7BL-7EL-7BL	658601392	744441451
III-7	XWC14-255-23	7BS·7BL-7EL	644113768	
III-6	XWC14-258-33	7BS·7BL-7EL	636622881	
III-5	XWC14-759-37	7BS·7BL-7EL	612074803	
III-4	XWC14-258-72	7BS·7BL-7EL	589963136	
III-1	XWC14-255-24	7BS·7BL-7EL	573165588	
VI-7	XWC14-260-62	7BS·7EL	306426320	
II-8	XWC14-260-17	7BS·7ES·7EL	48069029	
VIII-9	XWC14-703-11	7SS·7SL	738841955	
I-9	XWC14-704-4	7SS·7SL-7BL	738006554	
VIII-10	XWC14-703-17	7SS·7SL	736694967	
VIII-11	XWC14-703-14	7SS·7SL	732742014	
I-11	XWC14-705-21	7SS·7SL-7BL	718222302	
I-12	XWC14-705-8	7SS·7SL-7BL	716992026	
I-13	XWC14-707-8	7SS·7SL-7BL	709420199	
I-16	XWC14-709-3	7SS·7SL-7BL	693036264	

Rec. ID	Original recombinant code	Recombinant chromosome composition	Physical positions of recombination breakpoints (bp) ^a		
I-17	XWC14-705-1	7SS·7SL-7BL	684592274		
I-19	XWC14-705-18	7SS·7SL-7BL	681472263		
I-21	XWC14-703-22	7SS·7SL-7BL	673367983		
I-23	XWC14-93-11	7SS·7SL-7BL	664604963		
II-11	XWC14-706-19	7SS·7SL-7BL	662286861		
II-14	XWC14-704-22	7SS·7SL-7BL	657731776		
II-16	XWC14-708-8	7SS·7SL-7BL	647326484		
V-9	XWC14-95-8	7SS·7SL-7BL-7SL	647326484	745566679	-
V-10	XWC14-705-30	7SS·7SL-7BL-7SL-7BL	622198984	687726126	732742014
II-17	XWC14-704-43	7SS·7SL-7BL	622198984		
II-19	XWC14-709-4	7SS·7SL-7BL	596995366		
II-20	XWC14-707-11	7SS·7SL-7BL	592293885		
VI-9	XWC14-707-7	7SS·7BL	343026891		
III-9	XWC14-708-34	7SS-7BS-7BL	115332347		
III-10	XWC14-708-3	7SS-7BS-7BL	62038283		
IV-20	XWC14-704-24	7BS-7BL-7SL-7BL	698007708	756296711	-
IV-11	XWC14-704-21	7BS-7SS-7SL	698007708		
IV-16	XWC14-707-3	7BS-7BL-7SL	693036264		
IV-15	XWC14-95-19	7BS-7BL-7SL	689591306		
V-11	XWC14-709-44	7BS-7SS-7SL-7BL-7SL	73213887	622198984	684592274
IV-13	XWC14-709-36	7BS-7BL-7SL	684592274		
IV-12	XWC14-707-1	7BS-7BL-7SL	681472263		
III-23	XWC14-95-2	7BS-7BL-7SL	673367983		
III-20	XWC14-708-15	7BS-7BL-7SL	657731776		
III-18	XWC14-703-12	7BS-7BL-7SL	652745436		
III-17	XWC14-706-40	7BS-7BL-7SL	647326484		
V-12	XWC14-95-10	7BS-7BL-7SL-7BL	645240334	736694967	-
III-16	XWC14-95-15	7BS-7BL-7SL	622198984		
III-14	XWC14-705-10	7BS-7BL-7SL	614837023		
III-13	XWC14-707-21	7BS-7BL-7SL	588409728		

^aThe physical position of a recombination breakpoint was estimated according to the physical location of the middle point between the SNPs immediately flanking the recombination breakpoint in the IWGSC RefSeq v2.0 (<https://wheat-urgi.versailles.inra.fr/>).

Two highlighted recombination breakpoints were detected by SNP assay, but only one was visualized by GISH.

**APPENDIX I. THE COMPOSITE BIN MAP OF CHROMOSOME 7B AND
PARTITIONED CHROMOSOME BASED ON 7B-7E RECOMBINANTS AND 7B-7S
RECOMBINANTS**



The composite bin map of chromosome 7B and partitioned chromosome based on 7B-7E recombinants (a) and 7B-7S recombinants (b). Vertical bars indicate physical size of the bins, and curved lines indicate SNP numbers within each bin. All bins were color-coded according to their physical size and locations in the horizontal ideogram of chromosome 7B (*bottom*). Red triangles point to the centromere.

APPENDIX J. SNP-BASED PHYSICAL MAPPING OF THE 7B-7E AND 7B-7S

RECOMBINATION-RESOLVED BINS FOR CHROMOSOME 7B

Bins	Arm location	Estimated start point (bp)^a	Estimated end point (bp)^b	Bin size (bp)	SNPs/Bin
1	Short arm	427328	48069029	47641701	27
2	Short arm	48069029	62038413	13969384	23
3	Short arm	62038413	73213887	11175474	8
4	Short arm	73213887	115332347	42118460	24
5	Short arm	115332347	306426320	191093974	82
6	Long arm	306426320	573165588	266739268	107
7	Long arm	573165588	588409728	15244140	8
8	Long arm	588409728	589963136	1553408	5
9	Long arm	589963136	594148462	4185326	3
10	Long arm	594148462	596435648	2287187	1
11	Long arm	596435648	597397195	961547	1
12	Long arm	597397195	612074803	14677608	8
13	Long arm	612074803	614837023	2762220	1
14	Long arm	614837023	623635630	8798607	5
15	Long arm	623635630	636622881	12987251	9
16	Long arm	636622881	644113768	7490888	9
17	Long arm	644113768	645471478	1357710	4
18	Long arm	645471478	647326484	1855006	2
19	Long arm	647326484	652744324	5417841	14
20	Long arm	652744324	658601392	5857068	7
21	Long arm	658601392	662717968	4116577	2
22	Long arm	662717968	663739360	1021392	1
23	Long arm	663739360	664789155	1049795	3
24	Long arm	664789155	673367983	8578828	5
25	Long arm	673367983	681472263	8104280	1
26	Long arm	681472263	684592274	3120012	4
27	Long arm	684592274	687726126	3133852	7
28	Long arm	687726126	689591306	1865181	1
29	Long arm	689591306	691062100	1470794	1
30	Long arm	691062100	693036264	1974165	2
31	Long arm	693036264	698091479	5055215	2
32	Long arm	698091479	709419833	11328354	10
33	Long arm	709419833	716992026	7572193	37
34	Long arm	716992026	718222302	1230276	3

Bins	Arm location	Estimated start point (bp)^a	Estimated end point (bp)^b	Bin size (bp)	SNPs/Bin
35	Long arm	718222302	722231182	4008881	8
36	Long arm	722231182	732742014	10510832	23
37	Long arm	732742014	736694967	3952953	1
38	Long arm	736694967	738006554	1311587	1
39	Long arm	738006554	738841955	835401	3
40	Long arm	738841955	744441451	5599496	18
41	Long arm	744441451	745566679	1125228	9
42	Long arm	745566679	748818171	3251492	2
43	Long arm	748818171	756296711	7478541	14
44	Long arm	756296711	763311995	7015284	17

^{a,b}The bin start/end points were estimated according to the physical location of the middle point between the SNPs immediately flanking the recombination breakpoint in the IWGSC RefSeq v2.0 (<https://wheat-urgi.versailles.inra.fr/>).